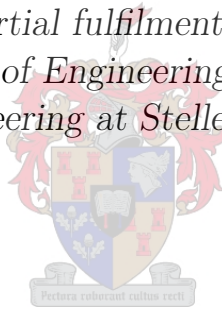


# Development of a Guidance and Intra-Arterial Flow Monitoring Catheter

by

Tys van der Merwe

*Thesis presented as partial fulfilment of the requirements for  
the degree of Master of Engineering (Mechatronic) in the  
Faculty of Engineering at Stellenbosch University*



Supervisors:

Mr. Johan van der Merwe Prof. Pieter Rousseau Fourie

December 2016

# Declaration

By submitting this thesis electronically, I declare that the entirety of the work contained therein is my own, original work, that I am the sole author thereof (save to the extent explicitly otherwise stated), that reproduction and publication thereof by Stellenbosch University will not infringe any third party rights and that I have not previously in its entirety or in part submitted it for obtaining any qualification.

Date: .....December 2016.....

Copyright © 2016 Stellenbosch University  
All rights reserved.

# Abstract

This thesis entails the development and testing of devices that can aid in guiding a needle into a blood vessel. Furthermore, a concept flow meter is also developed and tested. Physicians often have difficulty placing a needle in blood vessels. For a number of procedures access to blood vessels are required. Investigating methods to ease this process is thus beneficial to the medical field. Likewise, measuring blood flow is also of importance in the medical field. Measuring blood flow to the brain can prevent brain ischemia, which can lead to death of brain tissue.

Near infrared (NIR) light is used to guide the needle towards a blood vessel. Two optic fibre strands are placed inside the needle, one to transmit NIR light and one to receive reflected light. The reflected light, when pointing at blood, is different from other tissue types. The *in vitro* and *in vivo* tests both showed that there is a statistically significant difference ( $p < 0.001$ ) in reflected light when pointing at and away from a blood vessel.

Electrical impedance is used to determine when the needle enters a blood vessel. A sine wave is generated and passed through biological tissue. The measured impedance is different for blood and other tissue types. It was found that when a signal of 29.85 kHz was used, there was a statistically significant difference ( $p < 0.001$ ) between blood and muscle and blood and fat.

The flow meter works on the principle of thermal convection. The concept device that is developed, has an ambient temperature sensor and a second temperature sensor wrapped in a heating coil. In the presence of fluid flow, heat is carried away from the heater by thermal convection, causing a temperature drop. The device was tested *in vitro* in distilled water flow and blood flow at flow rates between 0.1 ml/s and 0.45 ml/s. Both the fluids had high variances in the temperature difference between the ambient and heater temperature. By removing the offsets, clear trends become visible. For the distilled water tests, a fit in the tested flow region was obtained with a coefficient of determination of  $R^2 = 0.9801$ . The blood tests however were more erratic and the best fit that could be obtained had a coefficient of determination of  $R^2 = 0.6056$ . In both cases however, CFD results indicate that this method is a viable method if some of the flow meter design aspects are improved.

The results indicate that a combination of the aforementioned technologies can be used to guide a needle into a blood vessel and measure flow rate. While further investigation is required to make this a product in the medical practice, the investigation in this thesis serves as a basis for future clinical trials in the development of a guidance and intra-arterial flow monitoring catheter.

# Abstrak

Die tesis behels die ontwikkeling en toets van toestelle wat 'n naald kan lei tot in 'n bloedvat. Verder is 'n konsep vloeimeter ook ontwikkel en getoets. Dokters beskou dit gereeld as 'n uitdaging om 'n naald in 'n bloedvat te plaas. Toegang tot sulke bloedvate is nodig vir 'n verskeidenheid prosedures. Vir dié rede is dit voordelig vir die mediese veld om metodes wat die proses vergemaklik te ondersoek. Net so is die meet van bloedvloeï ook belangrik in die mediese veld. Die meet van bloedvloeï na die brein kan brein isemie voorkom, wat kan lei tot die dood van breinweefsel.

Naby-infrarooi (NIR) lig word gebruik om die naald te lei na 'n bloedvat toe. Twee optiese vesels is binne in die naald geplaas. Een vesel dra die NIR lig van die lig bron af en die ander vesel lei gereflekteerde lig terug na 'n sensor toe. Die gereflekteerde lig is verskillend vir wanneer die naald na 'n bloedvat wys en weg van die bloedvat af wys. Die *in vitro* en *in vivo* toetse beide dui daarop dat daar 'n statistiese beduidende ( $p < 0.001$ ) verskil in gereflekteerde lig is wanneer die naald wys na 'n bloedvat en wanneer dit weg van die bloedvat af wys.

Elektrise impedansie word gebruik om te bepaal wanneer die naald 'n bloedvat binnedring. 'n Sinus golf word gegenereer en deur die biologiese weefsel gestuur. Die impedansie wat gevolglik gemeet word, is verskillend vir bloed as vir ander weefsel soorte. Dit was gevind dat vir 'n golf van 29.85 kHz, daar 'n statistiese beduidende verskil ( $p < 0.001$ ) tussen die impedansie van bloed en spier asook bloed en vet is.

Die vloeimeter werk met die beginsel van termiese konveksie. Die konsep toestel wat ontwikkel is, het 'n omgewingstemperatuur sensor en a temperatuur sensor wat in 'n verhittings spoel omvou is. Wanneer 'n vloeistof oor die verhitter vloei, word hitte weggedra en dit veroorsaak 'n verlaging in temperatuur. Die toestel was *in vitro* getoets in beide gedistilleerde watervloeï en in bloedvloeï met vloeï tempo's van tussen 0.1 ml/s en 0.45 ml/s. Beide vloeïstof toetse het hoë variansies gehad tussen die omgewingstemperatuur en die verhittingstemperatuur. Met verwydering van die relatiewe verskille tussen datastelle, het duidelike tendense in die data verskyn. Vir die gedistilleerde watertoetse is 'n pas gevind met 'n bepaaldheidskoeffisiënt van  $R^2 = 0.9801$ .

Vir die bloedtoetse was daar slegs 'n pas gevind met 'n bepaaldheidskoeffisiënt van  $R^2 = 0.6056$ . In beide gevalle alhoewel, het CFD resultate daarop gedui dat die metode wel 'n lewensvatbare metode is om vloeitempo te meet, mits sekere aspekte van die ontwerp verbeter word.

Die resultate dui aan dat 'n kombinasie van die bogenoemde tegnologieë gebruik kan word om 'n naald te lei tot in 'n bloedvat en om vloeitempo mee te meet. Verdere ondersoek word benodig om dié toestelle te omskep in 'n produk wat in die mediese praktyk gebruik kan word. Nietemin dien die ondersoek wat in dié tesis gedoen is, as 'n basis vir toekomstige kliniese ondersoeke wat kan bydra tot die ontwikkeling van 'n leidingsnaald en intra-arteriële bloedvloeimonitor.

# Acknowledgements

I would like to express my sincerest gratitude to Mr. J. van der Merwe and Prof. P.R. Fourie for their guidance throughout the course of this thesis. Furthermore, I would like to thank the Tygerberg animal testing unit and their staff for their professionalism and willingness to help. Also, I thank my colleagues, in particular Mr. G.J. Visser whom was always willing to provide insightful advice. Lastly, I thank my wife, father and mother for their unwavering support.

# Contents

<b>Declaration</b>	<b>i</b>
<b>Contents</b>	<b>vii</b>
<b>List of Figures</b>	<b>x</b>
<b>List of Tables</b>	<b>xiv</b>
<b>1 Introduction</b>	<b>1</b>
1.1 Objectives . . . . .	2
1.2 Motivation . . . . .	2
<b>2 Literature Review</b>	<b>4</b>
2.1 Relevant Anatomy and Physiology . . . . .	4
2.1.1 Blood Vessel Anatomy . . . . .	4
2.1.2 Circulatory System . . . . .	5
2.1.3 Blood Anatomy and Physiology . . . . .	7
2.1.4 Endovascular Procedures . . . . .	7
2.2 Technology Review . . . . .	8
2.2.1 Impedance . . . . .	8
2.2.2 Inductance . . . . .	10
2.2.3 Capacitance . . . . .	11
2.2.4 Near-Infrared . . . . .	13
2.2.5 Ultrasound . . . . .	14
2.2.6 Electromagnetism . . . . .	16
2.2.7 Laser . . . . .	17
2.2.8 Thermal Methods . . . . .	18
<b>3 Preliminary Technology Investigation and Theoretical Back-ground</b>	<b>20</b>
3.1 Near-Infrared . . . . .	20
3.2 Impedance . . . . .	22
3.3 Thermal Method . . . . .	24



## CONTENTS

<b>4</b>	<b>Design of Devices</b>	<b>27</b>
4.1	Near-Infrared Blood Vessel Location Detection . . . . .	27
4.1.1	Physical Design . . . . .	27
4.1.2	Electronic Design . . . . .	30
4.2	Impedance Blood Vessel Penetration Detection . . . . .	32
4.2.1	Physical Design . . . . .	32
4.2.2	Electrical Design . . . . .	33
4.2.3	AD5934 Communication and Sequencing . . . . .	36
4.3	Thermal Method Blood Flow Measurement . . . . .	38
4.3.1	Design . . . . .	38
4.3.2	Electronic Design . . . . .	40
4.3.3	CFD Simulation Setup . . . . .	43
<b>5</b>	<b>In Vitro Tests</b>	<b>45</b>
5.1	Fluid Circulation System . . . . .	45
5.2	Phantom for NIR Tests . . . . .	47
5.2.1	Blood . . . . .	47
5.2.2	Agar Phantom . . . . .	47
5.3	Experimental Procedure . . . . .	48
5.4	Blood Vessel Detection . . . . .	49
5.4.1	Results . . . . .	49
5.4.2	Discussion . . . . .	52
5.5	Blood Vessel Penetration Detection . . . . .	52
5.5.1	Results . . . . .	52
5.5.2	Discussion . . . . .	55
5.6	Blood Flow Measurement . . . . .	57
5.6.1	Results . . . . .	57
5.6.2	Discussion . . . . .	60
<b>6</b>	<b>In Vivo Tests</b>	<b>63</b>
6.1	Animal Testing Motivation . . . . .	63
6.2	Experimental Procedure . . . . .	64
6.3	Blood Vessel Detection . . . . .	66
6.3.1	Results . . . . .	66
6.3.2	Discussion . . . . .	71
6.4	Blood Vessel Penetration Detection . . . . .	73
6.4.1	Results . . . . .	73
6.4.2	Discussion . . . . .	75
<b>7</b>	<b>Conclusion</b>	<b>77</b>
7.1	Summary . . . . .	77
7.1.1	Near Infrared Blood Vessel Detection . . . . .	77
7.1.2	Electrical Impedance Blood Vessel Penetration Detection . . . . .	78
7.1.3	Thermal Convection Blood Flow Measurement . . . . .	78

CONTENTS

---

7.2 Potential Future Work . . . . .	79
7.3 Conclusion . . . . .	80
<b>List of References</b>	<b>82</b>
<b>Appendices</b>	<b>86</b>
<b>A Considered Technology</b>	<b>87</b>
A.1 Ultrasonic Doppler . . . . .	87
A.2 Capacitance . . . . .	88
<b>B Circuits</b>	<b>90</b>
<b>C Near Infrared Device Housing</b>	<b>93</b>
<b>D AD5934 Flow Chart</b>	<b>96</b>
<b>E Circulation System Heater Control</b>	<b>97</b>
<b>F In Vitro Experimental Procedure</b>	<b>98</b>
<b>G Pump Calibration</b>	<b>100</b>
<b>H Calibration</b>	<b>102</b>
<b>I Ethical Clearance Letter of Approval</b>	<b>104</b>

# List of Figures

2.1	Blood Vessel Anatomy (Marieb, 2012)	5
2.2	Circulatory system (Adapted from Villarreal (2009))	6
2.3	Impedance electrode set ups	9
	(a) Four electrode method	9
	(b) Two electrode method	9
2.4	Impedance guided arterial catheter (Schwartz, 2013)	9
2.5	Typical inductive sensor (Menke, 2014)	11
2.6	Capacitive proximity sensing	12
2.7	Real time visual projection of the brachial veins by the VeinViewer <sup>®</sup> (Strehle, 2010)	14
2.8	Ultrasonic guided needle (Gehlbach, 1992)	15
2.9	Electromagnetic blood flow meters (Moore and Zouridakis, 2004)	16
	(a) Chronic Dowel flow probe	16
	(b) Forceps flow probe	16
2.10	Thermal mass flow meter concept	19
3.1	Reaction of NIR light on skin with subcutaneous blood vessels	21
3.2	Relative fluence rate of muscle (left) and blood (right) in the presence of 880 nm light.	21
3.3	Monte Carlo simulation for a subcutaneous blood vessel in 880 nm light.	22
3.4	Preliminary test on NIR light response in fat and muscle	22
3.5	Basic biological tissue impedance models	23
	(a) Fricke-Morse model of biological tissue	23
	(b) Simplified model of biological tissue	23
3.6	Surface temperature response of heaters at different blood flow velocities	26
3.7	Visual CFD response of thermistor heater in different blood mass flow rates	26
4.1	NIR prototype setup	28
4.2	Optic fibre preparation (Photo: T. van der Merwe)	29
	(a) Optic fibre cut with ceramic wafer	29
	(b) Optic fibre sanded with 1200 grit paper	29

## LIST OF FIGURES

4.3	Needle with inserted optic fibre (Photo: T. van der Merwe) . . . . .	29
	(a) Front view . . . . .	29
	(b) Side view . . . . .	29
4.4	NIR LED and phototransistor setup . . . . .	30
4.5	NIR circuit potentiometers . . . . .	31
4.6	NIR device amplifier circuit . . . . .	32
	(a) AD620 amplifier circuit . . . . .	32
	(b) MAX660 voltage pump circuit . . . . .	32
4.7	Needle with inserted electrode (Photo: T. van der Merwe) . . . . .	33
	(a) Front view . . . . .	33
	(b) Side view . . . . .	33
4.8	AD5934 impedance converter connection . . . . .	33
4.9	Impedance signal circuit . . . . .	34
4.10	Impedance signals at 10 kHz with a 10 k $\Omega$ load . . . . .	35
4.11	Flow meter layout . . . . .	39
4.12	Thermistor wrapped in heating coil . . . . .	39
4.13	Heater circuit . . . . .	41
4.14	Thermistor Wheatstone circuit . . . . .	42
4.15	Thermistor circuit buffer . . . . .	43
4.16	Model used for the CFD simulations . . . . .	43
4.17	CFD simulation of flow sensor . . . . .	44
	(a) Visual temperature response of flow sensor in blood flow . . . . .	44
	(b) CFD simulation compared to analytical model . . . . .	44
5.1	Circulation system layout . . . . .	45
5.2	Fluid heating setup . . . . .	46
	(a) Fluid heater . . . . .	46
	(b) Heater control system . . . . .	46
5.3	<i>In vitro</i> testing procedure . . . . .	48
5.4	Normalised intensities of various tissues when probe is inserted into the tissue . . . . .	50
5.5	Normalised intensities when pointing probe at tube and pointing away from tube . . . . .	51
5.6	Impedance magnitudes and phase angles of tissue types with 95 % confidence intervals . . . . .	53
	(a) Tissue impedance magnitude . . . . .	53
	(b) Tissue impedance phase angles . . . . .	53
5.7	Interference ratios of blood and nearest tissue means . . . . .	54
	(a) Impedance magnitude interference ratios . . . . .	54
	(b) Impedance phase angle interference ratios . . . . .	54
5.8	Impedance magnitudes of fat and muscle compared to blood at 29.85 kHz . . . . .	55
	(a) Blood and muscle impedance magnitude . . . . .	55
	(b) Blood and fat impedance magnitude . . . . .	55

## LIST OF FIGURES

5.9	Impedance phase angle of fat and muscle compared to blood at 29.85 kHz . . . . .	55
	(a) Blood and muscle impedance phase angle . . . . .	55
	(b) Blood and fat impedance phase angle . . . . .	55
5.10	Raw response of thermal flow sensor in distilled water . . . . .	58
	(a) Temperature difference between ambient sensor and heater sensor . . . . .	58
	(b) Averaged ambient and heater temperatures during a test run . . . . .	58
5.11	Thermal flow sensor results with removed offset . . . . .	58
	(a) Test runs with no offset . . . . .	58
	(b) Error plot with 95 % confidence intervals. Solid line indicates fit. . . . .	58
5.12	CFD simulation results of thermal flow meter in water flow . . . . .	59
	(a) CFD results for different power settings . . . . .	59
	(b) CFD results over a larger flow range . . . . .	59
5.13	Raw response of thermal flow sensor in blood flow . . . . .	60
	(a) Temperature difference between ambient sensor and heater sensor . . . . .	60
	(b) Ambient and heater temperatures . . . . .	60
5.14	Thermal flow sensor results of blood tests with offset removed . . . . .	60
	(a) Test runs with no offset . . . . .	60
	(b) Error plot with 95 % confidence intervals. Solid line indicates fit. . . . .	60
5.15	CFD simulation results of thermal flow meter in blood flow . . . . .	61
	(a) CFD results for different power settings . . . . .	61
	(b) CFD results over a larger flow range . . . . .	61
6.1	<i>In vivo</i> testing procedure . . . . .	64
6.2	Incision near rabbit femoral artery . . . . .	65
6.3	Impedance needle placed into muscle tissue . . . . .	66
6.4	Normalised intensities of probe against blood vessel and away from blood vessel in surrounding tissue . . . . .	67
6.5	Normalised intensities of probe against skin, pointing at blood vessel and away from blood vessel . . . . .	68
6.6	Normalised intensities from inside muscle tissue near blood vessel for inverted scenarios . . . . .	69
	(a) Scenario 1 . . . . .	69
	(b) Scenario 2 . . . . .	69
6.7	Normalised intensities from inside muscle tissue near blood vessel . . . . .	70
6.8	Dynamic amplified voltage response of NIR device when moving over a blood vessel . . . . .	71
6.9	Impedance magnitudes and phase angles of rabbit tissue types with 95 % confidence intervals . . . . .	73

## LIST OF FIGURES

---

(a)	Rabbit tissue impedance magnitude . . . . .	73
(b)	Rabbit tissue impedance phase angles . . . . .	73
6.10	Interference ratios of blood and nearest rabbit tissue means . . . . .	74
(a)	Impedance magnitude interference ratios of rabbit tests . . . . .	74
(b)	Impedance phase angle interference ratios of rabbit tests . . . . .	74
6.11	Impedance magnitudes of fat and muscle compared to blood at 29.85 kHz for rabbit tests . . . . .	75
(a)	Blood and muscle impedance magnitude . . . . .	75
(b)	Blood and fat impedance magnitude . . . . .	75
6.12	Impedance phase of fat and muscle compared to blood at 29.85 kHz for rabbit tests . . . . .	75
(a)	Blood and muscle impedance phase angle . . . . .	75
(b)	Blood and fat impedance phase angle . . . . .	75
A.1	Doppler probe with attached needle . . . . .	87
A.2	Frequency mixer . . . . .	88
A.3	Capacitive sensing needle . . . . .	89
A.4	Capacitive sensing circuit . . . . .	89
B.1	Full thermal flow meter circuit . . . . .	90
B.2	Full near infrared device circuit . . . . .	91
B.3	Full impedance device circuit . . . . .	92
C.1	Near infrared device housing top cover . . . . .	94
C.2	Near infrared device bottom housing . . . . .	95
D.1	AD5934 flow chart (AD5934 datasheet) . . . . .	96
E.1	PID control of infusion warmer . . . . .	97
F.1	<i>In vitro</i> testing procedure . . . . .	99
G.1	Gilson Minipuls peristaltic pump . . . . .	100
G.2	Pump calibration . . . . .	101
H.1	Thermistors Calibration . . . . .	102
H.2	Ambient and heater thermistor Wheatstone bridge calibration . . . . .	103

# List of Tables

2.1	Mean impedance magnitude of various tissue types at 30 kHz (standard deviation in brackets) . . . . .	10
2.2	Depth of tissue penetration of 834 nm NIR light (standard deviation in brackets) . . . . .	13
3.1	Biological tissue impedance approximation . . . . .	24
4.1	AD5934 initial parameters for data acquisition . . . . .	37
4.2	Materials considered for heating element . . . . .	40
4.3	Wheatstone bridge resistance values . . . . .	42
5.1	Statistics of normalised NIR response in specific tissues at 880 nm (normalised to 0.4273 V) . . . . .	50
5.2	Statistics of normalised NIR response pointing at blood vessel and away from vessel at 880 nm (normalised to 0.4273 V) . . . . .	51
5.3	Impedance tests sample information . . . . .	53
5.4	Impedance magnitude statistics at 29.85 kHz . . . . .	56
5.5	Impedance phase angle statistics at 29.85 kHz . . . . .	56
5.6	Thermal flow results summary . . . . .	61
6.1	Statistics of normalised NIR response at blood vessel surface and in surrounding tissue 880 nm (normalised to 0.4778 V) . . . . .	68
6.2	Statistics of normalised NIR response at skin surface pointing at and away from blood vessel at 880 nm (normalised to 0.4778 V) . . . . .	69
6.3	Statistics of normalised NIR response when pointing at a blood vessel and away from the blood vessel at 880 nm (normalised to 0.4778 V) . . . . .	70
6.4	Impedance tests sample information for rabbit tests . . . . .	74
6.5	Impedance magnitude statistics at 29.85 kHz for rabbit tests . . . . .	76
6.6	Impedance phase angle statistics at 29.85 kHz for rabbit tests . . . . .	76
H.1	Steinhart-Hart constants . . . . .	103

# 1. Introduction

A common problem in the medical practise is that physicians often have difficulty locating blood vessels. A number of important medical procedures require the physician to access blood vessel. Knowing the location of blood vessels enables the physician to place a needle in the vessel, thereby gaining access to the vascular system. Overcoming the difficulty to locate and gain access to blood vessels thus becomes a topic of value. This leads to the need for methods of needle guidance to locate blood vessels.

The primary purpose of developing a guidance method, in the context of this thesis, is to create an access point for catheters to be inserted. While there are a number of different catheters that can utilise this access point, particular focus is placed on a catheter that can measure blood flow rate. Measuring blood flow rate to the brain during surgical operations is essential to ensure the safety of the patient. Investigating an appropriate method to continuously measure arterial blood flow and contributing to current studies on the topic thus becomes invaluable.

Physicians typically rely on their knowledge of the human anatomy to locate blood vessels. However, anatomical variations from person to person make this method somewhat unreliable. Other researchers have realised this problem too. Gehlbach (1992) patented a needle with an embedded ultrasonic crystal to locate blood vessels by means of ultrasonic Doppler. While this device does not feature much after the patent, it does show that others recognise the need for a guidance needle. The VeinViewer<sup>®</sup> is a product that can detect blood vessels near the surface of the skin by means of near infrared light. It cannot locate blood vessels that are far below the surface of the skin, but a study by Strehle (2010) shows that doctors still found this technology very useful. These are among a number of studies relating to the topic of locating blood vessels.

In terms of measuring blood flow rate, various methods have been studied, some of which are reviewed by Jayanthi *et al.* (2011). These include ultrasonic Doppler, laser Doppler as well as thermal conduction and convection methods. These studies emphasise the importance of measuring blood flow rate, particularly blood flow to the brain. A decrease in blood flow to the brain can cause



## 1. INTRODUCTION

---

brain ischemia, which can lead to the death of brain tissue. Furthermore, blood flow measurements play an important role in the diagnoses of some diseases. These factors contribute to the need for a study on appropriate methods to measure blood flow rate.

The technology that is feasible for needle guidance and intra-arterial flow monitoring are discussed and investigated in this thesis. Prototypes of the most viable technologies are developed and tested. This includes near-infrared, electrical impedance and thermal convection methods to locate blood vessels, determine blood vessel penetration and measure blood flow respectively. The theory behind these methods are briefly discussed and followed by tests on both an *in vitro* blood circulation model and *in vivo* on New Zealand white rabbits. The combination of these technologies are discussed and serve as a basis for future clinical trials.

### 1.1 Objectives

Developing a guidance and intra-arterial flow monitoring catheter can be broken down into three primary objectives. These objectives are to develop and investigate devices that have the ability to:

- Locate blood vessels prior to penetrating them. Thus the device must be able to identify a blood vessel when near or in contact with a blood vessel.
- Determine when the blood vessel is penetrated. The device must thus have a means of distinguishing when the tip of the needle has entered the blood vessel.
- Measure the flow rate of blood.

### 1.2 Motivation

A device that has the ability to guide a needle into a blood vessel and also measure the blood flow rate can potentially prove to have important benefits in the medical field. To fully grasp the importance of such a device, some possible applications are discussed.

In certain emergency cases it is crucial to gain quick access to blood vessels for a number of reasons. During resuscitation, for example, it is very important to insert an intravenous (IV) line to quickly administer adrenaline. Moreover, procedures such as emergency blood transfusion and insertion of temporary

## 1. INTRODUCTION

---

pacemakers all require quick access to blood vessels. Chemotherapy patients often have blood vessels that are difficult to locate due to the chemotherapy treatment. Additional pain by pricking a patient multiple times to find blood vessels for the chemotherapy can potentially be avoided by a device that can aid in guiding a needle into a blood vessel.

The device can also be used as an educational confidence builder. Medical students, even experienced physicians, oftentimes have difficulty locating blood vessels. This can also be beneficial to patients in general. When administering medication or nutrients via an IV line, it can be traumatising for the patient if the needle must be inserted multiple times. Measuring blood flow also has multiple important uses. In cerebral blood flow, not knowing the blood flow rate can result in brain tissue dying. Also, some diseases cause symptoms such as reduced or increased blood flow rate to certain organs. Blood flow rate measurements in these regions can help to diagnose diseases early on and thus avoid later complications.

Mentioned above are only a few possible applications for such a device. However, the real strength of the thesis lies in the research into different technologies and how they can be used to guide a needle into a blood vessel and measure flow rate. This lays a foundation for future research into similar devices.

## 2. Literature Review

### 2.1 Relevant Anatomy and Physiology

The purpose of this section is to provide the necessary background information in terms of the relevant anatomy and physiology. Information in this section is largely obtained from Marieb (2012).

#### 2.1.1 Blood Vessel Anatomy

The main carriers of blood in humans are veins, arteries and capillaries, collectively known as blood vessels. By referring to Figure 2.1 it can be seen that arteries and veins have very similar structures in that both have three coats, called tunics. The hollow area of these blood vessels are known as the lumen. The lumen is surrounded by the tunica intima which consists of epithelial cells to reduce the friction of blood flow. The next layer, tunica media, consists of smooth muscle that help to regulate blood pressure by changing the blood vessel diameter. The outer layer, known as the tunica externa, contain mostly fibrous tissue that acts as a support structure.

Broadly speaking, veins differ from arteries in that they carry blood towards the heart, whereas arteries carry blood away from the heart. There are however also structural differences. Arteries are generally under more pressure than veins and thus their walls are thicker. Furthermore, veins tend to have larger lumens and have valves to prevent blood from flowing back due to lower pressure. Veins and arteries are generally separated by a network of capillaries. Arteries branch into arterioles which then branch into capillaries. The capillaries then rejoin to form venules which flows into the veins. Capillaries are small blood vessels that consist only of endothelial cells and a membrane. The purpose of the capillaries is to come in close contact with surrounding cells and allow easy diffusion of oxygen ( $O_2$ ), carbon dioxide ( $CO_2$ ), nutrients and waste. The delivery of blood to these capillaries is known as perfusion.

## 2. LITERATURE REVIEW

---

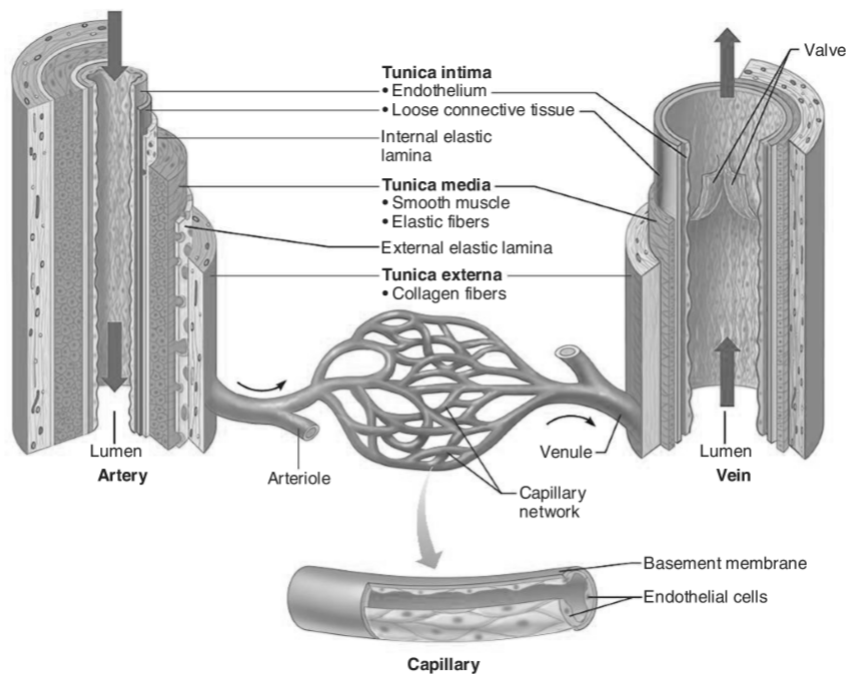


**Figure 2.1: Blood Vessel Anatomy (Marieb, 2012)**

### 2.1.2 Circulatory System

At the centre of the blood flow is the heart. Essentially the heart pumps blood through the body by contracting periodically. When the sinoatrial node (located on the heart) depolarizes it causes the heart to contract and pump blood. This electric pulse can be recorded in the form of an electrocardiogram (ECG) which illustrates the heartbeat. The heart pumps de-oxygenated (oxygen poor) blood into the right side of the heart via the superior and inferior vena cavae. Pulmonary arteries then carry this blood to the lungs where carbon dioxide is exchanged for oxygen. The oxygen rich blood then returns to the heart via the pulmonary veins. This blood is now pumped through the body, exiting the heart via the aorta. In this way, blood is circulated through the body with the required oxygen. Note that arteries will always carry oxygen rich blood and veins oxygen poor blood with the exception of the pulmonary blood vessels.

Several blood vessels branch from the aorta and the vena cavae. These blood vessels can be considered major blood vessels as they carry large volumes of blood to the rest of the body. For the purpose of this thesis only certain blood vessels are important. The reason for their importance is discussed in greater detail in Section 2.1.4. Referring to Figure 2.2, the carotid arteries are among the most important blood vessels that branch from the aorta. They supply blood to the brain. The subclavian arteries supply blood to the upper limbs via the brachial artery to the radial and ulnar arteries. The lower limbs

## 2. LITERATURE REVIEW

---

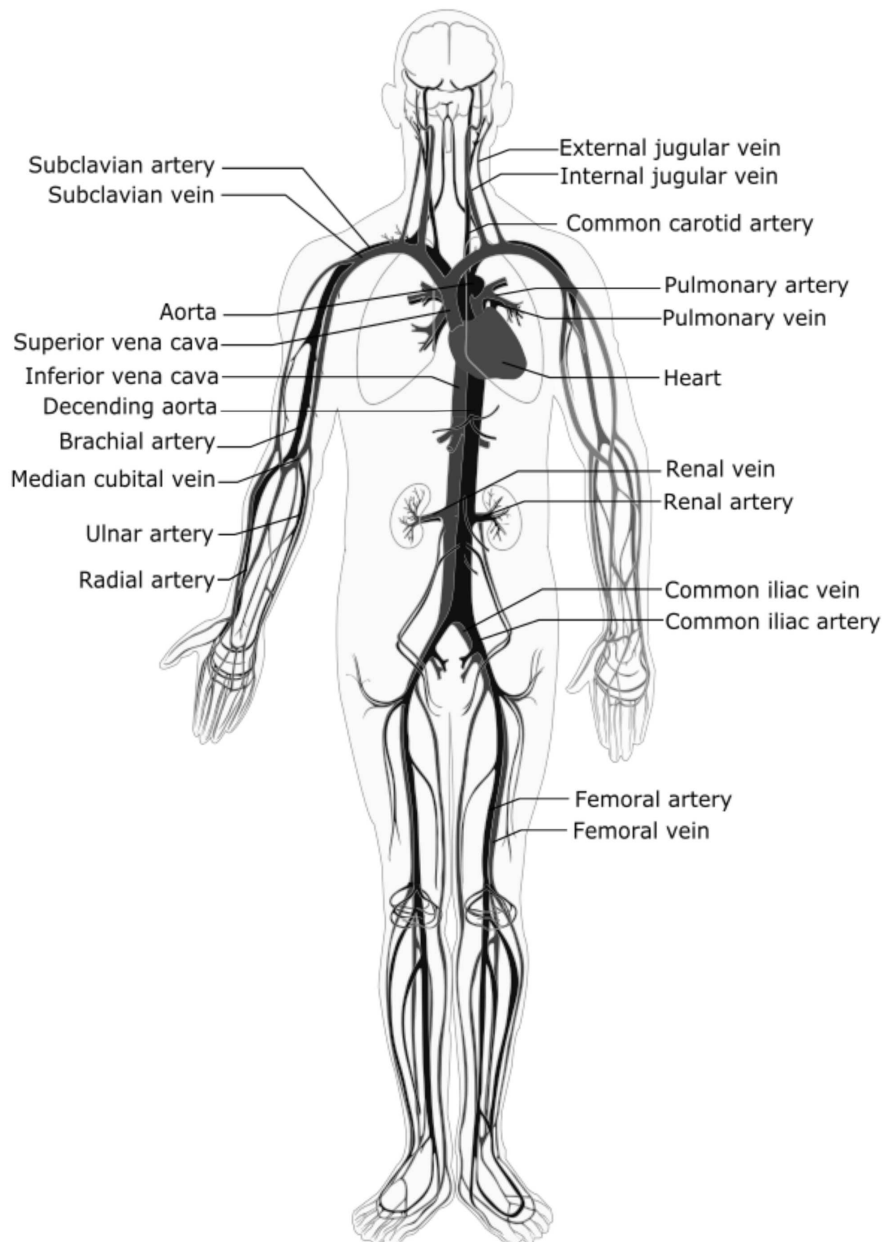


**Figure 2.2: Circulatory system (Adapted from Villarreal (2009))**

receive their blood from the iliac arteries. They branch further into the femoral arteries. Although not considered a major blood vessel, the renal artery that branches to the kidney is also of importance in certain procedures. The jugular veins transport oxygen poor blood away from the brain back to the superior vena cava. Oxygen poor blood from the upper limbs also flow to the superior vena cava via the subclavian vein.

## 2. LITERATURE REVIEW

---

### 2.1.3 Blood Anatomy and Physiology

Blood is essential in delivering nutrients, hormones and oxygen to the whole body. At the same time blood also plays a major role in the removal of waste product from the body as well as carbon dioxide. Blood can be separated into three components. About 55 % of blood consists of plasma of which about 90 % is water. Plasma also contain proteins and electrolytes. Electrolytes are ions that carry a charge. As is discussed in more detail in Section 2.2, these charges can be detected by certain devices. These ions include sodium ( $\text{Na}^+$ ), chloride ( $\text{Cl}^-$ ), potassium ( $\text{K}^+$ ), calcium ( $\text{Ca}^{2+}$ ) and magnesium ( $\text{Mg}^{2+}$ ) (Toffaletti, 2001). It must be noted that these ions will also be present in surrounding tissue.

Less than 1 % of the blood composition consists of leukocytes and platelets and this composition is known as the buffy coat. Leukocytes are more commonly known as white blood cells, which are largely responsible for immune defence. Platelets are responsible for the clotting of blood. The remaining 45 % consists of erythrocytes, more commonly known as red blood cells. Erythrocytes contain an important protein known as haemoglobin. Oxygen binds to the haemoglobin and it is then transported throughout the body. Carbon dioxide also binds to the haemoglobin, however to a much lesser extent.

### 2.1.4 Endovascular Procedures

Depending on the type of procedure that is done, it may be required to access either veins or arteries. Procedures that require access to blood vessels are known as endovascular procedures. Some of these procedures include the drawing of blood as well as intravenous (IV) therapy.

The process of making an incision in veins, typically for the purposes mentioned above, is known as venipuncture. Blood will usually be drawn from the median cubital vein. IV's may also be inserted at this position, but are usually inserted in veins present in the dorsal (back) side of the hand. The carotid artery transports blood to the brain. Being able to locate this artery and to measure the blood flow is of paramount importance to ensure that cellular death does not occur in the brain of patients.

The heart can be accessed with catheters for a number of medical procedures via the femoral artery. In cases such as this, it is important not only to locate the arteries, but also to guide the needle and prevent it from exiting the artery through the arterial wall. Once the catheter is inserted it is, in some cases, preferable to move the catheter into branching arteries to areas where inspection is required. An example of this is when a catheter is inserted in the femoral artery and guided along the aorta. From the aorta, the renal arteries can be accessed. This can allow the physician to inspect the kidneys.

## 2. LITERATURE REVIEW

---

### 2.2 Technology Review

Various technologies have been used in recent years to help guide a needle towards and into a blood vessel and then insert catheters once inside the blood vessels. Additionally, other technology that have not been used for these purposes show promise to be used for similar applications.

#### 2.2.1 Impedance

Impedance is broadly defined as the ratio between the voltage and current in a circuit (similar to resistance). Bioimpedance is thus defined as the ability of biological tissue to oppose, or impede, the flow of current (Grimnes and Martinsen, 2008). Although this applies to both direct current (DC) and alternating current (AC), it is of more use in the biomedical field to focus on AC. The reason for this is that different tissue types respond very differently to various voltage frequencies. The differences in the response of the tissues can be measured in terms of the magnitude of the impedance and also the phase angle. The phase angle is the difference between the phase of the voltage and the current. Measuring the phase angle and impedance magnitude upon applying different frequencies of electricity to biological tissue can then be used to determine which types of biological tissues are present. These measurements can be used to distinguish blood and blood vessels from surrounding tissue such as fat and muscle.

There are several considerations to be made in utilising this technology for the purpose of bioimpedance. Bioimpedance is measured by injecting a sinusoidal signal into the tissue. This leads to the first consideration, which is the choice of signal source. Either a voltage source or a current source can inject a signal. Current sources are typically used for bioimpedance measurements as a controlled current is safer for patients. Also, the signal to noise ratio is kept high because current injection can be maximised. Mohamadou *et al.* (2012) performed tests where he measured the impedance of various tissues with both a voltage source and a current source. While it is found that at high frequencies (above 500 kHz) the voltage source method outperforms the current source method, the voltage source has drawbacks. The voltage source requires a current sensing resistor and at low impedance loads the signal to noise ratio starts to decrease, which is unwanted.

The second consideration of using bioimpedance is the number of electrodes to use. The first common possibility is four electrodes. An input signal is given to the tissue and two electrodes between that signal measures the response as shown in Figure 2.3(a). The second method uses only two electrodes that serve both as a signal input and measuring terminals as shown in Figure 2.3(b). Chang *et al.* (2008) compared these two methods over a large frequency range.

## 2. LITERATURE REVIEW

It was found that from 100 Hz to 20 kHz the four electrode method performed the best, whereas the two electrode method performed the best from 12 MHz to 100 MHz. In between those frequencies both the methods gave similar performance. There is also a three electrode method, however it is not very common. The difference between the generated signal and the measured signal is then used to determine the impedance magnitude and phase angle.

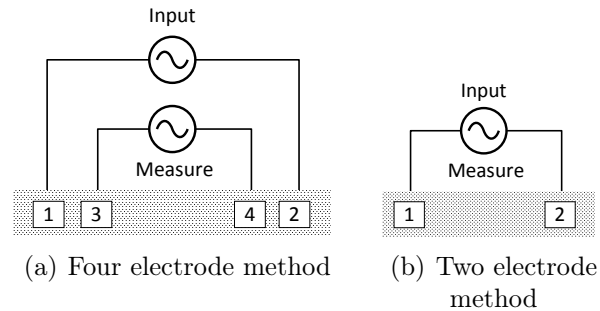


**Figure 2.3: Impedance electrode set ups**

The electrodes can be close to one another. Schwartz (2013) designed an impedance sensing device where the electrodes formed part of a hypodermic needle. Silver conductive material was placed in the lumen of the needle and looped around and placed under the cannula as shown in Figure 2.4.

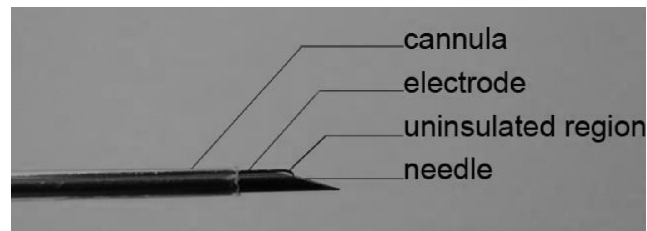


**Figure 2.4: Impedance guided arterial catheter (Schwartz, 2013)**

A recent study done by Kalvøy *et al.* (2009), *in vivo* on porcine, shows that for frequencies of up to 1 kHz blood can clearly be distinguished from both fat and muscle based only on the impedance magnitude. Frequencies greater than that also allow for distinction between blood, fat and muscle (Schwartz, 2013), however blood and fat are not as distinguishable as at lower frequencies. Based on phase angles, blood can again be easily distinguished from fat and muscle, however this is viable for frequencies of up to 1 MHz, with the exception of 10 kHz to 20 kHz where the different tissues have very similar phase angles.

The discrimination between tissue types is further verified by an impedance analysis by Martinsen *et al.* (2010). It shows the impedance magnitude and



## 2. LITERATURE REVIEW

---

phase angle at different frequencies of fat, muscle, arterial wall and blood. Arterial wall results seem volatile and at most frequencies the magnitude and phase angle are close to that of blood. From Martinsen *et al.* (2010), the biggest discrimination between tissues in terms of both magnitude and phase angle, lies at 30 kHz. The results are summarised in Table 2.1.

**Table 2.1: Mean impedance magnitude of various tissue types at 30 kHz (standard deviation in brackets)**

	Blood	Fat	Muscle	Artery
<b>Impedance Magnitude (Ohm)</b>	800 (173)	2690 (662)	2970 (334)	1651 (424)

### 2.2.2 Inductance

The concept of using electric induction to detect a conductor is based on two laws. Oersted's law states the flow of current through a conductive wire will result in a magnetic field around the wire. If alternating current (AC) is passed through the wire it will result in the varying magnetic field. According to Faraday's law this varying magnetic field can induce a voltage, or a current flow, in a conductor that falls within this magnetic field. This is known as electric induction and the conductor may induce a current in itself (self-induction) or surrounding conductors (mutual-induction).

In the medical field, an important use of an inductance sensor is for respiratory inductance plethysmography (RIP). RIP measures pulmonary ventilation (breathing). Wires in a coiled zigzag pattern are placed around the chest. Since the wires are in a zigzag shape, self-inductance will occur in the sections of the wire that are in close proximity to one another. When the chest circumference changes so will the self-induction as the zigzag shape will stretch. Lenz's law states that this change in induction will cause a current opposing the current that is already flowing in the wire. This change in current flow can be measured and used to determine the chest displacement with a resolution of as small as 10 nm (Wang and Liu, 2011). Although this specific application is not used to detect blood, it clearly indicates the precision capabilities of this technology.

Inductance sensors are very often used in industrial applications as a means of proximity sensing, as illustrated in Figure 2.5. This works by means of mutual-inductance. Generally the sensor has an oscillator that creates a high frequency magnetic field that in turn induces eddy currents in conductors that fall within the field. These eddy currents decrease the oscillation amplitude

## 2. LITERATURE REVIEW

---

since they are generating heat and subsequently energy is lost. The change in the oscillation amplitude of the magnetic field is used to determine the proximity of the conductor.

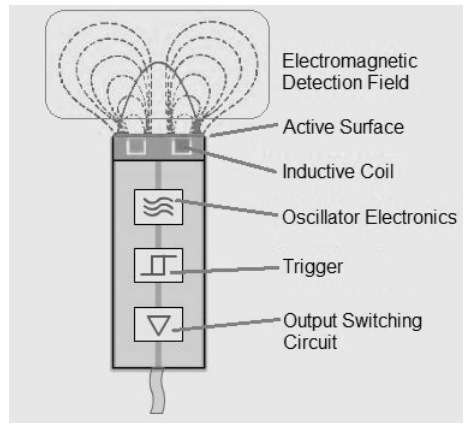


**Figure 2.5: Typical inductive sensor (Menke, 2014)**

The mutual inductance discussed above also has applications in the medical field. When a magnetic field is applied perpendicular to the flow of blood a voltage is induced as is discussed in more detail in Section 2.2.6. According to studies done by Wyatt (1961) the induction of voltage in the blood by an oscillating magnetic field will cause eddy currents in the blood. The eddy currents will again reduce the sensor oscillation amplitude which the sensor will then detect. The complication, however, is that the vascular wall and surrounding tissue can also have induced eddy currents, making tissue discrimination difficult.

Distinguishing between blood and other surrounding tissue may yet be possible. A study done by Gabriel *et al.* (2009) showed that the conductivity of blood is a  $0.6 \text{ S}\cdot\text{m}^{-1}$ , whereas fat and muscle is  $0.078 \text{ S}\cdot\text{m}^{-1}$  and  $0.17 \text{ S}\cdot\text{m}^{-1}$  respectively. This relative difference means that induction may occur more easily in blood than in other surrounding tissue.

As stated, the major drawback of this technology is that it would be difficult to clearly distinguish between certain biological tissue and blood vessels, especially if the blood vessel is deep below the surface of the skin. Also a high power voltage oscillator may be required.

### 2.2.3 Capacitance

A capacitor is a device that can store an electric charge on two terminals and create a potential difference across them. This is usually done by attaching

## 2. LITERATURE REVIEW

---

the positive and negative terminals of a cell (battery) to two separate conductive electrodes, separated by a dielectric material. Electrons (-) travel to the one electrode and since like charges repel, the other plate loses electrons and becomes positively charged. This process continues until equilibrium is reached.

The ratio between the accumulated charges of the plates and the voltage across the terminals is defined as the capacitance of the capacitor. The charges on the plates causes an electric field to surround them. When an external conductive object comes within the vicinity of the of the electrodes, the charges in the object start to separate as shown in Figure 2.6. The charge distribution of the external object causes the charge distribution on the electrodes to change, which in turn causes the capacitance to change. Since biological tissue contains ions, the charge distribution in the biological tissue can be changed in the presence of an electric field. The tissue can thus cause a change in capacitance of a nearby capacitor and this is the concept on which capacitive sensing is based (Du, 2014).

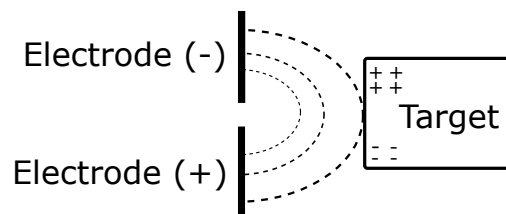


**Figure 2.6: Capacitive proximity sensing**

A common use for capacitive sensing is in touch screen technology. Several patents have been issued for use in touch screens, but these do not distinguish between different biological tissues and rather act as proximity sensors. In other words, blood cannot necessarily be distinguished from surrounding tissue. The only real use of capacitive sensors for blood related measurements is for measuring blood pressure. Halperin *et al.* (1996) designed an implantable capacitive blood pressure sensor. The sensor is concentrically placed around a blood vessel. The part of the sensor that is in contact with the blood vessel acts as one plate of the capacitor and the second plate is separated by an air gap. Pressure causes the inner membrane to displace which changes the capacitance. Previous studies done by Frobenius *et al.* (1973) showed that this type of device results in a linear change in capacitance for change in blood pressure making it easier to determine the blood pressure. The principle is however different from the one used in touch screens and cannot be used to detect a blood vessel noninvasively.

Capacitive proximity sensing of blood may be possible if one uses the differences in dielectric constants of various biological tissues. The dielectric

## 2. LITERATURE REVIEW

---

constant is a measure of how a material responds in an electric field. The dielectric constants of blood, as determined by Pethig (1987), and that of fat and muscle, as determined by Jaspard *et al.* (2003), can be compared. Fat has a distinctly lower dielectric constant than blood at all frequencies tested, however muscle is very similar to that of blood, making it difficult to distinguish once again. The influence of tissue surrounding a blood vessel on capacitance will hinder attempts to measure the capacitance of the blood vessel. Also, any grounded objects that come into contact with this device will result in inconsistent readings.

Capacitive sensing has drawbacks in detecting blood vessels, however a major advantage of this technology is the scale of the capacitive sensors. Micro-scale capacitive proximity sensors have been available for a number years. Such a sensor was already patented in 1996 by Chen and Luo (1996) of which the electrodes separation was as small as 1  $\mu\text{m}$ .

### 2.2.4 Near-Infrared

Near-infrared (NIR) light is light with a wavelength that ranges between 760 nm to 2500 nm (Davies, 2005), falling just short of the visible spectrum. Erythrocytes (red blood cells) in the blood contain proteins known as haemoglobin, as discussed in Section 2.1.3. The NIR light can penetrate the skin. Tissue that surrounds the blood vessels, such as fat and muscle, reflects the NIR light, whereas the hemoglobin in the blood absorbs the light (Strehle, 2010). A study done by Stolik *et al.* (2000), showed that NIR light can penetrate fat and muscle a lot deeper than blood, since blood absorbs the light (refer to Table 2.2). Sensors detect the returning NIR light and it is then determined where the blood vessels are based on the absence of NIR light.

**Table 2.2: Depth of tissue penetration of 834 nm NIR light (standard deviation in brackets)**

	Blood	Fat	Muscle
<b>Depth of penetration (mm)</b>	0.51 (0.06)	2.79 (0.49)	3.72 (0.92)

NIR technology is used in several medical devices. Helfer *et al.* (1993) designed a NIR device that used light of wavelengths ranging between 1000 nm to 2500 nm to locate diseased tissue among healthy tissue. This device focused on the reflective properties of the various tissues.

More recently commercial devices emerged on the medical market. Devices such as the AV400 Vein Viewing System by AccuVein<sup>®</sup> and the VeinViewer<sup>®</sup>

## 2. LITERATURE REVIEW

---

by Christie Medical Holdings use NIR technology to detect and visually display veins in real time on the surface of the skin. NIR light is emitted onto the skin by these devices and it is then determined where the veins are. Figure 2.7 shows how an image is projected onto the skin by the VeinViewer<sup>®</sup>. The image is a visual representation of the reflected NIR light showing clearly where the veins are.

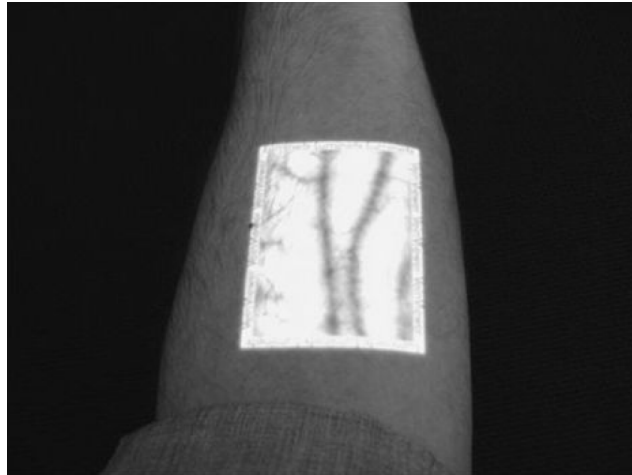


**Figure 2.7: Real time visual projection of the brachial veins by the VeinViewer<sup>®</sup> (Strehle, 2010)**

The VeinViewer<sup>®</sup> was the subject of a study done by Strehle (2010), where the aim was to determine whether such a novel device would be advantageous for detection of veins to ease phlebotomy in children. The VeinViewer<sup>®</sup> used in the study has a peak wavelength of 760 nm and has the ability to penetrate the skin up to about 10 mm deep and still give accurate readings. 72 % of the paediatricians involved in the study said that the technology did in fact help them.

The concept of using NIR to detect blood vessels is proven to work. There are minor drawbacks however. Detecting blood vessels that are further below the surface of the skin than 10 mm can become problematic. In addition to this drawback, it is also difficult to determine the depth of the blood vessel below the surface of the skin (Strehle, 2010).

### 2.2.5 Ultrasound

Ultrasound is defined as sounds with a frequency above 20 kHz (human audible range). Most medical diagnostic devices, however, use frequencies in the range of 2 MHz to 10 MHz (Bushberg, 2002).

## 2. LITERATURE REVIEW

---

Generally in the medical practice ultrasound is used by allowing the high frequency sound waves to directionally penetrate biological tissue. The sound is partially reflected by certain tissue types. This reflected sound is then used to determine the position of subcutaneous bodies such as organs. This makes it possible to obtain a two-dimensional visual representation of the reflected sound.

In terms of detecting blood flow, and indirectly the blood vessel, the ultrasound is used in conjunction with the Doppler effect. A transducer emits ultrasound at an angle into a blood vessel. The sound is then reflected off of the flowing blood and because of the velocity of the blood, the frequency of the reflected sound is different from the initial sound input. Another transducer then receives the sound and the blood flow velocity is then determined based on the Doppler shift (Franklin *et al.*, 1961).

Detecting whether blood flow is indeed present is also possible as a means to locate a blood vessel. Gehlbach (1992) designed a needle that has a directional ultrasound transducer within the needle as show in Figure 2.8. The transducer is a piezoelectric crystal. Depending on the angle and distance from the blood vessel, the Doppler shift caused by the blood would be different. An audible signal is then used to interpret the position of the blood vessel. An advantage of this technology in this particular design is that it can also be used to determine the appropriate angle of needle insertion. However, there are, to the best of our knowledge, not any validation studies of this product after the patent was published.

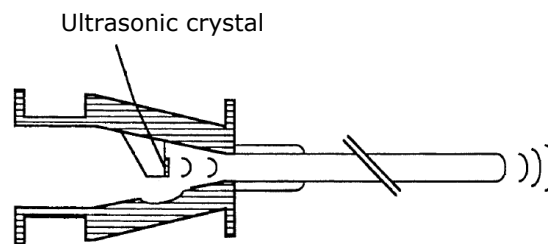


**Figure 2.8: Ultrasonic guided needle (Gehlbach, 1992)**

Ultrasound technology has a few minor drawbacks. Ultrasound does not propagate well in gasses such as air. It does however propagate well in fluid and for this reason the ultrasound emitter and receiver must be in contact with a fluid. As in the case of Gehlbach (1992) a solution, such as saline, has to fill the needle and the needle then has to be in contact with the skin to aid the sound propagation. Another drawback is that the mounting of the transducers in the needle is challenging as Gehlbach (1992) described. A study done by Smith *et al.* (2011) showed that it is in fact possible to fabricate 10-5 micron ultrasound transducers that can both emit and detect ultrasound in

## 2. LITERATURE REVIEW

---

the range of 5 GHz to 30 GHz. The transducers however have to be excited by an external femtosecond laser.

The promising aspect of ultrasound technology is that it can be used not only to detect blood vessels, but also to determine the appropriate angle of penetration into the blood vessel. Once in the blood vessel the technology can further be used to guide the needle.

### 2.2.6 Electromagnetism

Electromagnetism is often used in the medical field to measure blood flow. Farady's law of electromagnetic induction is the basis for the measurement of blood flow. When a magnetic field is applied at a right angle to flow of a current carrying conductor, blood in this case, a voltage (or electromotive force) is generated in the blood (Teferra, 2012). The voltage induced is then measured by means of electrodes on either side of the applied magnetic field.

The magnetic field is usually applied by a probe placed around the blood vessel, as illustrated in Figure 2.9. An electromagnetic Dowel flow probe is a good example of a chronic blood flow measuring device. A blood vessel is placed through the circular hole of the probe (Figure 2.9(a)) and the flow is then measured. The technology can also be used acutely such as in the case of the Forceps flow meter (Figure 2.9(b)). The Forceps flow meter is primarily used to measure blood flow through the aorta (Moore and Zouridakis, 2004).

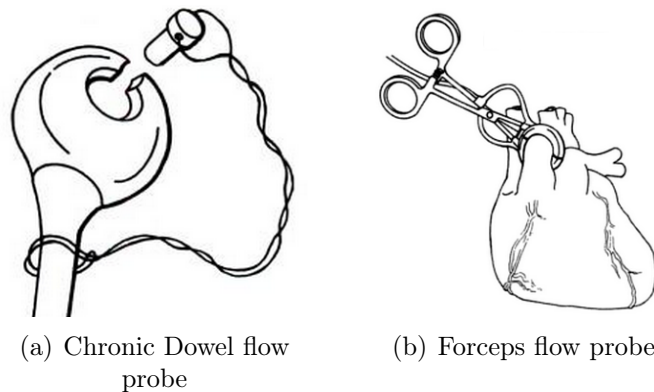


**Figure 2.9: Electromagnetic blood flow meters (Moore and Zouridakis, 2004)**

The technology can also be used noninvasively. A patent issued by Ogle (1999) proposed that if a magnetic field is generated parallel and perpendicular to the blood vessel, ECG electrodes can be used to detect the voltage generated

## 2. LITERATURE REVIEW

---

in the blood. Subsequently the flow rate of the blood can then be determined. This method does not appear regularly in the medical field however.

A variation of the electromagnetic technology is the Hall effect. When a magnetic field passes through the flow of current, such as in blood, the ions (or charges) separate, causing the one side of the conductor to be negatively charged and the other side positively charged. This charge separation creates a voltage known as the Hall voltage. In the case of blood vessels, the voltage can be measured on either side of the blood vessel perpendicular to the magnetic field.

In terms of measuring blood flow, electromagnetism shows promise. However, the drawback with this technology is that it requires a magnetic field perpendicular the blood vessel. The most practical manner in which this is done, requires that a probe be placed around the blood vessel. This procedure is highly invasive and the method of using ECG simply does not have enough literature support to prove that it actually works.

### 2.2.7 Laser

Laser light is amplified light of which the wavelengths are constant and the light waves have the same phase, i.e. the light waves are coherent (Siegman, 1986). There are various applications of lasers in the medical field to date in terms of detecting blood vessels and more specifically determining blood flow. In the medical field this technology is known as laser-Doppler flowmetry (LDF). Typically LDF meters make use of laser light in the range of 660 nm to 800 nm, which ranges from red to near infrared light. (Shepherd and Öberg, 1990).

LDF is used in different ways in the medical field. The first method is used to detect blood flow intravenously by means of a catheter. The catheter has a laser light emitter and a receiver. The light that is emitted from the catheter strikes moving blood cells and this results in a change of frequency of the light, known as a Doppler shift. The receiver detects the new frequency and this is used to determine the blood velocity. This method can also be used to determine the direction of blood flow. Blood that flows away from the sensor causes the wavelength to increase, known as red shift. Blue shift occurs when the blood flows towards the sensor. This technique does however require the light to strike the blood flow at a known angle, which does pose some problems.

Similarly LDF is used non-invasively to determine muscle perfusion. An emitter focuses laser light onto a region where capillaries are present and a receiver determines the Doppler shift. This technology has also been used in rats to measure cerebral cortical blood flow (Dirnagl *et al.*, 1989). Detecting subcutaneous blood vessels does, however, pose several challenges. Shepherd



## 2. LITERATURE REVIEW

---

and Öberg (1990) stated that the laser light signal with a wavelength of 800 nm has attenuated to 37 % incident light on the receiver at a depth of only 1.2 mm. The reliable depth of penetration is thus limited with this technology.

### 2.2.8 Thermal Methods

Thermal methods can be used to determine blood flow rates. Thermal flow meters work on the principle of heat transfer from a source to the surrounding fluid flow. The source is typically a resistance heating element. The source temperature is controlled by changing the electric current flow to the source. The electric current required to maintain a specific source temperature can be used to determine power output. Ultimately this can be used to determine the amount of heat transferred to the fluid, which is an indication of flow rate. Alternatively, a constant power can be used and the change in temperature can be used to calculate the flow rate.

In 1954 Fegler introduced one of the older thermal methods of measuring blood flow, known as thermodilution. Instead of determining the electric power used by a heating element, a cool fluid is injected into a blood vessel. A measurement of the temperature downstream of the injection is then used to determine heat transfer or thermal diffusion (Ganz and Swan, 1972). The drawback of this method is that it cannot be used continuously and only instantaneous measurements can be taken.

The method of using a heating element and controlling the power output to determine heat transfer can be used to determine either blood flow velocity or the mass flow rate of blood. Both methods work on the principle of heat transfer, however different methods of calculation are used. Nelson (1992) developed a probe that uses a heater and thermocouples to measure flow velocity in the aorta. Ambient temperature is measured upstream of the flow and the temperature is measured at the heating element. By knowing the power output of the element, heat transfer by convection is determined and used to determine flow velocity. Li *et al.* (2015) developed a similar device to measure cerebral blood flow. Micro resistance temperature sensors were etched near a heating pad. By raising the temperature of the heater to 2 °C above ambient temperature, the flow rate could be determined.

The flow velocity of blood is often not as important as the volume flow rate of blood. Blood flow velocity can be used to calculate volume flow rate by determining the cross sectional area of the blood vessel. This is often times not known and is only approximated. Determining the mass flow rate of blood works on the principle of conductive heat transfer rather than convective heat transfer. Refer to Figure 2.10 for a simplified concept that is especially used in industrial applications to measure fluid mass flow. A heating element is

## 2. LITERATURE REVIEW

---

placed within the fluid flow. Power is applied to the element and conductive heat transfer occurs. Downstream and upstream of the heater, there are two temperature sensors. The difference between the downstream and upstream temperatures can be used to determine mass flow rate if the heating cross sectional area is known. This method requires a lot of power, especially in liquid flow. When the upstream sensors starts to measure ambient temperature, the heat from the element no longer reaches the sensor. This results in inaccurate readings.

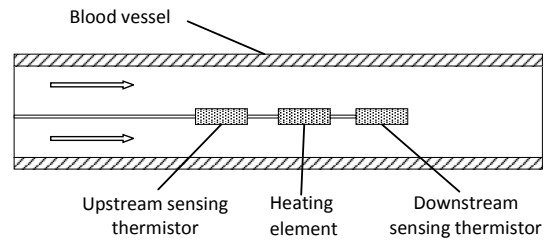


**Figure 2.10: Thermal mass flow meter concept**

## 3. Preliminary Technology Investigation and Theoretical Background

This chapter briefly covers the theoretical background of the technologies that are chosen for the design phase. Some basic simulations and analytical models are also included in this preliminary investigation to further demonstrate the principles upon which these technologies work. Appendix A briefly describes technology that were also considered.

### 3.1 Near-Infrared

In this thesis, near infrared (NIR) light is used as a means to locate blood vessels. As mentioned in the literature review, NIR light responds differently to various tissue types. Blood, for example, contains haemoglobin that absorbs NIR light, whereas skin and fat reflects the light. An example of this is shown in Figure 3.1. In this photo, NIR light is projected onto skin. A NoIR (no infrared filter) raspberry pi camera is used to capture the image. It is clear that skin reflects a large amount of the light, whereas the blood vessels absorb the light. The blood vessel can be identified by the darker lines on skin. The response of NIR light in the presence of various tissue types thus serves as a basis for locating blood vessels.

There are several properties, that differ between tissue types, and this influences how photons travel through the tissue. Among these optical properties are the scatter coefficient ( $\mu_s$ ), absorption coefficient ( $\mu_a$ ) and the tissue anisotropy ( $g$ ). The scatter coefficient is a measure of the number of particles that cause a photon to scatter in a different direction. Similarly the absorption coefficient refers to the number of chromophores that can absorb the photons. Lastly the tissue anisotropy describes the forward motion of the photon after a scattering particle has been struck.

### 3. PRELIMINARY TECHNOLOGY INVESTIGATION AND THEORETICAL BACKGROUND

---

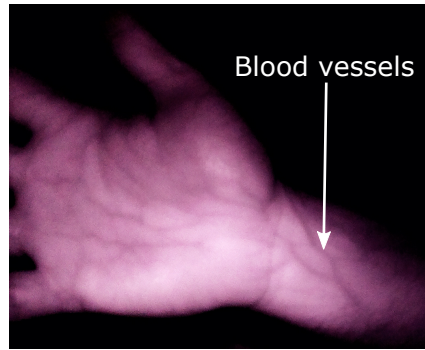


**Figure 3.1: Reaction of NIR light on skin with subcutaneous blood vessels**

These variables describe the optical properties of the tissue. By knowing the approximate values of these variables for different tissue types, the photon paths can be roughly estimated by means of a Monte Carlo simulation. Monte Carlo simulation software, written by Prof Jacques from the Oregon Health and Science University, provides good visual information regarding the propagation of photons throughout various tissue types. The software allows for customisation, specifically for the tissue types used and their properties, along with the wavelength of the light used. The results are displayed in terms of relative fluence. This is a measure of the number of photons incident at specific unit volumes during the simulation. Figure 3.2 displays the difference in absorption of 880 nm light passing through epidermis into muscle (left image) and into blood (right image). Clearly more light is absorbed by the blood. Furthermore, Figure 3.3 shows how light is absorbed in the presence of a blood vessel.

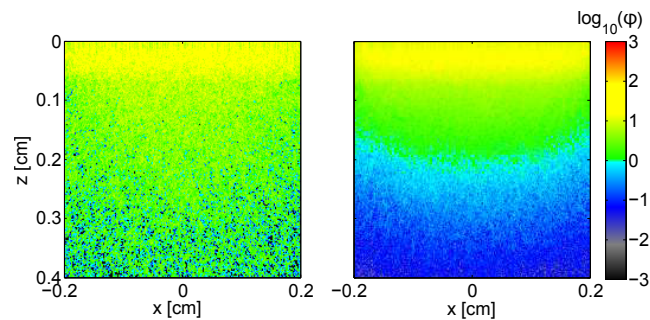


**Figure 3.2: Relative fluence rate of muscle (left) and blood (right) in the presence of 880 nm light.**

### 3. PRELIMINARY TECHNOLOGY INVESTIGATION AND THEORETICAL BACKGROUND

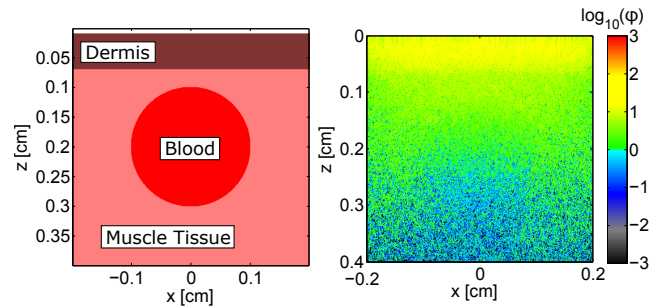


**Figure 3.3: Monte Carlo simulation for a subcutaneous blood vessel in 880 nm light.**

The aforementioned information provide reasonably good evidence as to why NIR light is a good method to locate blood vessels. Figure 3.4 shows the response of NIR light being transmitted via optic fibres when firmly placed on the surface of porcine fat and then moved to the muscle tissue. While this does not indicate whether a blood vessel can be located by means of NIR light, it does show that the method is capable of detecting differences between fat and muscle. This further confirms the viability of NIR methods to detect blood vessels.

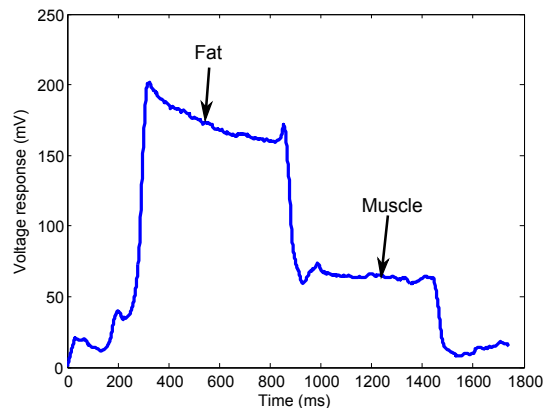


**Figure 3.4: Preliminary test on NIR light response in fat and muscle**

## 3.2 Impedance

The differences in the electric impedance of various tissue types are used to distinguish between which tissue type the probe is currently in. This allows one to know when a blood vessel is penetrated. In this thesis the probe is

### 3. PRELIMINARY TECHNOLOGY INVESTIGATION AND THEORETICAL BACKGROUND

---

in the form of a needle. To provide more background as to how this works, consider the model in Figure 3.5(a) from Giannoukos and Min (2014). The model is known as the Fricke-Morse model and represents the impedance of biological tissue, where  $R_i$  is the intracellular resistance,  $R_e$  the extracellular resistance and  $C$  the membrane capacitance of the cells. The impedance of the model is described by Equation 3.1, where  $\omega$  is the frequency in radians. A highly simplified version of this model is shown in Figure 3.5(b), where  $R$  is a lumped version of the tissue resistance. Impedance is then represented by Equation 3.2.

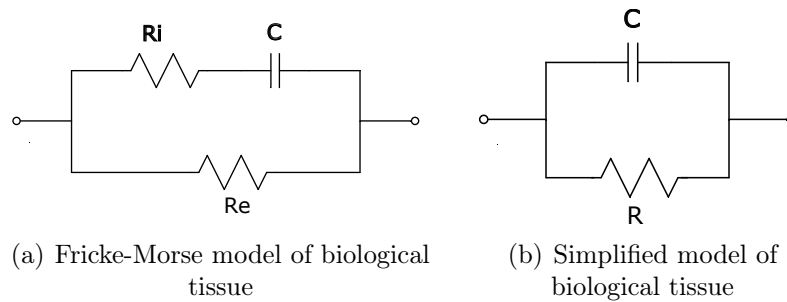


**Figure 3.5: Basic biological tissue impedance models**

$$Z = \frac{R_e(1 + jR_iC\omega)}{1 + jC\omega(R_i + R_e)} \quad (3.1)$$

$$Z = \frac{R}{1 + jCR\omega} \quad (3.2)$$

This is a highly simplified model of biological tissue and does not taken into account dispersion and relaxation of tissue at certain frequencies. Also electrode polarization does not form part of this model. There are other equations, such as the Cole equation, that can be empirically determined to provide more accurate results. In terms of basic principles, the model from Figure 3.5(b) will suffice.

Impedance of different tissue types can roughly be compared by means of the aforementioned model. The capacitive and resistive properties of tissues used in this model also change with frequency. Thus, to properly distinguish between tissue types, signals at appropriate frequencies must be used when determining tissue impedances. Andreuccetti *et al.* (1996) has developed an internet resource that calculates the conductance ( $\sigma$ ) and relative permittivity ( $k$ ) of various tissues at specific frequencies. These values correspond to that obtained by Gabriel *et al.* (1996). By using the respective conductance and relative permittivity the tissue resistance and capacitance can be determined by Equation 3.3 and Equation 3.4 respectively.  $A$  represents the cross sectional area between electrodes,  $l$  the distance between electrodes and  $\epsilon_0$  as constant of  $8.854 \times 10^{-12}$  F/m.

### 3. PRELIMINARY TECHNOLOGY INVESTIGATION AND THEORETICAL BACKGROUND

---

$$R = \frac{l}{A\sigma} \quad (3.3)$$

$$C = \frac{k\epsilon_0 A}{l} \quad (3.4)$$

Table 3.1 summarises the approximate impedance magnitudes and phase angles of blood, muscle and fat. This is based on the simplified model described by Equation 3.2. It should be noted that the results displayed here are not expected to be the same during actual testing as a large number of assumption are made in the simplified model. The results do however indicate very noticeable differences between tissue types that indicates that electrical impedance can be used to distinguish between tissue types.

**Table 3.1: Biological tissue impedance approximation**

Tissue	Conductance, $\sigma$ (S/m)	Relative Permittivity, $k$	Impedance magnitude ( $\Omega$ )	Phase Angle (Degrees)
Blood	0.70031	5224.2	$1.428 \times 10^2$	-0.713
Muscle	0.34754	12468	$2.872 \times 10^2$	-3.426
Fat	0.024121	290.93	$4.145 \times 10^3$	-1.153

### 3.3 Thermal Method

The literature review briefly mentions how the thermal method can be used to determine the flow rate. The thermal mass flow meter, based on thermal conduction, makes use of a flow area of known diameter with a heater and upstream and downstream temperature sensors. This method requires complex manufacturing methods and typically is not used in liquid flow, due to the high temperature requirements. In this thesis, primarily convective heat transfer principles are used, although conductive and radiation heat transfer do also play a role. Constant power is applied to a heating element. This causes the temperature at the heater to rise. When a fluid flows over it, heat is carried away by convection and the temperature drops. This drop in temperature can be related to flow velocity, and if the vessel diameter is known, as well as the blood density, mass flow rate can be calculated. A major advantage of this method, compared to the traditional thermodilution method, is that the flow rate can be continuously be measured and not only instantaneously.

Pure convective heat transfer principles clearly show that a temperature drop can be expected when a heater is exposed to fluid flow. Consider Equa-

### 3. PRELIMINARY TECHNOLOGY INVESTIGATION AND THEORETICAL BACKGROUND

---

tion 3.5. This equation predicts how much power in the form of heat will be carried away from a heated object.

$$Q = hA(T_s - T_\infty) \quad (3.5)$$

$Q$  is the power dissipated,  $h$  the thermal convection coefficient,  $A$  the surface area of the object,  $T_s$  the surface temperature and  $T_\infty$  the ambient temperature. The convection coefficient  $h$  is a function of the Nusselt number ( $Nu$ ), the thermal conductivity of the fluid ( $k$ ) and the effective diameter of the object ( $D$ ), which is geometry dependent. This is shown Equation 3.6

$$h = \frac{kNu}{D} \quad (3.6)$$

The Nusselt number is highly dependent on the specific chosen geometry and is furthermore a function of the Prandtl number (dimensionless parameter based on fluid characteristics) and the Reynolds number. The Reynolds number ( $Re$ ) is a function of the fluid velocity ( $v$ ), the kinematic viscosity ( $\nu_k$ ) and the effective diameter ( $D$ ) which is again geometry dependent. The Reynolds number can be used to determine whether a flow is turbulent or laminar and is given by Equation 3.7

$$Re = \frac{vD}{\nu_k} \quad (3.7)$$

By using these equations and parameters an estimation of the flow velocity can be made. The drop in surface temperature, based only on thermal convection, can be seen in Figure 3.6 for a sphere, cylinder and flat plate. The fluid used is 38 °C blood and the heater is set at 200 mW. For the sake of simplicity, the assumption is made that blood acts as a Newtonian fluid, which will not be the case in practice. The simulation does however still indicate that there is a considerable drop in temperature when exposed to fluid flow.

This concept is further illustrated by means of a basic CFD simulation performed on Autodesk CFD 2016, as illustrated in Figure 3.7. A heater, in the shape of a typical thermistor, is exposed to blood flow in a tube. The image to the left is the response of the heater in a low fluid flow rate, whereas the right side is of a higher flow rate. Arrows indicate the direction of the flow. It is clear that more heat is carried away in higher flow rates, as is expected.



### 3. PRELIMINARY TECHNOLOGY INVESTIGATION AND THEORETICAL BACKGROUND

---

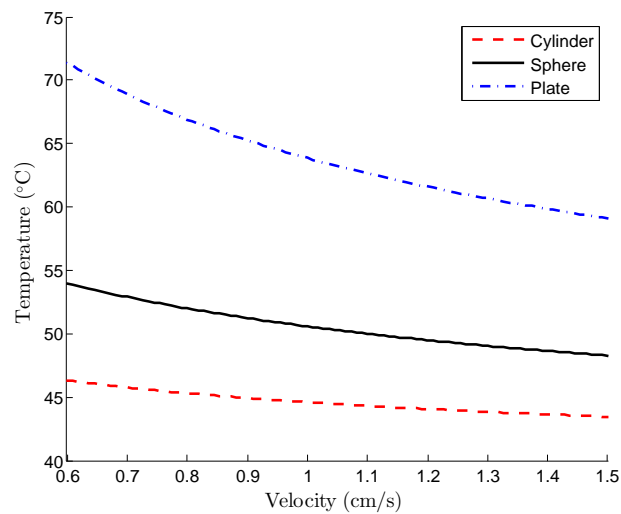


**Figure 3.6:** Surface temperature response of heaters at different blood flow velocities

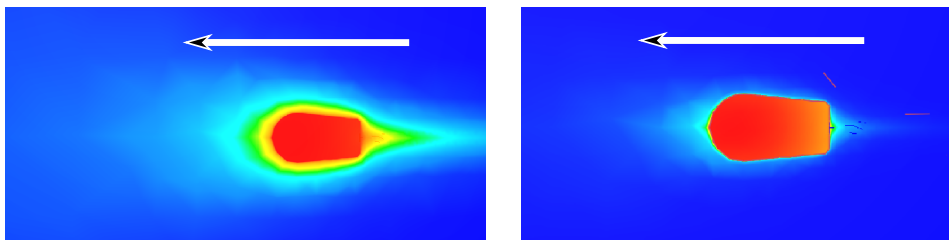


**Figure 3.7:** Visual CFD response of thermistor heater in different blood mass flow rates

## 4. Design of Devices

This chapter describes the physical and electronic design of the devices that are developed to detect blood vessel location, detect blood vessel penetration as well as measure blood flow rate. The full circuits of each device can be seen in Appendix B.

### 4.1 Near-Infrared Blood Vessel Location Detection

Based on the preliminary technology validation (Section 3), near-infrared (NIR) is the most feasible method to use to locate blood vessels.

#### 4.1.1 Physical Design

NIR light attenuates as it penetrates different tissue types. Since the device is intended to be used to locate blood vessels near the tip of the needle, the light source is required to be near the needle tip. The most practical way to accomplish this is by means of optic fibre. In this way, the light is channelled from the original light source (an LED) to the tip of the needle. Reflected light is then channelled back via another strand of optic fibre, towards a phototransistor. The optic fibre approximately acts as a point source and this implies that the phototransistor will receive most of its light from the direction in which the device is pointing. This allows for the locating of blood vessels (see Section 3 for theory explanation). Compared to the VeinViewer<sup>®</sup>, this device is designed to be capable of detecting blood vessels at any depth as opposed to only blood vessels near the surface of the skin.

The device developed in this thesis works with an SFH 4585 IR LED as the source of light. The IR receiver is a QSE114 phototransistor. The LED emits light with wavelengths between 775 nm and 1000 nm, however, the peak intensity occurs at 880 nm. Similarly the peak sensitivity of the phototransistor is 880 nm. A 1 mm diameter hole is drilled in the tip of the LED. This serves

#### 4. DESIGN OF DEVICES

---

as an attachment point for the optic fibre. The optic fibre has a diameter of 500 microns and is held in place by means of a connector and clear epoxy. Care is taken to ensure that the epoxy does not touch the tip of the optic fibre. This ensures that good contact is made and that a maximal amount of light is transmitted to the tip of the needle. The optic fibre is placed inside a 16 gauge needle (outer diameter of 1.65 mm). Another optic fibre is also placed inside the needle that receives reflected light and transmits it to the phototransistor. A connector and epoxy secure the tip of the optic fibre to the phototransistor. Figure 4.1 illustrates the layout of the design. The housing is 3D-printed and made of ABS. A detailed schematic can be found in Appendix C.

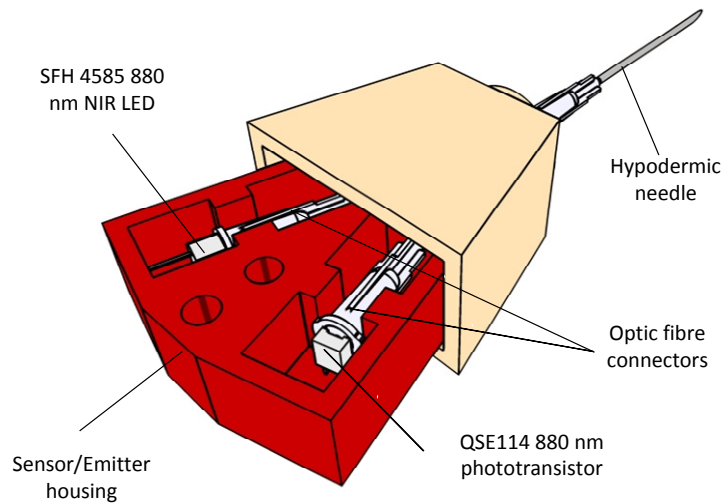


**Figure 4.1: NIR prototype setup**

In terms of the physical design of this prototype, there are several points to be considered:

**Optic fibre cutting** The manner in which the optic fibre is cut affects the surface finish of the fibre. This can cause the light to disperse in various directions and may also reduce the surface area for light to be transmitted or received. In this thesis a ceramic wafer is used to slightly cut the surface of the optic fibre to weaken it. The fibre is then lightly tapped near the cut, causing it to have a smooth fracture. Usually there is a part that does not fracture properly (Figure 4.2(a)) and 1200 grit sanding paper is used to remove this edge. The result is a slightly rough finish as shown in Figure 4.2(b). Despite the rough surface, light is still transmitted sufficiently.

**Relative movement of optic fibre** There is always some internal reflection of NIR light. When NIR strikes the tip of the optic fibre some of that light

#### 4. DESIGN OF DEVICES

---

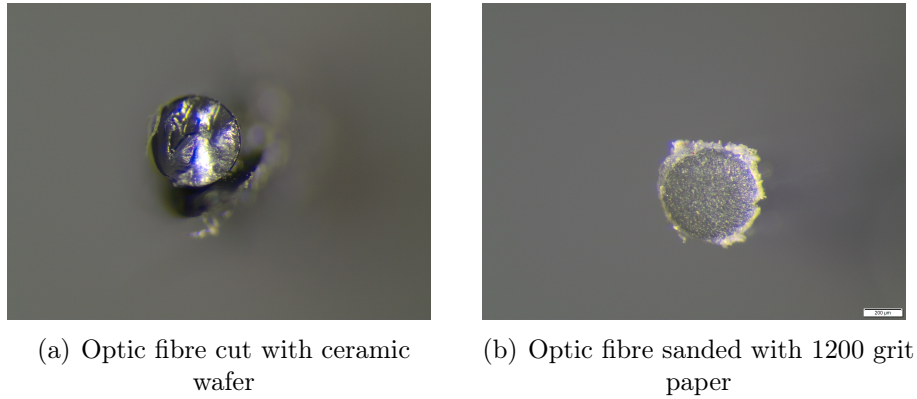


**Figure 4.2: Optic fibre preparation (Photo: T. van der Merwe)**

can be reflected into the adjacent optic fibre which affects the reading. This is not a problem if the two optic fibres are fixed relative to one another. Relative change to external observed light will not be affected by internal reflected light as the internal light remains constant. In this design, the optic fibres are held together with epoxy. This ensures that no relative motion occurs.

**Protruding of optic fibre outside of the needle** Care is taken to ensure that the optic fibre does not protrude outside of the bevel of the needle as shown in Figure 4.3. The reason for this is to ensure that when penetrating tissue, the needle bevel will carry all the load and the optic fibre will not break or bend.

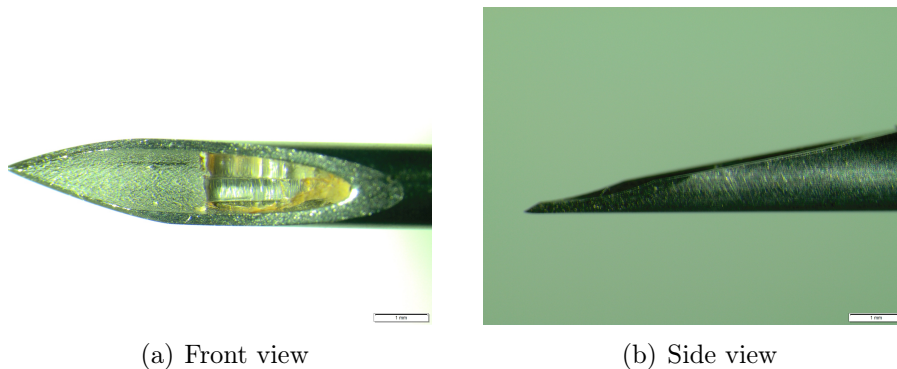


**Figure 4.3: Needle with inserted optic fibre (Photo: T. van der Merwe)**

**Separation of internal and external light sources** The phototransistor is completely isolated from direct and indirect external light. It is also sep-

## 4. DESIGN OF DEVICES

---

arated from the internal LED. Any interference of light, other than that of the optic fibre, creates another variable that influences the results and must be avoided.

### 4.1.2 Electronic Design

The main components of importance in the circuit are the SFH 4585 LED and the QSE114 phototransistor and are shown in Figure 4.4. The LED is powered by 5 V from a micro controller. The LED consumes around 80 mA of current and has a forward voltage of 1.5 V.

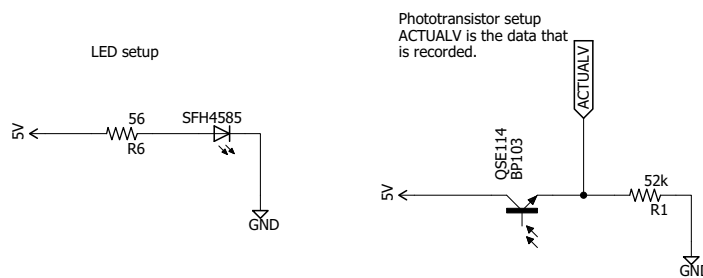


**Figure 4.4: NIR LED and phototransistor setup**

The phototransistor is the important part, as all the data are gathered from this sensor. The sensor is logarithmically linear for low light intensity and high light intensity. Since there is a large amount of attenuation of NIR light in the optic fibre, the phototransistor functions in the low linear region only. The phototransistor is used in a similar fashion as a voltage divider. Current is generated when light strikes the phototransistor and flows through a 56 k $\Omega$  resistor to ground. The voltage over the resistor is the signal that is used to determine the light intensity.

The voltage over the aforementioned resistor serves as the first input to an AD620 instrumentation amplifier. This amplifier amplifies the difference between two voltages. The second input is provided by a potentiometer. The potentiometer is set near the baseline response of the phototransistor so any change can be easily observed. If the second input voltage differs too much from the first input, clipping of the data would occur when amplified. The circuit developed in this thesis provides an option for a manual analog 10 turn 10 k $\Omega$  potentiometer or a 10 k $\Omega$  digital potentiometer. This can be seen in Figure 4.5.

For the purpose of data acquisition the manual potentiometer is used in this thesis as it remains constant. In the testing environment, the ambient light remains constant and the optic fibre tips are cleaned regularly to obtain

## 4. DESIGN OF DEVICES

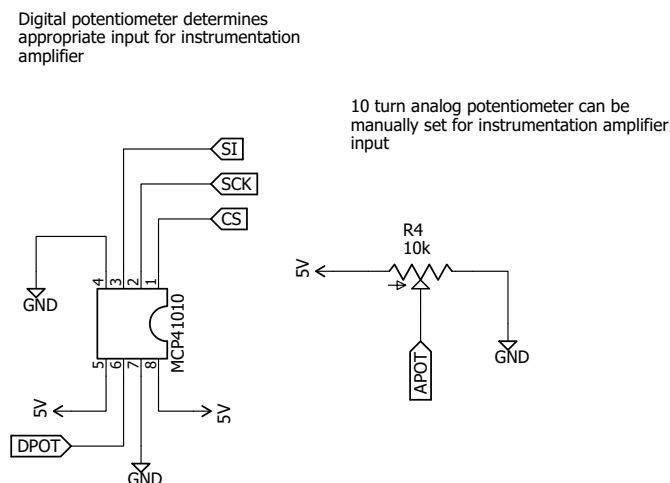


**Figure 4.5: NIR circuit potentiometers**

data with the least amount of variables. In a practical setting this is not always the case. Ambient light may differ in certain environments and also the optic fibre tips may accumulate different tissue types as it penetrates a patient's body. The purpose of the digital potentiometer is for self-calibration. A microcontroller (the Atmega328 in this case) communicates with an MCP41010 digital potentiometer with SPI communication protocol. The microcontroller runs through a range of resistances until the output of the instrumentation amplifier is in a suitable range. This allows for the use of the NIR device in various environments, without the need of constantly cleaning the optic fibre.

The AD620 amplifies the difference between the two input signals. Refer to Figure 4.6(a). The gain in this circuit is set to approximately 50.4. The output of the AD620 passes through a low pass filter with a cut-off frequency of 132 Hz to remove any unnecessary noise. The signal then passes through a buffer in the form of a LM324 opamp. This creates a low impedance to input in to the data acquisition hardware.

The AD620 encounters problems with amplification at lower voltages if it is run in single supply. In this circuit it is thus run in dual supply, where a negative 5 V is obtained from the MAX660 voltage pump (Figure 4.6(b)). Furthermore the AD620 supply pins are accompanied by 1 nF decoupling capacitors.

The Atmega328 is only used for the digital potentiometer. For testing purposes a USB-6009 National Instruments DAQ is used along with the analog potentiometer because a dynamic potentiometer adds an unwanted variable to the testing. The relatively basic electronic design, along with minimal components gives this design great potential to be very compact. This is especially true when compared to other methods as described in Section 2.

## 4. DESIGN OF DEVICES

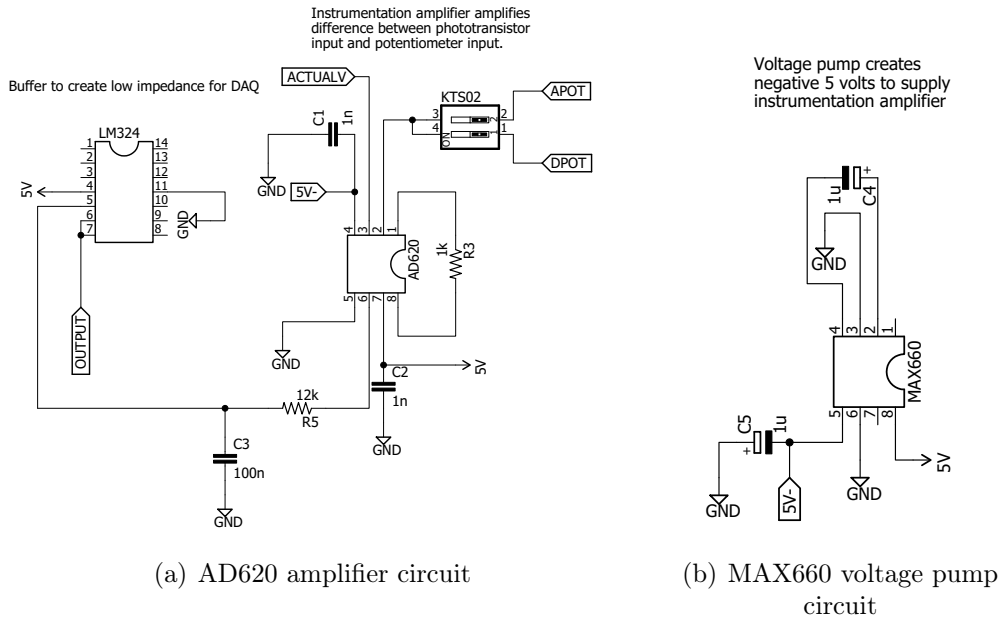


Figure 4.6: NIR device amplifier circuit

## 4.2 Impedance Blood Vessel Penetration Detection

Based on the preliminary technology validation (Section 3), electrical impedance is the most feasible method to use to determine penetration of blood vessel.

### 4.2.1 Physical Design

There are several ways to place electrodes to determine the electrical impedance of tissue. Section 2.2.1 describes the use of two, three and four electrode methods. While the four electrode method is typically used for determining bio-impedance, the most practical method for a hypodermic needle is the two electrode method. While the four electrode method is slightly more accurate, the two electrode method will suffice as discriminating between tissues does not require maximal accuracy.

The two electrodes may be placed in any manner with the condition that the electrodes not make contact with one another. The design used in this thesis uses the stainless steel needle as the one electrode and an additional conductive pin placed within the needle. This can be seen in Figure 4.7. The pin is separated from the surrounding electrode by means of an epoxy. The physical aspect of this sensor is relatively simple and easy to manufacture. As a design note, avoid using electrodes with exposed copper. Blood will cause

#### 4. DESIGN OF DEVICES

the copper electrodes to break down over time, which will result in inconsistent results and eventual failure of the device.

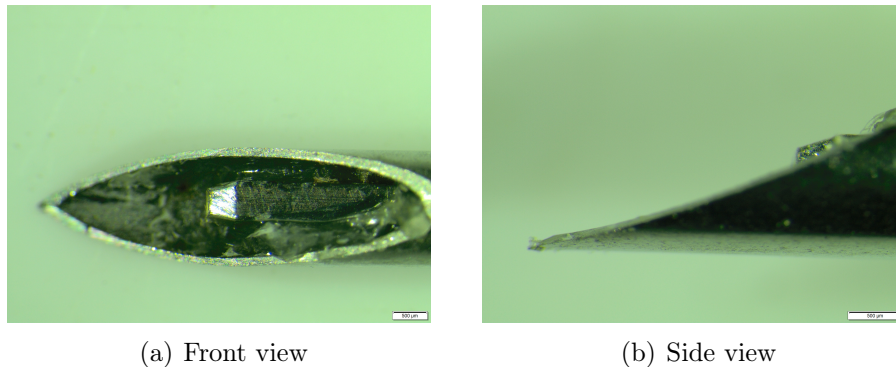


**Figure 4.7:** Needle with inserted electrode (Photo: T. van der Merwe)

#### 4.2.2 Electrical Design

The electrical design of this device is based around an IC known as the AD5934 impedance converter. The operation and communication of the AD5934 are discussed in more detail in Section 4.2.3. There are a range of sections of the circuit that are required to properly use the AD5934. Figure 4.8 displays how the AD5934 is connected to the rest of the circuit, each label being explained throughout this section.

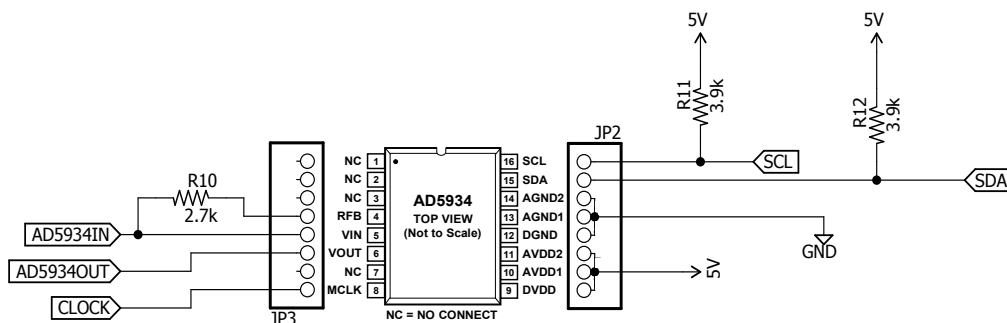


**Figure 4.8:** AD5934 impedance converter connection

Pins 9 to 11 are all connected to a common voltage source. In this case it is a 5 V voltage source provided by an Arduino microcontroller. Pins 12 to 14 are all connected to a common ground. The AD5934 communicates with the



#### 4. DESIGN OF DEVICES

Arduino by means of I<sup>2</sup>C protocol. Pins 15 and 16 are the data and clock lines respectively and are needed for I<sup>2</sup>C communication. These pins are pulled high with 3.9 k $\Omega$  resistors (more information in Section 4.2.3). Pin 8 is a input pin for an external clock. The more expensive AD5933 has an internal clock. For the AD5934 an external clock is necessary. The direct digital synthesizer in the AD5934 makes use of a clock signal, 16.000 MHz in this case, to accurately generate its signals. An MEC MO-12B crystal oscillator is used as a clock for the AD5934. Pin 6 is the voltage frequency signal output pin that is used to determine the impedance over the needle electrodes. The user specifies a frequency range and the amplitude for the signal. A corresponding voltage signal is then generated at pin 6 and oscillates around mid supply voltage (2.5 V in this case).

There are however several considerations to take into account regarding the signal for bio-impedance tests. Section 2.2.1 provides some background regarding the use of a voltage source and a current source. The device developed in this thesis makes use of a voltage controlled current source. This implies that the voltage signal generated at pin 6 is converted into a current signal. When the current signal passes through tissue, the device will record the return voltage signal. Figure 4.9 illustrates how the signal travels from the AD5934 output pin to the input pin. It is discussed step by step below with the signal simulation displayed in Figure 4.10:

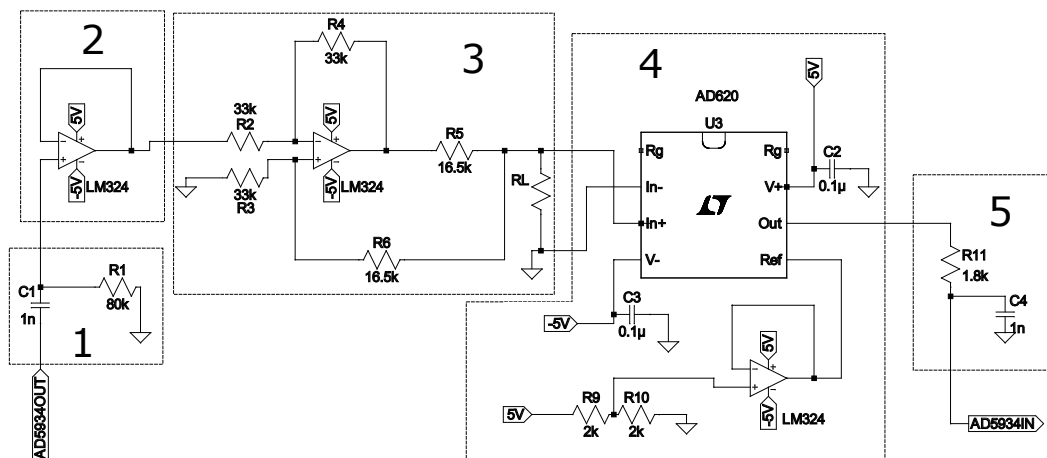


**Figure 4.9: Impedance signal circuit**

1. Bioimpedance measurement requires that the signal be alternating current (AC) centred around zero. Since the AD5934 outputs a signal that oscillates around 2.5 V, the DC offset of the signal is first removed before being converted to a current signal. The voltage signal passes through

## 4. DESIGN OF DEVICES

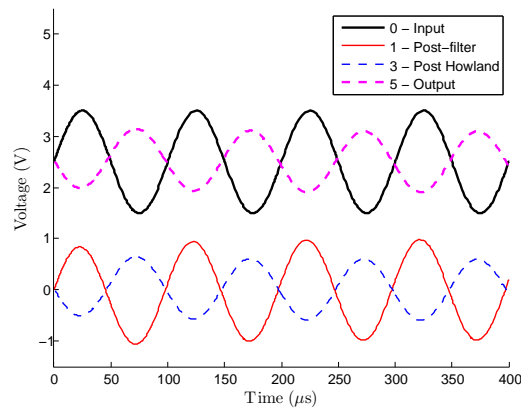


**Figure 4.10: Impedance signals at 10 kHz with a 10 k $\Omega$  load**

a high pass filter with a cut-off frequency of 1989 Hz. This completely removes the DC offset.

2. The signal then passes through a buffer in the form of a LM324 opamp to provide a low impedance prior to entering the voltage controlled current source.
3. There are several methods that can be used to make a controlled current source, however, the enhanced Howland current source has been shown to perform reliably between 100 Hz to 100 kHz (Islam *et al.* (2013) ; Cheng *et al.* (2006)). The load current obtained from the Howland current source is described by Equation 4.1.

$$I_L = -\frac{V_i R_4}{R_5 R_2} \quad (4.1)$$

Where  $V_i$  is the voltage from phase 2. Note that the current is negative for positive input voltages. This causes the load voltage to be inverted, relative to the input voltage. The load current is not dependent on the load resistance. Cheng *et al.* (2006) states that the ideal impedance for this circuit is obtained when Equation 4.2 is true.

$$R_4 R_3 = R_2 (R_5 + R_6) \quad (4.2)$$

4. The signal then enters the AD620 differential amplifier. The difference between the load voltage and ground is then measured. Note that even if there is no load, a signal will still enter the amplifier. This is a disadvantage of the two electrode method, but in the presence of a n impedance load, relative changes are still detected. The reference pin is given mid-supply voltage (2.5 V), which gives the signal a DC offset back to the original position of the input signal.

## 4. DESIGN OF DEVICES

---

- Prior to the final signal entering the AD5934, it passes through a last low pass filter with a cut-off frequency of 88419 Hz. This is to remove most of the noise from the signal.

The final signal reaches pin 5 of the AD5934, where it passes through an internal opamp. The amplification is set with a resistor connected between pin 5 and pin 4.

All of the amplifiers in this circuit are powered in dual supply (i.e. +5 V and -5 V). This is accomplished by means of the MAX660 charge pump. A schematic is shown in Figure 4.6(b).

### 4.2.3 AD5934 Communication and Sequencing

The AD5934 is an affordable, 12-bit impedance converter. It has a signal generator that can perform frequency sweeps and records signals from analog to digital at 250 kilo samples per second. An on-board digital signal processing engine performs discrete Fourier transforms on the digital signal, allowing one to obtain both the real and imaginary parts of the impedance.

Generating a signal and interpreting the results with the AD5934 requires that the communication be executed in the correct sequence as specified by the manufacturers (see Appendix D for flow chart). I<sup>2</sup>C communication protocol is used to write values to specific registers within the AD5934. The information in these registers is used to perform the frequency sweeps as the user specifies. The Arduino is chosen for this communication because of its available libraries that greatly simplify the I<sup>2</sup>C communication. The manner in which the device is used in this thesis is discussed below:

- Prior to the start of the sweep, the start frequency, frequency increment and the total number of steps are set. Both the start frequency and the frequency increment are recorded over three registers each. This results in 24-bit (3 byte) representation of the frequency. The hexadecimal code is determined by the Equation 4.3.

$$Frequency\ code = \left( \frac{Desired\ frequency}{\left( \frac{Clock\ Frequency}{16} \right)} \right) \times 2^{27} \quad (4.3)$$

The number of increments is represented by 9 bits allowing for a total number of 511 steps. The values used for data acquisition are displayed in Table 4.1.

## 4. DESIGN OF DEVICES

Table 4.1: AD5934 initial parameters for data acquisition

Parameter	Register Addresses	Hexadecimal Code	Value
Start Frequency	0x82 ; 0x83 ; 0x84	0x0A3D70	5 kHz
Frequency Increment	0x85 ; 0x86 ; 0x87	0x005C46	175 Hz
Number of Steps	0x88 ; 0x89	0x01FF	511

The values in Table 4.1 are for the purposes of data acquisition, to obtain the impedance of tissue types over a range of frequencies. In the practical usage of the device a frequency region will be chosen where the impedance differences between muscle, blood and fat are the greatest (near 30 kHz according to literature). The sweep will occur within a few hertz of that frequency. This way, the user will easily be able to detect when a blood vessel is penetrated.

2. The start frequency is initialised in this step by writing 0x11 to address 0x80 in the control register. Some high impedance systems require that the frequency signal be active for a short period of time, however this is not important for the purposes of the bioimpedance being tested in this thesis. This step must however be included to properly use the AD5934.
3. The frequency sweep is now started by writing 0x21 again to address 0x80. The first frequency is now being generated.
4. During this phase, the Arduino constantly checks the 0x8F register of the AD5934. This register indicates whether valid real and imaginary data have been gathered. This is indicated by a binary 0000 0010 in register 0x8F. If no valid data has been gathered yet, the frequency remains unchanged.
5. As soon as valid data is obtained, it is recorded and the device continues to the next frequency. This is done by writing 0x31 to register address 0x80.
6. The previous two steps are repeated until the Arduino reads the binary code 0000 0100 from register 0x8F. This indicates that the sweep is complete. For the purpose of controlled data acquisition this process is repeated by manually resetting the Arduino to repeat all the previous steps. In practice however, the Arduino would simply restart the process automatically, to continuously provide impedance information to the user.

## 4. DESIGN OF DEVICES

---

Once all the real ( $R$ ) and imaginary ( $X$ ) data have been gathered the impedance magnitudes ( $|Z|$ ) and phase angles ( $\theta$ ) at a given frequency can be determined by means of Equation 4.4 and Equation 4.5 respectively.

$$|Z| = \sqrt{R^2 + X^2} \quad (4.4)$$

$$\theta = \tan^{-1} \left( \frac{X}{R} \right) \quad (4.5)$$

### 4.3 Thermal Method Blood Flow Measurement

Based on the preliminary technology validation (Section 3), thermal convection is the most feasible method to use to determine flow rate within blood vessels. This method can easily be scaled with the correct manufacturing methods and contains no moving parts. Also, since this method requires the probe to be inside a blood vessel, it is considerably less invasive than for example the electromagnetic flow probes (Figure 2.9) which must be placed around a blood vessel.

#### 4.3.1 Design

There are several methods in which the laws of thermal convection and conduction can be used to determine the flow rate of a fluid. A more detailed explanation of the method used in this thesis is given in Section 3. This method makes use of an ambient temperature sensor and a temperature sensor situated within a coiled heater. This design makes use of thermal convection to determine flow rate. An overall layout of the device is shown in Figure 4.11.

The temperature sensors are Epcos G540 ultra-miniature NTC thermistors. While the 0.8 mm diameter thermistor is too large to properly place into small blood vessels, it is small enough to conceptually test in tubes as shown in Section 5. This device is only conceptually tested in this thesis, and future work would include miniaturising it to use *in vivo*.

Typically in thermal air flow measurement devices, the thermistor also acts as a heater. This is generally possible as the power required to raise the temperature of the thermistor to a usable temperature will not damage the thermistor. However, this is different in the case of liquid fluid flow since the thermal convection becomes considerably higher and more power is required. Custom platinum etched thermistors can be used in this way, but become

## 4. DESIGN OF DEVICES

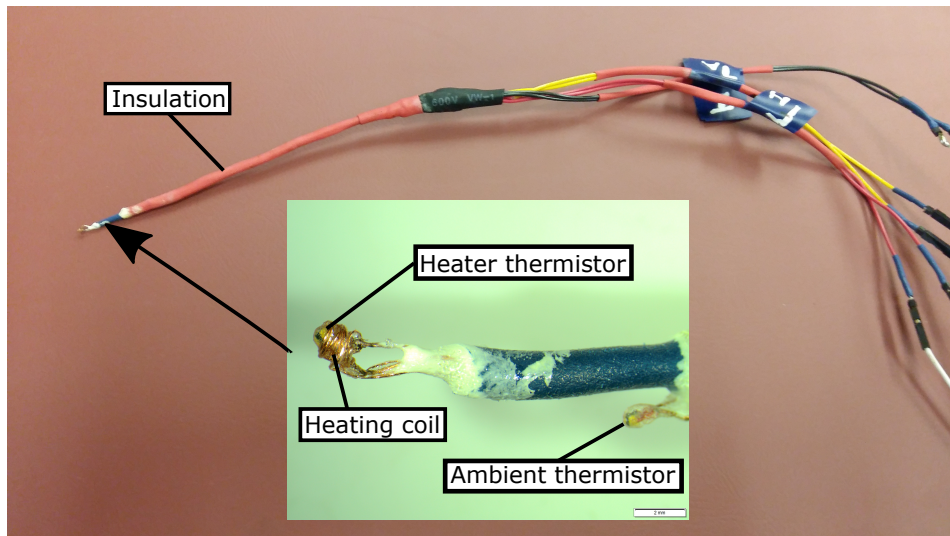


**Figure 4.11: Flow meter layout**

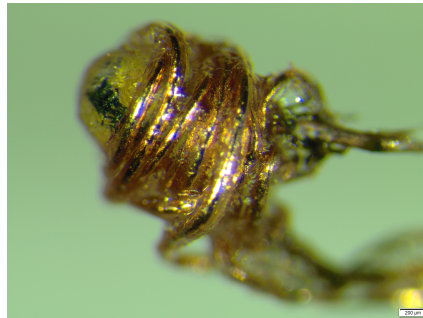


**Figure 4.12: Thermistor wrapped in heating coil**

expensive and complex to manufacture. For this reason, the one Epcos G540 thermistor is wrapped in a heating coil as shown in Figure 4.12.

The heating coil produces heat independently of the thermistor. To avoid any self heating of the thermistor, a  $30\text{ k}\Omega$  thermistor is chosen as a large voltage would be required for the unwanted effect of self heating. Also a large voltage (approximately  $42\text{ V}$ ) would be required to exceed the  $18\text{ mW}$  maximum power limit. Note that in Figure 4.12 there is a thin layer of epoxy insulation over the heating coil and the lead wires of the thermistor. This is to ensure that the copper never comes into contact with the blood, as blood will erode the copper.

There are several materials that were considered for use as the heating element. Some of the materials considered are listed in Table 4.2 (values obtained from Turner (2013)). These are average values and provide a basis for selection.

## 4. DESIGN OF DEVICES

**Table 4.2: Materials considered for heating element**

Material	Resistivity - $\rho$ ( $\Omega m$ ) $\times 10^{-8}$	Temperature coefficient of resistance ( $K^{-1}$ )
Copper	1.77	0.0068
Platinum	10.58	0.003
Titanium	88	0.046
Tungsten	5.5	0.0045
Nichrome	112	0.00017

This device makes use of a constant power supply to the heater as opposed to a constant temperature heater. For this reason it is important to use a material of which the resistance does not change over a temperature range. Titanium is thus excluded from the selection, albeit a good choice for a constant temperature heater. Platinum heaters are typically etched and platinum wire is extremely cost inefficient. Tungsten wire is too brittle for this application. Nichrome has a good resistivity and temperature coefficient of resistance, however the wire is mostly supplied in diameters of 500  $\mu m$  and larger, which is too large for this device.

From the aforementioned, copper is chosen as the heater material. The copper wire that is used is 200  $\mu m$  in diameter and is insulated and will thus not be eroded by blood. The resistance of the wire heater is measured to be 1.4  $\Omega$ .

### 4.3.2 Electronic Design

There are two parts in the electrical design that function independently. The first part is the heating circuit, which includes a power monitor. The second circuit is the two thermistor circuit. These are discussed below.

The heating circuit is relatively simple especially since it makes use of a constant power. Constant power is easy to maintain as the heater resistance remains constant as well as the voltage from the power supply. Figure 4.13 illustrates the layout of the heater circuit. A variable voltage source supplies power to the heater circuit. Current flows through a shunt resistor of 0.1  $\Omega$  with 1 % precision. The current then flows through the heater to ground. A flyback diode is inserted as a safety measure, to ensure that possible coil inductance in the heater does not cause a harmful reverse current.

The shunt resistor in Figure 4.13 forms part of the INA219B current sensor. As current flows through the shunt resistor, a voltage drop occurs over the

## 4. DESIGN OF DEVICES

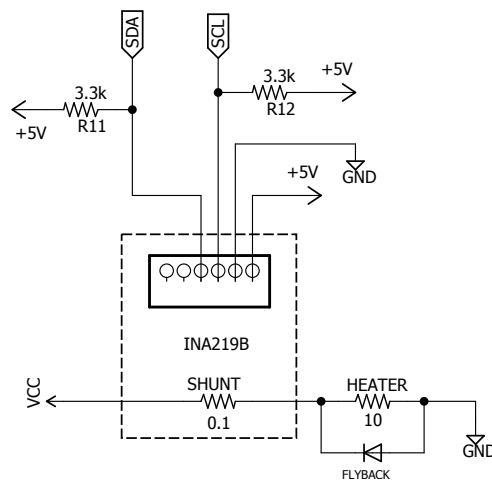


**Figure 4.13: Heater circuit**

resistor in accordance with Ohm's law. The INA219B measures this voltage drop by converting the analog signal to a 12-bit digital signal. By knowing the resistance and the voltage drop, the current is subsequently internally determined. It should be noted that the shunt resistor is placed on the supply side of the heater. This provides two advantages. Firstly, the heater ground does not change with a change in current. Secondly, and more importantly, the bus voltage (supply voltage) can also be measured. The INA219B records the bus voltage. By knowing both the bus voltage and the circuit current (from the shunt voltage), the power can be calculated. The bus voltage and shunt voltage can be retrieved from the INA219B by means of I<sup>2</sup>C communication (performed by an Arduino). The data (SDA) and clock (SCL) lines that go to the corresponding Arduino pins, are pulled high with 3.3 k $\Omega$  resistors.

The next part of the electrical design is the temperature sensor circuit. As mentioned, the temperature sensors are thermistors. The resistance of thermistors change with a change in temperature. This implies that by knowing the resistance, the temperature can be calculated once calibrated. This is further described in Appendix H. A Wheatstone bridge is used for each thermistor to accurately determine the resistance of the thermistor. Figure 4.14 illustrates how the Wheatstone bridge is used. An AD620 instrumentation amplifier is used to amplify the voltage between  $V_A$  and  $V_B$ . This can be used to determine the thermistor resistance by using Equation 4.6.

$$V_o = \left( \frac{R_2}{R_1 + R_2} - \frac{R_{thermistor}}{R_3 + R_{thermistor}} \right) V_i \quad (4.6)$$

Where  $V_o = V_A - V_B$  and  $V_i$  is the supply voltage (5 V in this case).



## 4. DESIGN OF DEVICES

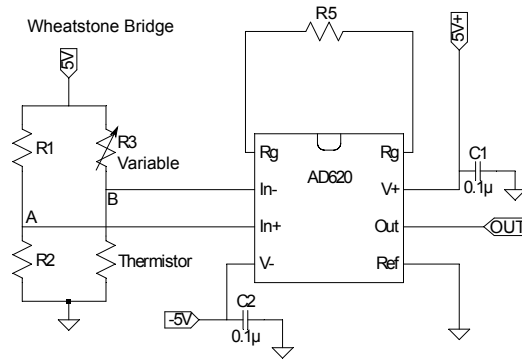


**Figure 4.14: Thermistor Wheatstone circuit**

The Wheatstone bridge in Figure 4.14 is used for both the ambient and heater thermistors. The -5 V supply is obtained from the MAX660 IC shown in Figure 4.6(b). The values of the resistances in the Wheatstone bridge are important for calculating the unknown thermistor resistance. Since the resistors that are used have a tolerance, the exact resistances are recorded in Tabel 4.3. The variable resistor  $R_3$ , is adjusted in accordance with the temperature at which the device will be used.

**Table 4.3: Wheatstone bridge resistance values**

Thermistor Usage	$R_1$ (Stock Value)	$R_2$ (Stock Value)	$R_5$ (Stock Value)	Approximate Amplification by $R_5$
Heater	9.974 k $\Omega$ (10 k $\Omega$ )	3.971 k $\Omega$ (4 k $\Omega$ )	9.978 k $\Omega$ (10 k $\Omega$ )	5.95
Ambient	10.033 k $\Omega$ (10 k $\Omega$ )	4.184 k $\Omega$ (4 k $\Omega$ )	9.945 k $\Omega$ (10 k $\Omega$ )	5.97

The output of both the ambient and the heater thermistor circuit passes through a buffer in the form of a LM324 opamp. This creates a low impedance output for the DAQ. Figure 4.15 illustrates this, where HOUT and AOUT are the outputs of the heater thermistor and ambient thermistor circuits respectively.

## 4. DESIGN OF DEVICES

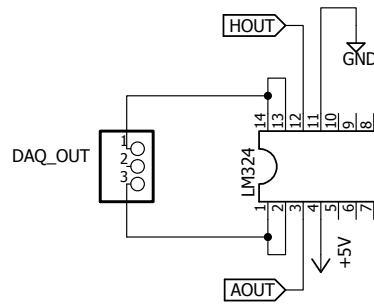


**Figure 4.15: Thermistor circuit buffer**

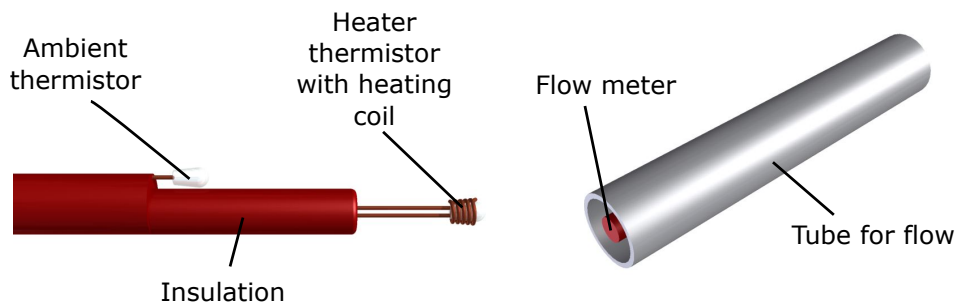


**Figure 4.16: Model used for the CFD simulations**

### 4.3.3 CFD Simulation Setup

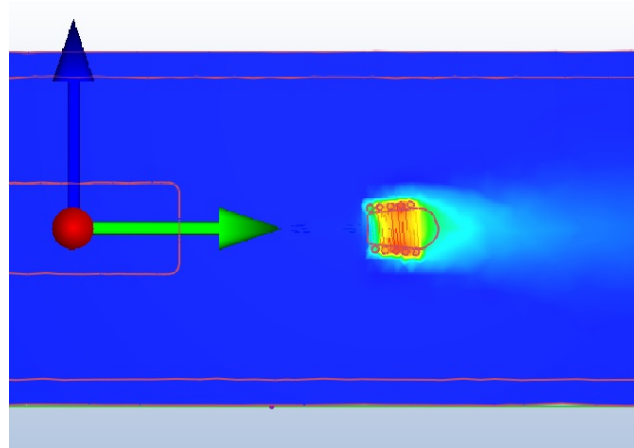
Autodesk CFD 2016 is used to simulate a model of the device discussed in this section. The simulation results are later compared to that of the *in vitro* tests. Figure 4.16 displays the model used for the CFD simulations. Both the thermistors have the properties of glass assigned to them, whereas the heating element is assigned as copper. The right side of the figure displays the flow meter inserted in a tube. The one end of the tube has a boundary condition specifying the volume flow rate as well as the temperature (38 °C). The other end has a zero gage pressure.

Figure 4.17(a) displays a visual representation of the heated flow sensor when exposed to blood flow. Figure 4.17(b) shows the CFD calculated temperatures over a number of volume flow rates. The analytical plot is based on Equation 3.5 from Section 3.3. The analytical model assumes the heater is a spherical shape and makes use of the same power output and velocity flow rates as given in the CFD simulation. The analytical model has higher temperatures, but has a very similar trend. This difference can be attributed to a number of factors. The analytical model assumes a mean flow velocity over a smooth spherical sensor which is not the case in the CFD simulation.

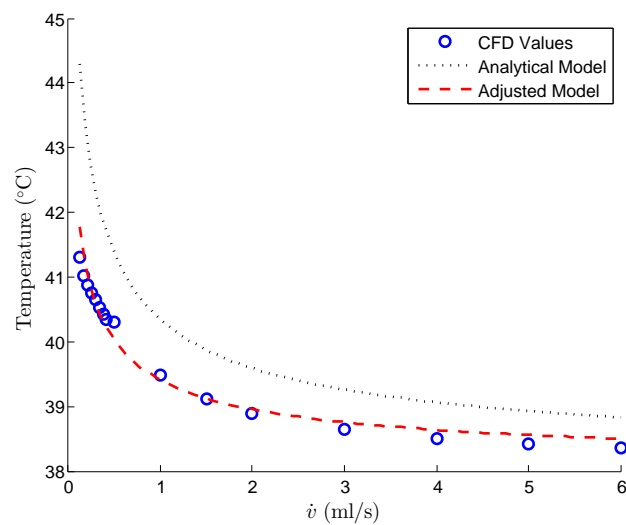
#### 4. DESIGN OF DEVICES

---

Also no radiation or conduction heat transfer is included. Thus, by reducing the power output of the analytical model, the CFD and the analytical model are nearly the same. This indicates that the CFD trend is most likely correct.



(a) Visual temperature response of flow sensor in blood flow



(b) CFD simulation compared to analytical model

**Figure 4.17: CFD simulation of flow sensor**

## 5. In Vitro Tests

The *in vitro* tests were performed on a fluid flow circulation system. These tests provide a better understanding of how the devices work and what can be expected from the *in vivo* tests.

### 5.1 Fluid Circulation System

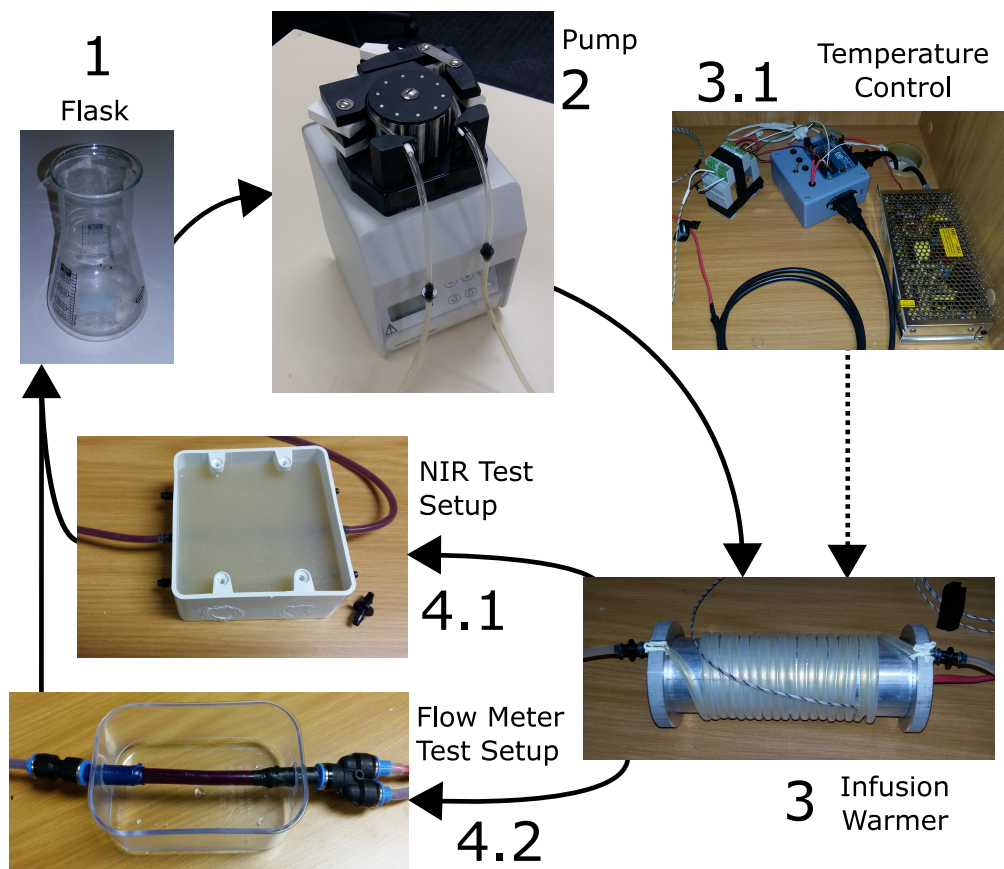


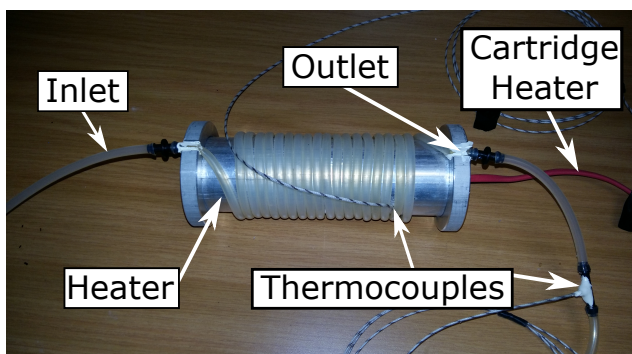
Figure 5.1: Circulation system layout

## 5. IN VITRO TESTS

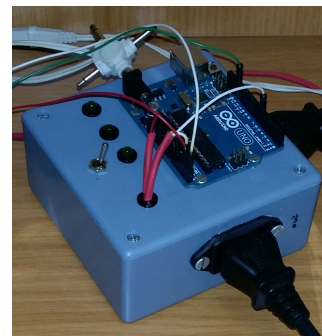
---

The circulation model consist of several parts as shown in Figure 5.1. The steps are briefly described below:

1. The fluid that is used during the testing is placed in a glass flask. Note that blood does not react with glass, so this is a suitable flask for blood tests.
2. The fluid is circulated by means of a Gilson Minipuls peristaltic pump. A peristaltic pump provides two main advantages. Firstly, it pumps at very accurate and repeatable flow rates. Secondly, and more importantly, none of the fluid ever comes into contact with the pump. Fluid is drawn from the flask via silicon tubing. The fluid reaches the pumping area and flows through a piece of Tygon R3607 tubing and continues through the system in silicon tubing. Since fluid only ever comes into contact with the flask and the silicone tubing, this pumping system is suitable for blood. Blood does not react with either silicon or Tygon.
3. In the third step, the fluid passes through a section of silicon tubing that is wrapped around an aluminium cylinder as shown in Figure 5.2(a). The aluminium is heated by a cartridge heater. This then heats up the fluid without the fluid ever coming into contact with the heater. The heater is controlled by a PID controller shown in Figure 5.2(b). Thermocouples on the heater surface and in the outlet tube provide temperature information to the controller. The system maintains a fluid temperature of 38 °C at the outlet thermocouple. Also, the surface thermocouple ensures that the blood will never reach temperatures higher than 50 °C at which point red blood cells begin to damage. Appendix E briefly illustrates the PID control results.



(a) Fluid heater



(b) Heater control system

**Figure 5.2: Fluid heating setup**

## 5. IN VITRO TESTS

---

4. This step is separated into two parts. 4.1 and 4.2 are interchanged depending on whether the NIR device or the flow meter is being tested respectively. The setup displayed in 4.2 is simply a tube with an Y-adaptor that allows both blood to flow in and the thermal device to be inserted without leaking. The setup in 4.1 has a few more considerations to be taken into account and is discussed in Section 5.2.

### 5.2 Phantom for NIR Tests

The materials used and the setup for the NIR tests are discussed in this section.

#### 5.2.1 Blood

While artificial substances, such as Naphthol green dye, can mimic blood, it still has limitations when compared to blood. For this reason actual blood is rather used for the tests.

During the course of these tests, two batches of blood from two different horses are used. The blood was obtained from the Medical Research Council (MRC). A factor that particularly has an influence on near infrared absorption, is the haemoglobin concentration. Horses tend to have a lower haemoglobin concentration than humans. Humans generally have haemoglobin concentrations between 12 g/dl to 17 g/dl. The blood from the two horses have haemoglobin concentrations of 8.5 g/dl and 8.6 g/dl (as tested by the EKF Diagnostics Hemo Control analyser). It is expected that the lower concentration of haemoglobin will result in slightly less absorption of the NIR light. This implies that in humans the absorption will likely be more noticeable.

The blood was stored between 2 °C and 6 °C as suggested by manual issued by the World Health Organisation (WHO, 2005). Even though literature suggests that blood can last longer, MRC advised that the blood should be used within five days. Hence the tests were all performed within that period.

#### 5.2.2 Agar Phantom

The ability of the near infrared (NIR) device to locate blood vessels is assessed in this section. To effectively accomplish this, a model is required that simulates a blood vessels (with blood flow) within tissue, typically muscle.

An exact model that includes the complexities of skin, fat, muscle, blood and a blood vessel does not exist. The simplified model used for the *in vitro* tests consists of three major parts:

## 5. IN VITRO TESTS

**Agar** Agar is a gelatine-like substance that is easily attainable and can mimic the optical and thermal properties of muscle tissue. Jaime *et al.* (2013) states that a 52 g/l mixture of agar and distilled water provides an absorption coefficient in the agar that is very similar to that of muscle in the region of 800 nm. This mixture is used for the NIR tests in this thesis.

**Silicon and PVC tubing** The tubing allows light to pass through into the blood.

**Blood** As indicated in the previous section, horse blood is used for the tests. This is more accurate than using artificial absorption fluids.

### 5.3 Experimental Procedure

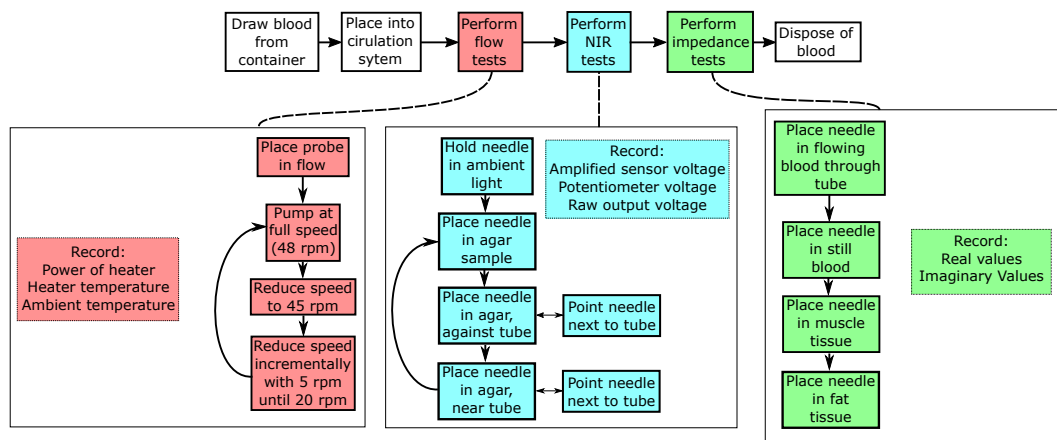


Figure 5.3: *In vitro* testing procedure

The general testing procedure was performed as shown in Figure 5.3 and is explained below (Appendix F has an enlarged version of Figure 5.3):

1. Approximately 100 ml of blood was drawn from the vacuum sealed blood container for each test set.
2. The blood was then placed into the flask and the pump turned to full speed. This was to quickly fill the whole circulation system with blood, particularly the heating area.
3. Once the system was filled with blood, the heater control was activated. The system was then left until a steady temperature of approximately 38 °C is achieved.

## 5. IN VITRO TESTS

---

4. In this step the tests on the devices were performed. This occurred in the following order:

**Flow tests** The thermal flow probe was placed into the flow tube (represented by 4.2 in Figure 5.1). The pump was set to full speed at 48 rpm. The next step was performed at 45 rpm after which the speed was incrementally decreased until 15 rpm in steps of 5 rpm. This resulted in eight steps. At each increment the power, heater temperature and ambient temperature were measured with the probe. These steps were repeated several times until an adequate amount of data was obtained.

**NIR tests** The amplified output from the phototransistor, potentiometer voltage and the raw output from the phototransistor were recorded for each step in these tests. The first set of measurements were taken in ambient light, after which measurements were taken in various places within the agar sample. This was followed by measuring the response when the needle was placed against the tube (filled with blood), and then next to the tube. This same step was repeated at a short distance from the tube.

**Impedance tests** The real and imaginary impedance values, as given by the AD5934, were recorded for each frequency in each step. The first set of measurements were taken in flowing blood, by placing the needle through the tube in the flow. This was followed by measurements in still blood. Additional tests were then done on post mortem porcine muscle and fat tissue.

5. After the set of tests had been completed the blood and needles were disposed of in the appropriate containers. BCL Medical Waste Management Services correctly then disposed of the containers.

## 5.4 Blood Vessel Detection

### 5.4.1 Results

The method used in this thesis to detect the location of blood vessels is based on near infrared technology. In order to give an indication of the viability of such a device, there are several tests that can be performed. Measurements in various tissues, such as blood, muscle and fat, can provide insight into how clearly tissues can be distinguished from one another. This does however not indicate clearly if the device can indicate the position of a blood vessel that is filled with blood. A more appropriate test is one where the response of the needle when pointing at a blood vessel and when pointing away from the blood



## 5. IN VITRO TESTS

---

vessel is recorded. This leads to the hypothesis that the mean measurement of reflected light when pointing at a blood vessel is different than when pointing away from the vessel.

Figure 5.4 displays the normalised results that were obtained by placing the optic fibre directly into the corresponding tissue. The values are normalised to the highest reading obtained during this section of the tests (0.4273 V). For the flowing blood, the needle was inserted through the wall of the tubing. Table 5.1 summarises the statistics of the tests. A two sample t-test is used to determine the p-value. Note that for this particular test, blood from one horse was used, but the measurements were taken at different points in the flow. Similarly, samples from the fat and muscle were taken at different points on two separate sets of tissue.

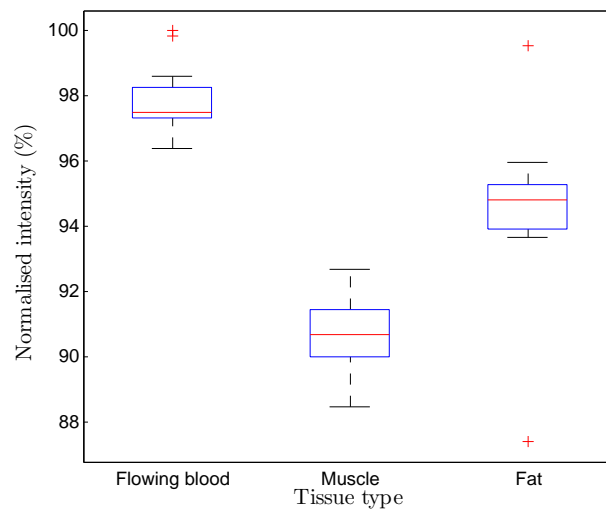


**Figure 5.4: Normalised intensities of various tissues when probe is inserted into the tissue**

**Table 5.1: Statistics of normalised NIR response in specific tissues at 880 nm (normalised to 0.4273 V)**

Tissue type	Number of samples	Mean (%)	Standard deviation (%)	p-Value (compared to blood)
Blood	20	97.73	0.9731	NA
Muscle	21	90.69	1.1591	$2.2659 \times 10^{-22}$
Fat	21	94.62	2.1251	$6.3186 \times 10^{-7}$

## 5. IN VITRO TESTS

It is clear from Table 5.1 that when the probe is placed directly in fat and muscle, both can be clearly distinguished from blood. The means of blood, fat and muscle are all significantly different from one another. This indicates that the needle can likely be used to located blood vessels, although not conclusive.

Figure 5.5 displays the results obtained when the needle is place near the blood vessel (PVC tubing in this case) and pointed at the blood vessel. It also displays when it is pointed away. The empty vessel shows that it is in fact not the vessel itself that is causing the difference in measurements, but rather the blood. The samples were obtained by recording measurements at various points in two agar phantoms over six separate tubes. The results are summarised in Table 5.2.

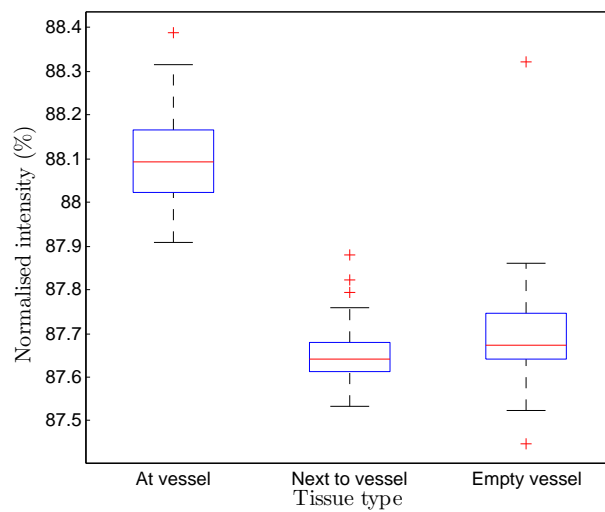


**Figure 5.5: Normalised intensities when pointing probe at tube and pointing away from tube**

**Table 5.2: Statistics of normalised NIR response pointing at blood vessel and away from vessel at 880 nm (normalised to 0.4273 V)**

Tissue type	Number of samples	Mean (%)	Standard deviation (%)	p-Value
At vessel	30	88.10	0.1071	$9.0996 \times 10^{-26}$
Away from vessel	30	87.66	0.0789	
Empty tube	18	87.70	0.1820	NA

## 5. IN VITRO TESTS

---

### 5.4.2 Discussion

The data obtained from the *in vitro* testing shows a significant difference in the light intensity between when pointing at a blood vessel, filled with blood, and when pointing away from the blood vessel. There are however several things to consider.

Starting with the results displayed in Figure 5.4, there is a very significant difference between blood, muscle and fat in terms of the light intensity. However, it is unexpected that blood has a higher intensity response than muscle and fat. A possible reason for this is that when the light source is in direct contact with blood, the reflectance component overpowers the absorption component. This means that a large amount of light is immediately reflected, whereas when the light passes through another tissue type and then through blood, more light is absorbed. Furthermore, when pointing at the tube filled with blood there is also a significant difference from surrounding tissue. Although the response that is recorded is higher for blood in the tube than in the agar, it should be noted that the overall response is lower than that of muscle and fat. This implies that the agar possibly did not simulate the optical properties of real muscle tissue. It is also shown that the higher reading is not due to the reflectance of the tube, as an empty tube had almost no effect on the reading.

Ultimately it is clear from the tests that blood causes a significant difference in diffuse reflectance compared to other tissue types. This is also clear when the needle pointed at the artificial blood vessel. While the data shows that a vessel that contains flowing blood can be located using this device, *in vivo* testing will provide the most reliable results. This is due to the fact that the phantom used, cannot simulate all the complexities of biological tissue.

## 5.5 Blood Vessel Penetration Detection

### 5.5.1 Results

Electrical impedance is the method of choice that is used to detect whether a needle has penetrated a blood vessel (i.e. inside blood) or not. Determining whether this is possible is dependant on whether the impedance magnitude and phase angle between blood and muscle, and blood and fat are significantly different at a specific frequency. Thus, the null hypothesis states that the mean impedance magnitudes and phase angles are the same, whereas the alternative hypothesis states that blood and muscle, and blood and fat differ.

Detecting the penetration of blood vessels with impedance requires only one frequency (or frequency range) at which tissue types can be distinguished from

## 5. IN VITRO TESTS

one another. To determine a suitable frequency, all tests were performed by a frequency sweep, ranging from 5 kHz to 75 kHz, which is in line with literature. Figure 5.6(a) and Figure 5.6(b) illustrates the mean results obtained during the frequency sweeps for impedance magnitude and phase angle respectively. The figures also display their respective 95 % confidence intervals. This is based on the number of samples displayed in Table 5.3. Note that each sample consists of a number of readings. The total number of readings performed are indicated in the last column. Also, the muscle and fat samples were obtained from different points in two separate sets of porcine tissue. The blood samples were obtained from one set of horse blood at different points in the flow.

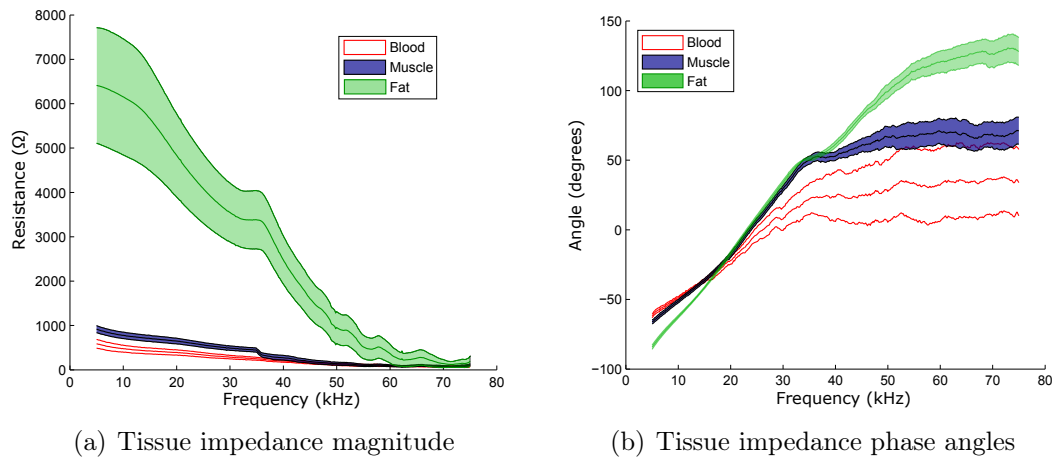


**Figure 5.6: Impedance magnitudes and phase angles of tissue types with 95 % confidence intervals**

**Table 5.3: Impedance tests sample information**

Tissue type	Number of samples	Total Readings (some samples consists of multiple readings)
Blood	9	46
Muscle	20	96
Fat	20	97

The purpose of these results is to find a frequency at which blood can be individually distinguished from muscle and fat. Equation 5.1 is used to find an optimal frequency. The difference between the mean of blood and the nearest other tissue mean is calculated. This is then divided by the sum of the 95 % confidence intervals (CI) from each mean. Hence, if this interference ratio

## 5. IN VITRO TESTS

---

( $I_{ratio}$ ) is less than one, the confidence interval of blood interferes with that of another. A value larger than one is thus preferable.

$$I_{ratio} = \frac{\text{Mean of blood} - \text{Nearest mean}}{\text{Blood CI from mean} + \text{Nearest tissue CI from mean}} \quad (5.1)$$

Equation 5.1 is applied to both the impedance magnitudes and phase angles. The resulting interference ratios are illustrated in Figure 5.7.

It would be preferable to distinguish between tissue types by means of both impedance magnitude and phase angle. For this reason, based on the data gathered, the optimal frequency can be chosen by calculating the product of the interference ratios of the impedance magnitude and phase angle. The optimal frequency will be the product with the highest value. The maximum value of 7.3825, occurs at a frequency of 29.85 kHz.

The box plots in Figure 5.8 and Figure 5.9 illustrate the data for the impedance magnitude and phase angle respectively. In all four cases the 95 % confidence intervals never intersect. Since the impedance mean of blood is being compared individually to that of muscle and fat, a two sample t-test is used to determine the p-values. The t-test results is summarised in Table 5.4 and Table 5.5 for impedance magnitude and phase angle respectively.

The t-tests for the four cases all indicates that the difference between the mean impedance magnitude and phase angles of blood and muscle and blood and fat are significantly different. This implies that at 29.85 kHz the device can clearly distinguish between blood and other tissues (fat and muscle)

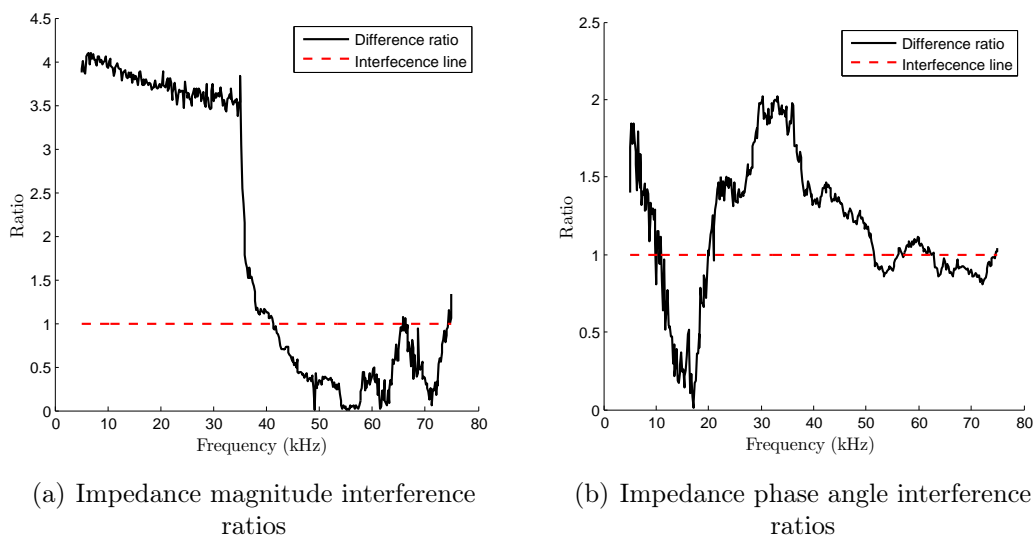
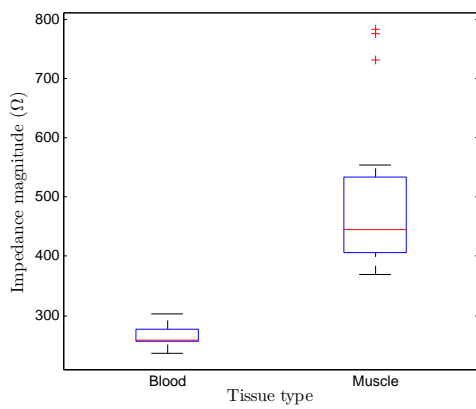
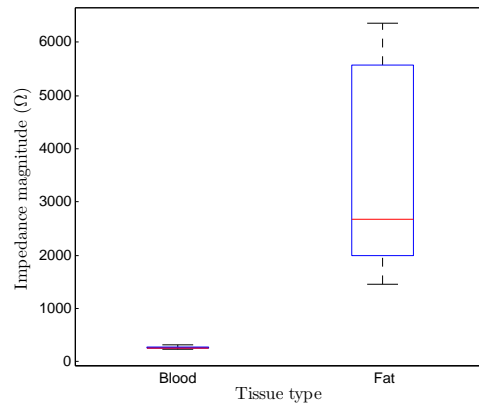


**Figure 5.7: Interference ratios of blood and nearest tissue means**

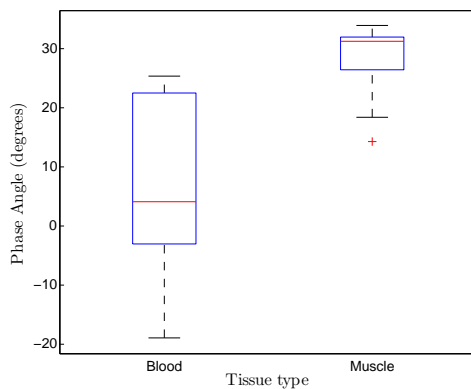
## 5. IN VITRO TESTS



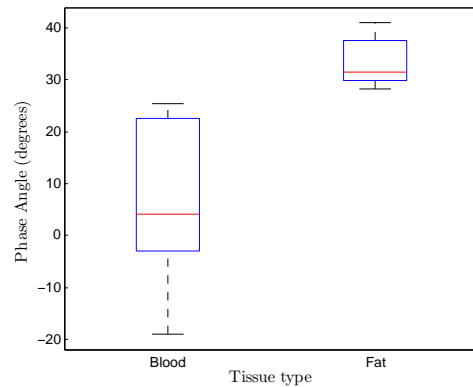
(a) Blood and muscle impedance magnitude



(b) Blood and fat impedance magnitude

**Figure 5.8: Impedance magnitudes of fat and muscle compared to blood at 29.85 kHz**

(a) Blood and muscle impedance phase angle



(b) Blood and fat impedance phase angle

**Figure 5.9: Impedance phase angle of fat and muscle compared to blood at 29.85 kHz**

## 5.5.2 Discussion

The hypothesis that at certain frequencies the means of the impedance magnitudes and phase angles differ significantly between blood, muscle and fat are clearly supported by the results. In fact there are a range of frequencies where this is true. Some frequencies have erratic behaviour among the different samples. This implies that at these frequencies it is possible to distinguish between tissue types, however the chances of a getting false positive becomes greater. It is found that at 29.85 kHz the 95 % confidence intervals of impedance mag-

## 5. IN VITRO TESTS

Table 5.4: Impedance magnitude statistics at 29.85 kHz

Tissue type	Mean ( $\Omega$ )	Standard deviation ( $\Omega$ )	p-Value (compared to blood)	Null rejected
Blood	265.88	18.53	NA	NA
Muscle	491.39	126.67	$2.1547 \times 10^{-5}$	Yes
Fat	3558.29	1728.29	$7.6754 \times 10^{-6}$	Yes

Table 5.5: Impedance phase angle statistics at 29.85 kHz

Tissue type	Mean (degrees)	Standard deviation (degrees)	p-Value (compared to blood)	Null rejected
Blood	7.25	14.58	NA	NA
Muscle	28.95	5.45	$5.9864 \times 10^{-6}$	Yes
Fat	33.35	4.02	$1.1042 \times 10^{-7}$	Yes

nitude and phase angles of blood and the nearest tissue are furthest from one another. While the data from Figure 6.11 and Figure 6.12 do show that some minimum values of muscle overlap with the impedance of blood, the combined use of impedance magnitude and phase angle will reduce the chance of false positives.

It should be noted that several factors could influence the results obtained. The fact that the blood is citrated (form of anticoagulation) could potentially have affected the results. Also, the tissue tests were performed on post mortem tissue samples. While the effect is not expected to be significant, the *in vivo* tests are the only way to confirm these results.

In conclusion, this device can be used to discriminate between tissue types, particularly between blood and other tissue types. Under the given test conditions with the samples used, the needle can detect when a blood vessel is penetrated at 29.85 kHz, however, live animal testing is required to confirm. Note that the results obtained by both Schwartz (2013) and Martinsen *et al.* (2010) (see Section 2) also suggest that the frequency at which blood can be discriminated from other tissues the best, is at 30 kHz.

## 5. IN VITRO TESTS

---

### 5.6 Blood Flow Measurement

The concept of using principles of thermal convection to determine blood flow rate was tested in this thesis. This section displays the results obtained from the device developed in Section 4.3 along with predicted values of the device for larger flow rates, based on simulations. Calibration data for the pump and the thermistors can be found in Appendix G and Appendix H respectively.

#### 5.6.1 Results

The sensors were placed inside a flexible PVC tube with a inner diameter of 8 mm. Due to way in which this device is intended to be used, it was arbitrarily inserted into the tube, i.e. the sensor position relative to the centre of the tube was not controlled. When placed into a blood vessel this can also not be controlled. It was, however, approximately placed near the centre. This was repeated for each set of eight flow rates used.

The first set of tests were performed on distilled water. This was done as a preliminary step to get an estimation of how the device performed. Water is simpler than blood in that water is a Newtonian fluid and blood not. Figure 5.10(a) displays the temperature differences between the ambient temperature sensor and the heater sensor for a number of different flow rates. The mean of the power supplied for all of the tests is 1.331 W, with the minimum and maximum being 1.327 W and 1.336 W. A trend is clearly noticeable among each set of readings, however the difference in temperature for different test sets fluctuate. From Figure 5.10(b) it becomes apparent that the heater temperature is the cause for this shift as the average temperature per run changes for each set. This is discussed in the discussion section.

Meaningful data can be extracted from these results by taking the temperature difference of the highest flow rate measurement from each individual test run. These measurements serve as an offset reference value for its corresponding test run. By deducting this reference value from each reading in that test run, the offset will be removed and the highest flow rate temperature difference will now have a zero offset. Figure 5.11(a) displays the results of removing the offset. Figure 5.11(b) is an error plot with a linear fit with an adjusted coefficient of determination of  $R^2 = 0.9801$ .

A linear fit over this range provides a good coefficient of determination. These results can now be compared to a CFD model of the test set up. Figure 5.12(a) displays CFD results for various power settings. It should be noted that the power settings for the CFD differs greatly from the actual power recorded for the tests. There are two reasons for this. Firstly, the wires that carry the current to the heater dissipate a large amount of power. Secondly,



## 5. IN VITRO TESTS

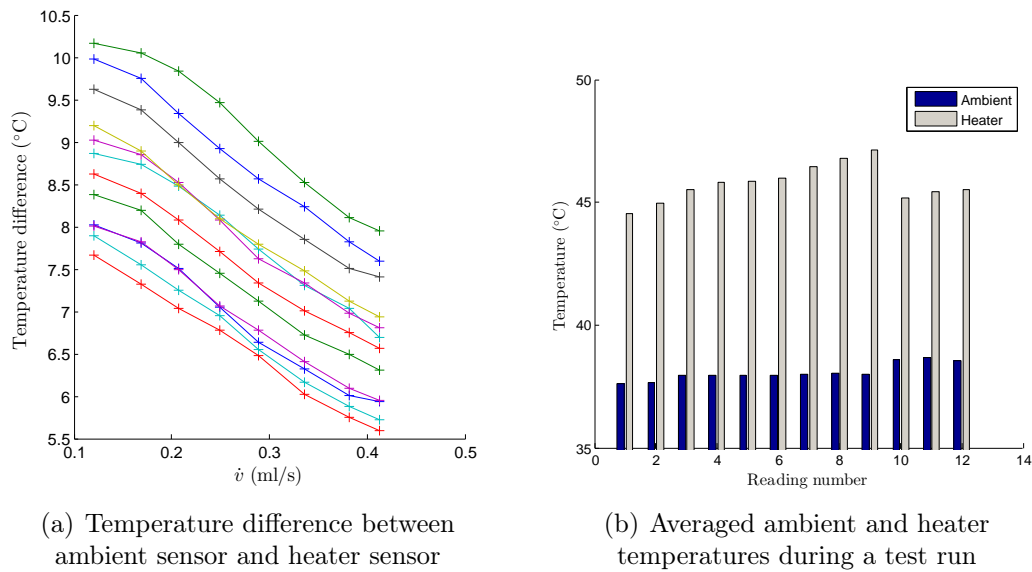


**Figure 5.10: Raw response of thermal flow sensor in distilled water**

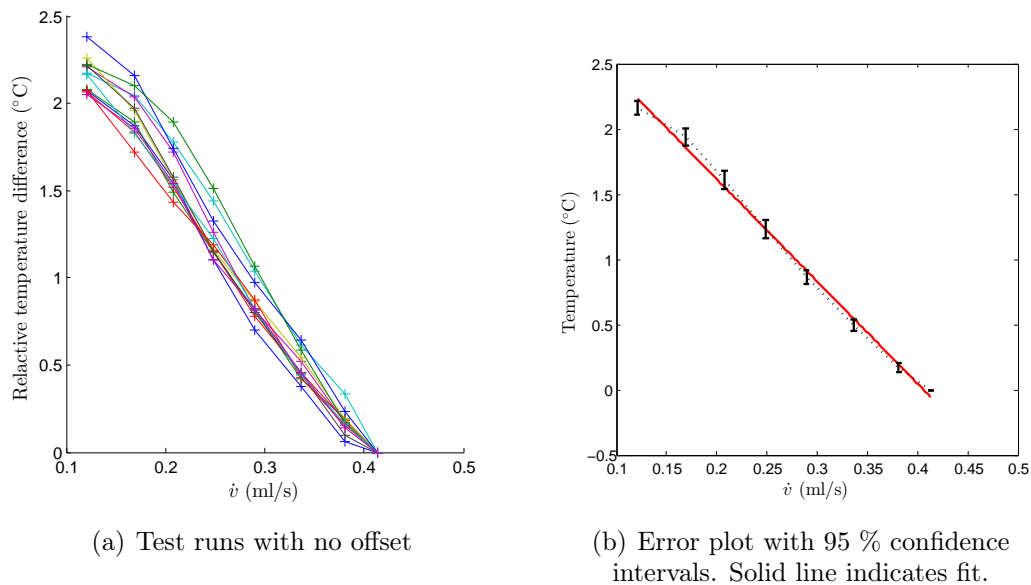


**Figure 5.11: Thermal flow sensor results with removed offset**

the maximum temperatures in the CFD simulation are used for the plot and not necessarily the temperature that the thermistor will record at its core. Several power settings are thus used iteratively to fit the recorded data as close as possible to get a reasonable model to estimate the temperature response for cases of higher flow rate. Figure 5.12(b) displays the predicted response of the model at flow rates of up to 6 ml/s. Note that the temperature offset remains

## 5. IN VITRO TESTS

the same as in the previous figures to simplify comparison.

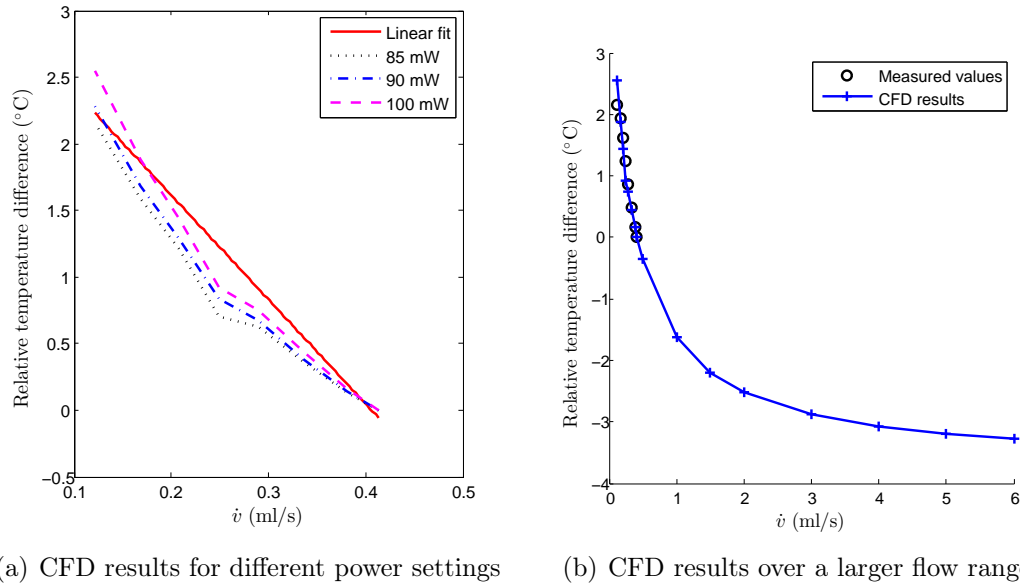


**Figure 5.12: CFD simulation results of thermal flow meter in water flow**

The tests with the horse blood were performed in the same manner as the distilled water tests. An average power of 1.336 W was applied to the heater with a minimum and maximum power of 1.326 W and 1.342 W respectively. The results however were a bit more erratic. Figure 5.13(a) shows the difference in ambient and heater temperature, similar to the water tests. The differences are, however, widely spread. From Figure 5.13(b) it can be seen that the largest temperature differences occurs in the final runs. Reasons for this is explained in the discussion section (Section 5.6.2).

The offset can once again be removed as explained in the water tests. Figure 5.14(a) shows the blood test results with the offset removed. Again, the results are erratic compared to the water tests. Figure 5.14(b) displays the summary of all the readings. The black bars represent the 95 % confidence intervals and the solid line represents a second order polynomial fit. The fit has an adjusted coefficient of determination of  $R^2 = 0.6056$ .

The second order polynomial fit is the best fit over the test region. Figure 5.15(a) shows the temperature response of various power settings of the heater. As explained in the water tests, the CFD heater power is far below the recorded values. The CFD model is again adjusted to fit the data points as close as possible. Figure 5.15(b) shows the predicted temperature response over larger flow range (CFD heater set to 75 mW). The results are briefly summarised in Table 5.6.

## 5. IN VITRO TESTS

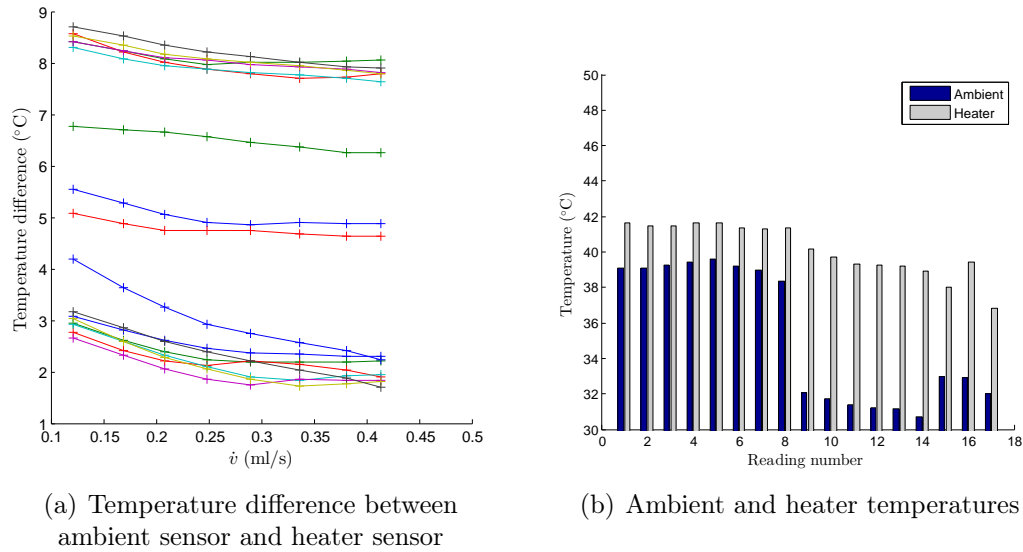


**Figure 5.13: Raw response of thermal flow sensor in blood flow**

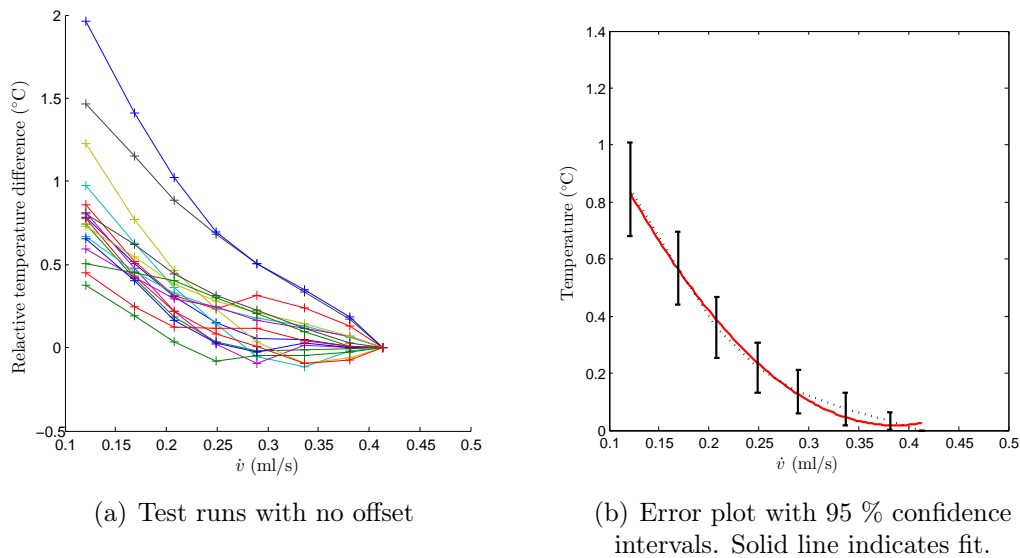


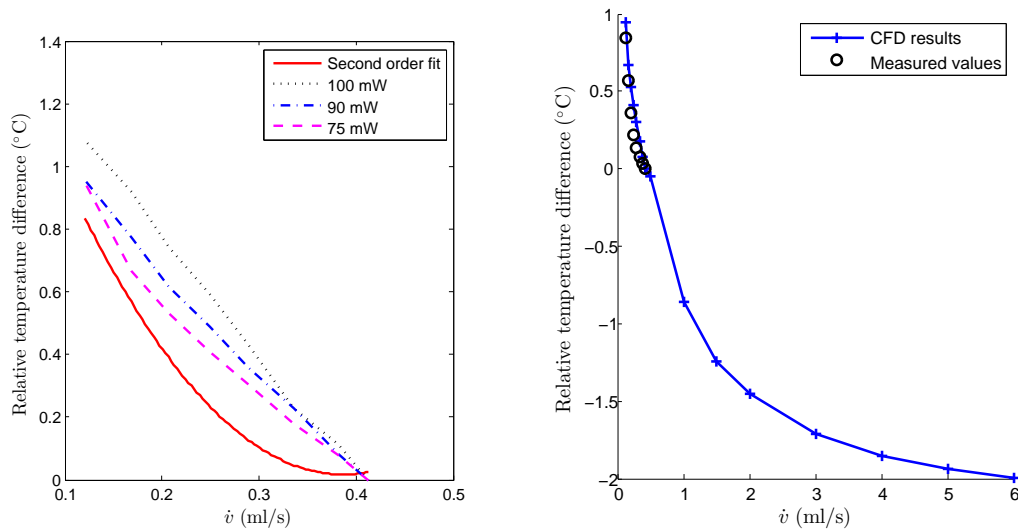
**Figure 5.14: Thermal flow sensor results of blood tests with offset removed**

## 5.6.2 Discussion

The purpose of these tests is to determine whether the thermal flow meter, described in Section 4.3, can be used to determine flow rate in blood vessels. The results indicate that it is in fact possible but with a number of considerations.

The first issue to address is the fluctuating differences in temperature across test runs. In both the water tests and the blood tests the problem clearly

## 5. IN VITRO TESTS



(a) CFD results for different power settings      (b) CFD results over a larger flow range

**Figure 5.15: CFD simulation results of thermal flow meter in blood flow****Table 5.6: Thermal flow results summary**

Test medium	Number of tested flow rates	Total number of samples	Fit type used over test range	Coefficient of determination $R^2$
Water	8	96	Linear	0.9801
Blood	8	144	Second order polynomial	0.6056

originates from the heating thermistor. A possible reason for this is that heat starts to get trapped in the heating coil. In the case of the water tests, small bubbles formed on the sensor which can also trap heat. In the case of the blood tests, some blood cells started to get trapped in the copper coil. This could all contribute to a rise in heater temperature over the period of testing. In some cases, the time between test sets were longer than others, allowing the heating coil to cool down again. This could cause unpredictable offsets between the test sets. The most practical solution to the problem would be to have a smooth surface heater instead of a coil.

Once the relative offset of the temperature differences are removed there is a clear trend in the data. The blood tests provided the least consistent

## 5. IN VITRO TESTS

---

results and is likely due to the fact that blood cells became trapped in the heater coil. The water tests results appeared to be approximately linear. This is not completely as expected, however a linear fit provided a good coefficient of determination. This implies that in the tested region, the volume flow rate can be estimated with little error. Results of a CFD simulation is compared to these results and falls near the linear fit however do not appear to be linear. Expanding the water flow rate to 6 ml/s the trend becomes very similar to that of convective heat transfer as explained in Section 3.3. This is to be expected and while the model does not exactly fall on the measured data it provides a good idea of what can be expected at higher flow rates.

The blood test results do not appear to be linear. A second order polynomial fit to the data provided a moderate coefficient of determination, although better than that of linear and third order polynomials. This is due to the large variances in data at each point. The CFD results again do not match the measured results exactly. The results do however appear similar to that of the water tests that is consistent with convective heat transfer.

The widely spread data from the blood tests indicate that this specific device will not be able to accurately determine blood flow rates in the tested region. However, the results from the water tests and the CFD simulations clearly indicated that it is theoretically possible to determine the blood flow rate with convective heat transfer methods. The device should however have a smooth heating element that prevents blood cells from becoming trapped. It should also be noted that this device has a temperature drop proportional to flow velocity. To determine volume and mass flow rates the diameter of the vessel along with the density must be known.

## 6. In Vivo Tests

The *in vivo* testing was performed on New Zealand white rabbits. Ethical clearance was obtained for the protocol number SU-ACUD15-00106 (proof in Appendix I). Only the impedance and NIR devices were tested on the rabbits. The thermal flow meter was only conceptually tested *in vitro*.

### 6.1 Animal Testing Motivation

The *in vitro* tests of Section 5 made use of approximated models of human anatomical features. Needless to say, the complexities of the human anatomy cannot be exactly replicated. Live mammalian testing is thus the best alternative. For this reason adult New Zealand white rabbits were used for testing. Choosing a viable mammal as a translational model to humans and viable test subject, requires two main factors to be taken into account:

**Blood vessel diameter** The technology that is tested is used both inside and outside of blood vessels. Performing these tests require that the blood vessels be large enough for the devices to be used. Generally adult rabbits have femoral blood vessel sizes between 1.5 mm to 1.8 mm (Shen-Xiu and Ti-Sheng, 1986). The NIR device has an active sensing diameter of 1.6 mm. Note that this device does not enter the blood vessel and is only used to locate the blood vessel. The impedance method uses a 14 gauge needles with an outer diameter of 1.83 mm. Since this device penetrates blood vessels, it will be used prior to terminating the subject.

**Blood composition** The blood composition, particularly haemoglobin concentration, is important for NIR technology. This is true since the concentration partly determines how much NIR light will be absorbed. A recent study by Tokarz-Deptuła *et al.* (2014) shows that New Zealand rabbits have a haemoglobin concentration of 11 g/dl to 13 g/dl. In terms of the NIR capabilities, this is comparable to that of humans, which ranges from 12 g/dl to 17 g/dl (Johnson *et al.*, 2015).

## 6. IN VIVO TESTS

---

Testing on rabbits, based on the aforementioned facts, thus provides results translatable to humans in terms of basic physiology. Furthermore, testing of the invasive technology on humans require that the device be approved based on animal testing results. Thus, the animal testing provides a basis for future clinical trials.

### 6.2 Experimental Procedure

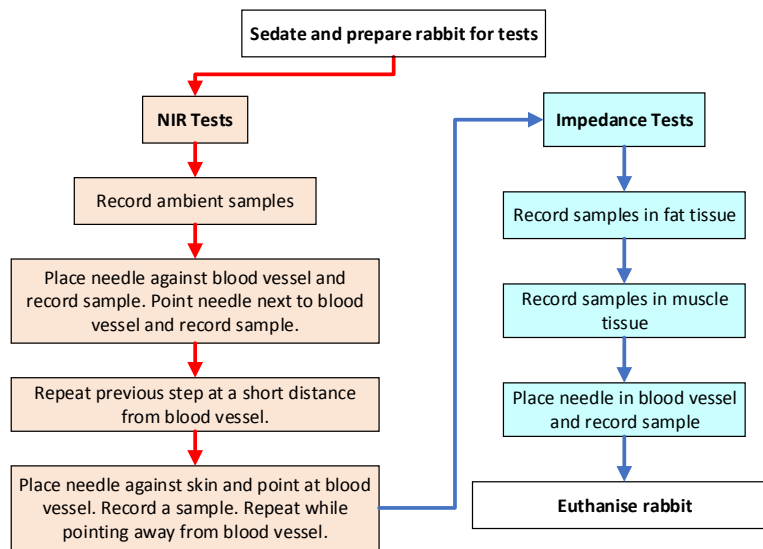


**Figure 6.1:** *In vivo* testing procedure

The testing done on the rabbits followed the general procedure as illustrated in Figure 6.1. Five rabbits were used for the testing, of which two rabbits died prematurely.

The first step was to prepare and sedate the rabbit. The rabbit was induced with between  $20 \text{ mg kg}^{-1}$  and  $50 \text{ mg kg}^{-1}$  ketamine intramuscularly. To maintain anaesthesia, Isoflurane vapour was administered via a tracheostomy at a flow rate of  $0.5 \text{ l/min}$ . Additionally  $40 \%$  oxygen was given. Ventilation was maintained between 20 to 40 breaths per minute with peak pressures of 12 to  $18 \text{ cm H}_2\text{O}$ . Ringer's lactate intravenous fluids were administered at a rate of  $15 \text{ to } 20 \text{ ml/kg/hr}$ .

The first set of tests that were performed was with the NIR device. The reason for this is that this device never penetrates the blood vessels. Due to the large diameter of the impedance needle, a punctured blood vessel will not seal up and the rabbit could potentially bleed out. Thus the impedance tests,

## 6. IN VIVO TESTS

---

with the large needle size, were performed last. The testing was performed in the following order:

1. The response of the NIR device in ambient light was recorded. This provided a baseline reference of the device response.
2. The next set of readings were taken at the surface of the blood vessel. This was done by making an incision near the femoral artery that made the artery visible as shown in Figure 6.2. This alternated with readings next to the blood vessel and in the muscle tissue. Note that it was important to place the needle such that the optic fibre came into firm contact with the corresponding tissue. The test was repeated for several different points along the blood vessel as well as at the other femoral artery.



**Figure 6.2: Incision near rabbit femoral artery**

3. The next set of readings were taken while placing the needle into tissue near the blood vessel (near the incision). The device was pointed at the blood vessel and the response was recorded. Note that the physician performing the test only had an estimate of where the blood vessel was located. By viewing the real time voltage response of the needle, using his knowledge of anatomy and having a slight visibility of the blood vessel, the vessel was located and data recorded. The needle was then turned away from the blood vessel in an arbitrary direction, where the next data points were collected. Again this was repeated several times at different points along the femoral arteries.
4. The last set of NIR tests were performed in a similar fashion as the previous steps, however, this time, the recordings were made at the surface of the skin. The NIR device was pointed at visible arteries near the skin surface. The arteries needed to be visible in order to get accurate readings.



## 6. IN VIVO TESTS

---

5. The impedance device was then tested. The device was first placed into fat. The rabbits used in these tests had very little fat. The needle was thus placed in to areas with visible fat among the muscle tissue. Several frequency sweeps were performed per sample area. Each sample was obtained from a different point.
6. This was followed by inserting the impedance needle into muscle tissue. To avoid having multiple variables, the needle was inserted approximately the same depth in each sample. Figure 6.3 shows the inserted needle for the muscle tests. Again each sample was recorded at a different area.

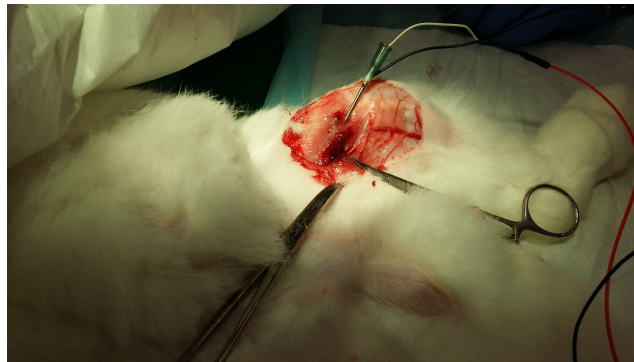


**Figure 6.3: Impedance needle placed into muscle tissue**

7. The last set of readings were taken inside the carotid artery of the rabbit. Each sample consisted of a number of frequency sweeps and samples were taken at different depths into the artery. Only the carotid arteries were used, as they were large enough for the needle to fit.

After all the tests were completed the rabbit was euthanised. The rabbit was given a lethal dose of Ketamine. The body of the rabbit was then disposed of in the appropriate container supplied by BCL Medical Waste Management Services.

## 6.3 Blood Vessel Detection

### 6.3.1 Results

The *in vitro* testing on the circulation system provided reasonable evidence that a blood vessel can be located by means of NIR light. There are a number

## 6. IN VIVO TESTS

---

of factors that could simply not be simulated by the circulation system. The tests on New Zealand white rabbits provides a much better approximation of what can be expected on humans. The complex anatomical features such as muscle with blood supply and fat deposits provide a testing environment that simulates the practical environment in which this device is intended to be used. Similarly to the *in vitro* tests, the hypothesis that is tested is that the mean relative light intensity when pointing at a blood vessel is different from when pointing away from a blood vessel. The null hypothesis being that the means of the relative intensities are the same. Note that the samples were obtained from various regions on three separate rabbits.

Figure 6.4 displays the normalised intensity results that were obtained by placing the optic fibre directly against a blood vessel and then placing it in the tissue next to the blood vessel. The intensities are normalised to the maximum measurement during the tests at 0.4778 V. Table 6.1 summarises the statistics of the tests. Note that a two sample t-test is used to determine the p-values. A p-value of less than 0.05 is considered statistically significant.

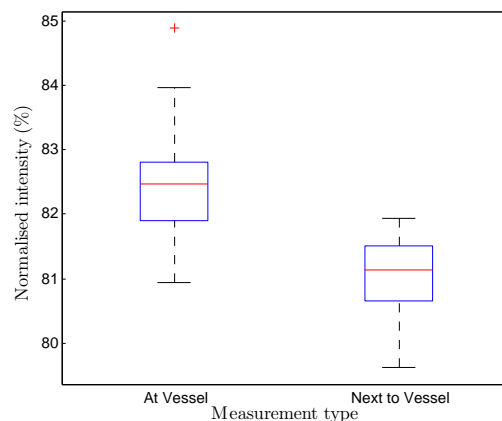


**Figure 6.4: Normalised intensities of probe against blood vessel and away from blood vessel in surrounding tissue**

Clearly there is a considerable difference between the blood vessel and surrounding tissue. The needle was firmly placed against the blood vessel to allow no direct exposure from external light. When pointing next to the vessel, the optic fibre slightly penetrated the surrounding tissue, which prevents exposure from external light sources.

The next step is to determine whether the needle can detect the presence of a blood vessel from the surface of the skin. This aims only to locate a blood vessel near the surface of the skin. To accurately perform these tests, the physician needed to be able to see the blood vessel. For this reason a

## 6. IN VIVO TESTS

**Table 6.1: Statistics of normalised NIR response at blood vessel surface and in surrounding tissue 880 nm (normalised to 0.4778 V)**

Test type	Number of samples	Mean (%)	Standard deviation (%)	p-Value
Point at blood vessel	34	82.46	0.8847	$2.2780 \times 10^{-11}$
Point next to blood vessel in tissue	34	81.01	0.5761	

visible artery near the surface of the skin was used. The needle was placed against the skin and pointed directly at the blood vessel and then next to the blood vessel. Figure 6.5 illustrates the results that were obtained. Table 6.2 summarises the test statistics. Again a t-test is used.

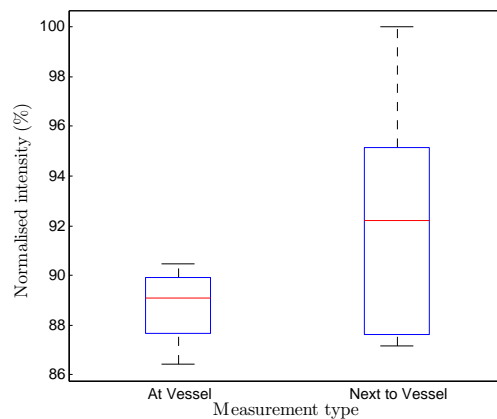


**Figure 6.5: Normalised intensities of probe against skin, pointing at blood vessel and away from blood vessel**

The results at the skin surface are somewhat erratic. This is most likely due to small strands of rabbit hair at the skin surface. Nonetheless, the null hypothesis is still rejected and statistically the device can distinguish between pointing at a blood vessel and away from said blood vessel. From the t-test, with an error probability of  $\alpha = 0.05$ , the statistical power of these results is determined to be 0.98.

## 6. IN VIVO TESTS

**Table 6.2:** Statistics of normalised NIR response at skin surface pointing at and away from blood vessel at 880 nm (normalised to 0.4778 V)

Test type	Number of samples	Mean (%)	Standard deviation (%)	p-Value
Point at blood vessel	25	88.69	1.3133	$3.8791 \times 10^{-4}$
Point next to blood vessel	25	92.04	4.1802	

The next set of tests had some difficulty in that the physician could not physically see the location of the blood vessel. The visible part of the blood vessel was followed into the tissue. The needle was then approximately inserted where the blood vessel was expected to be. To aid the physician the real-time response of the needle was displayed on a computer screen. The physician knew what to expect in terms of the response signal. The result is that the physician could mistakingly point at surrounding tissue when told to point at a blood vessel and vice versa. Figure 6.6(a) and Figure 6.6(b) display two scenarios. In each the physician is instructed to point at a blood vessel and away from the blood vessel as indicated. The response of a high or low signal was however inverted for the two scenarios, without physician knowing.

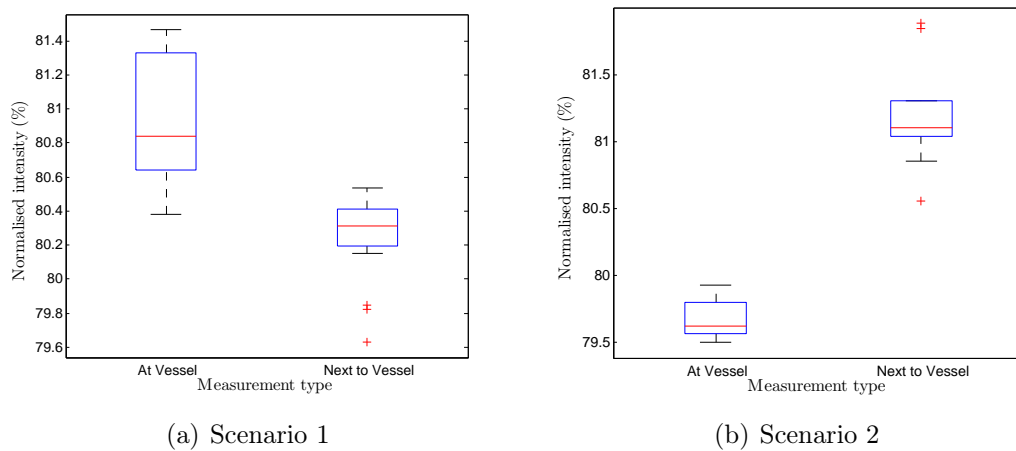


**Figure 6.6:** Normalised intensities from inside muscle tissue near blood vessel for inverted scenarios

## 6. IN VIVO TESTS

Both the scenarios from Figure 6.6 display statistically significant differences between pointing at the blood vessel and pointing away from the blood vessel. However, the results in both scenarios were opposite. This implies that the physician had to rely on the real time response to locate the blood vessel. While the results are inverted, in each scenario one set of readings definitely pointed at the blood vessel and one pointed away from the blood vessel. It cannot be entirely certain which is which. Figure 6.7 displays what the results would look like had the signal not been inverted for one scenario. From the previous data, it is expected that the lower intensity set of readings corresponds to the needle pointing at the blood vessel (see discussion). The t-test results are displayed in Table 6.3.

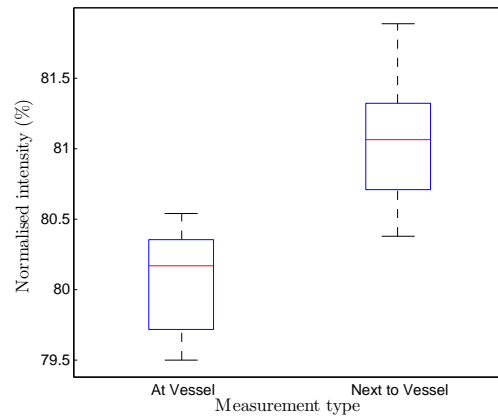


**Figure 6.7:** Normalised intensities from inside muscle tissue near blood vessel

**Table 6.3:** Statistics of normalised NIR response when pointing at a blood vessel and away from the blood vessel at 880 nm (normalised to 0.4778 V)

Test type	Number of samples	Mean (%)	Standard deviation (%)	p-Value
Point at blood vessel	28	80.05	0.3536	$1.2067 \times 10^{-13}$
Point next to blood vessel	28	81.03	0.3909	

## 6. IN VIVO TESTS

---

Figure 6.8 displays how the device reacted over time when moving over a blood vessel. The physician was instructed to place the needle near the vicinity of the blood vessel. The needle was then moved over the blood vessel from side to side.

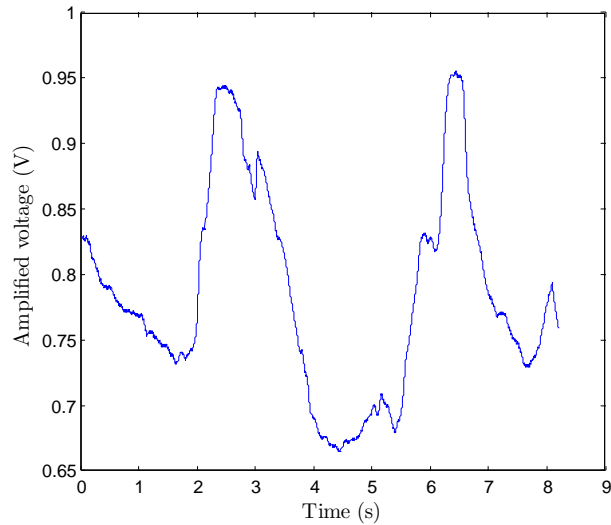


**Figure 6.8: Dynamic amplified voltage response of NIR device when moving over a blood vessel**

### 6.3.2 Discussion

The data obtained from the *in vivo* testing clearly supports the hypothesis that the mean intensity when pointing at a blood vessel differs from when pointing away from a blood vessel. This applies for several cases, such as when the needle is placed directly on the blood vessel, through a thin layer of skin and also when the needle is in muscle. While all the results do indicate statistically significant differences between pointing at and away from a blood vessel, the minimum and maximum values still intersect in some cases. This can be caused by several factors including the needle angle with respect to the blood vessel and the blood content of the muscle tissue. These factors will always play a role in a practical environment. The factors can be reduced somewhat by using a calibration potentiometer as described in Section 4.1.2. By calibrating the needle inside muscle tissue any significant relative changes is expected to be clearly noticeable.

Most of the results that were obtained are as expected. Haemoglobin absorbs NIR light. This phenomena is shown in the skin surface tests in Fig-

## 6. IN VIVO TESTS

---

ure 6.5. When the probe is aimed at the blood vessel less light is reflected. Light travels through the dermis and epidermis with high scattering and low absorption coefficients. Thus a large amount of light is reflected along its path from the transmitter to the receiver. When a blood vessel is encountered, light is absorbed by the haemoglobin, subsequently resulting in a lower intensity reading by the receiver.

The tests where the needle was inserted into the muscle tissue and pointed at the blood vessel show similar results. While it cannot be confirmed where exactly the needle is pointing, since the physician himself could not see the blood vessel, the higher set of intensities correspond to the values obtained for pure muscle tissue throughout the rabbit tests. This implies that the lower set of readings most likely correspond to pointing at a blood vessel.

The results where the probe makes direct contact with the blood vessel are unexpected however. The results displayed in Figure 6.4 indicates that more light is reflected when the needle is placed against the blood vessel directly, than when the needle is slightly inserted into the muscle tissue. A possible reason for this is that when the optic fibre makes *ex situ* surface contact with the vessel, reflectance plays a larger role than absorbance. Incident light at the surface of the vessel is immediately reflected at the blood vessel and optic fibre interface. The *in vitro* tests had similar results when the needle was placed directly into the blood. The reflected light reading was higher than that of muscle and fat. However, when pointing at the tube, filled with blood, the response was lower than that of muscle and fat.

A limitation of this device is that the sensitivity may not allow for the exact placing of the needle, i.e. it will not be able distinguish if the needle is pointing at the centre of the blood vessel or at the side wall of the blood vessel. This does not imply that the NIR technology cannot be used to locate the centre of a blood vessel, however, further studies are required to if it is possible.

This technology can in fact be used to locate a blood vessel. The user should however get the tip of the needle near the vicinity of the blood vessel for detection to be possible. A higher intensity light and more sensitive receiver may increase the sensing distance and can be considered in future designs. Whether the relative change in light intensity between pointing at a blood vessel and pointing away from said blood vessel is more or less, also requires some further investigation to confirm.

## 6. IN VIVO TESTS

## 6.4 Blood Vessel Penetration Detection

## 6.4.1 Results

The hypotheses remain the same as for the *in vitro* tests. The null hypothesis states that the mean impedance magnitudes and angles are the same, whereas the alternative hypothesis states that means of blood and muscle, and blood and fat differ. This applies only to specific frequencies.

The rabbit impedance tests were performed by means of a frequency sweep, ranging from 5 kHz to 75 kHz. Figure 6.9(a) and Figure 6.9(b) illustrates the mean results obtained during the frequency sweeps for impedance magnitude and phase angle respectively. The figures also display their respective 95 % confidence intervals. This is based on the number of samples displayed in Table 6.4. Note that each sample consists of a number of frequency sweeps. The total number of readings performed are indicated in the last column. The muscle and fat samples were obtained at different points on three separate rabbits. The blood samples were obtained from two rabbits only.

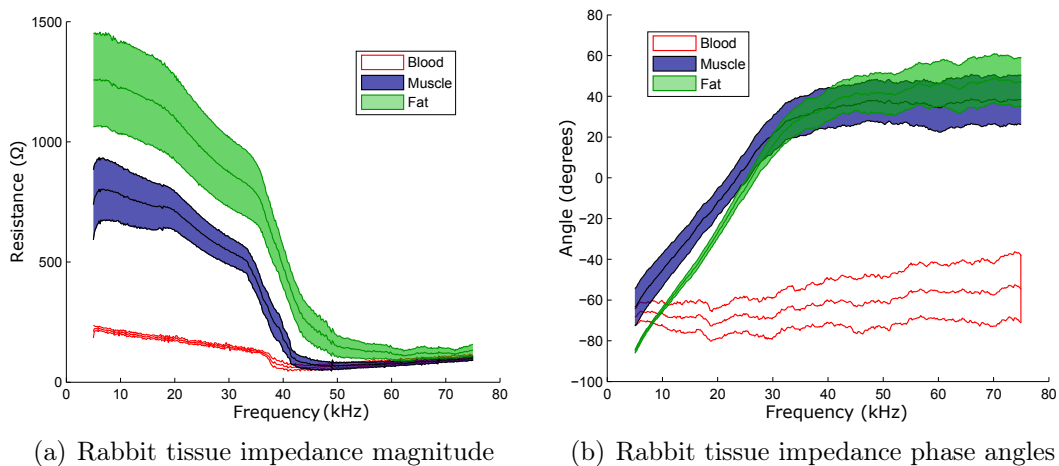


**Figure 6.9: Impedance magnitudes and phase angles of rabbit tissue types with 95 % confidence intervals**

Figure 6.9(a) shows strong similarities to the results obtained in the *in vitro* testing. Figure 6.9(b) however has a distinctly lower impedance phase angle for blood. This is elaborated on in Section 6.4.2. The interference ratios, as described by Equation 5.1 are illustrated in Figure 6.10. Values larger than one indicate that at that specific frequency the 95 % confidence intervals of blood and the nearest tissue do not overlap and is thus preferable.

The optimal frequency is determined by taking the product of the impedance magnitude and phase angle interference ratios. The optimal frequency will be



## 6. IN VIVO TESTS

Table 6.4: Impedance tests sample information for rabbit tests

Tissue type	Number of samples	Total Readings (some samples consists of multiple readings)
Blood	15	20
Muscle	37	78
Fat	31	61

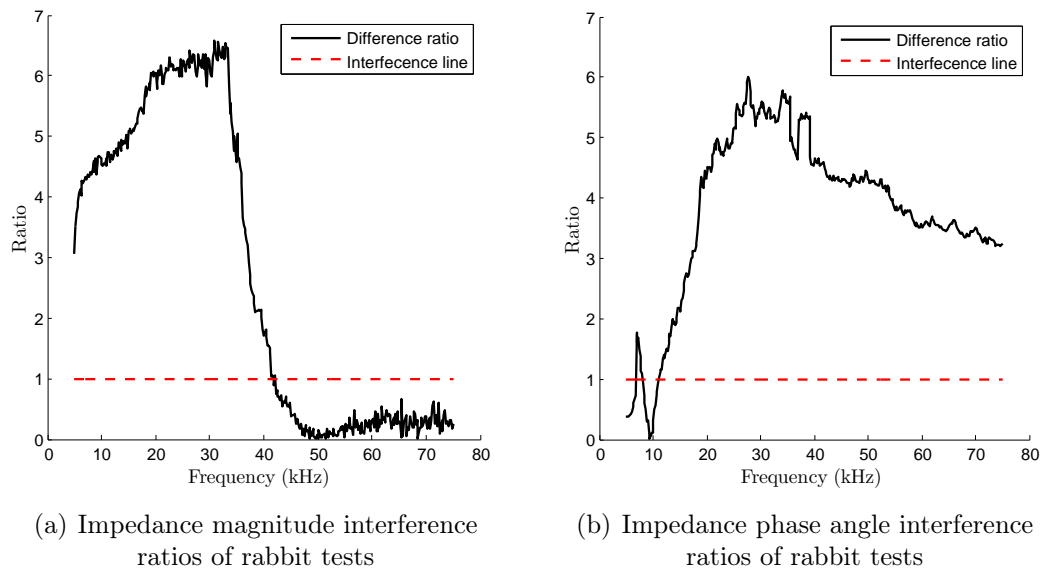
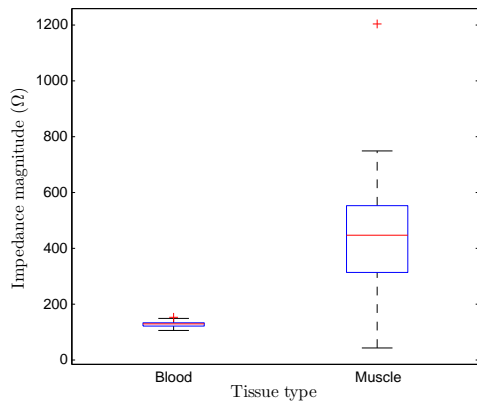


Figure 6.10: Interference ratios of blood and nearest rabbit tissue means

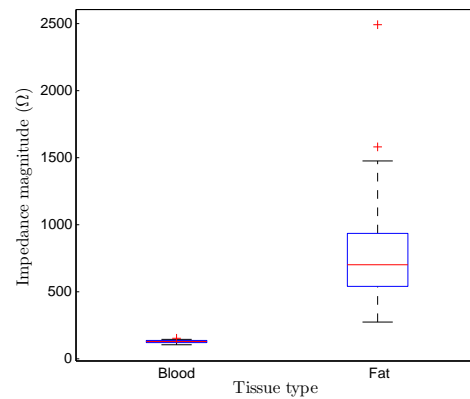
the product with the highest value. The maximum value of 37.77, occurs at a frequency of 27.93 kHz. For the sake of relating the tests to that of the *in vitro* tests, the same frequency as used there is analysed. The frequency is 29.85 kHz, now with an interference ratio product of 34.35.

Figure 6.11 and Figure 6.12 again show that in all four cases the 95 % confidence intervals never intersect. Determining whether the difference between blood and muscle, and blood and fat, is statistically significant, is accomplished by means of a t-test. The summary of the test given in Table 6.5 and Table 6.6 for impedance magnitude and phase angle respectively. Based on the results of the t-tests it is clear that the impedance device can clearly distinguish between blood and muscle, and blood and fat at 29.85 kHz. This can be done by using both impedance magnitude and impedance phase angle.

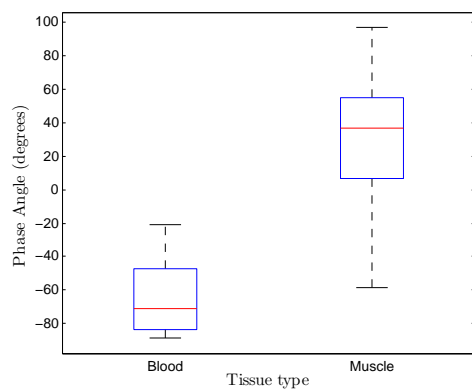
## 6. IN VIVO TESTS



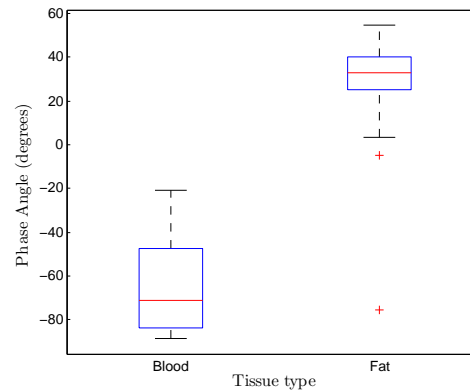
(a) Blood and muscle impedance magnitude



(b) Blood and fat impedance magnitude

**Figure 6.11: Impedance magnitudes of fat and muscle compared to blood at 29.85 kHz for rabbit tests**

(a) Blood and muscle impedance phase angle



(b) Blood and fat impedance phase angle

**Figure 6.12: Impedance phase of fat and muscle compared to blood at 29.85 kHz for rabbit tests**

## 6.4.2 Discussion

The data displayed in the results section, similar to that of the *in vitro* test, again clearly support the hypothesis that at certain frequencies the means of the impedance magnitudes and phase angles differ significantly between blood, muscle and fat.

As discussed in the *in vitro* tests (Section 5.5.2), at a frequency of 29.85 kHz, blood is highly distinguishable from fat and muscle tissue. It should be noted that the phase angle of blood differs from the *in vitro* tests. This could be

## 6. IN VIVO TESTS

Table 6.5: Impedance magnitude statistics at 29.85 kHz for rabbit tests

Tissue type	Mean ( $\Omega$ )	Standard deviation ( $\Omega$ )	p-Value (compared to blood)	Null rejected
Blood	148.72	13.05	NA	NA
Muscle	549.83	210.14	$1.2027 \times 10^{-6}$	Yes
Fat	873.56	475.56	$4.3436 \times 10^{-7}$	Yes

Table 6.6: Impedance phase angle statistics at 29.85 kHz for rabbit tests

Tissue type	Mean (degrees)	Standard deviation (degrees)	p-Value (compared to blood)	Null rejected
Blood	-69.22	22.08	NA	NA
Muscle	20.58	31.38	$4.6943 \times 10^{-13}$	Yes
Fat	15.32	17.90	$1.6761 \times 10^{-16}$	Yes

caused by a number of factors, likely the fact that the blood in the *in vitro* tests contained anticoagulant. Nonetheless, in both sets of tests there is still a significant difference between the phase angle of blood and both muscle and fat at 29.85 kHz.

During the course of these tests, the needle tip was cleaned when excessive amounts of tissue accumulated near the electrodes. If the needle penetrates through various tissues toward the blood vessel, the accumulated tissues can cause variability in the results. Future studies can investigate this possibility, however the effect is not expected to be large, especially when in blood, since the liquid will fill the majority of the space between the electrodes.

In conclusion, this device can be used to discriminate between tissue types, particularly between blood and other tissue types. Thus, at 29.85 kHz, the needle can detect when a blood vessel is entered. The results obtained by both Schwartz (2013) and Martinsen *et al.* (2010) (see Section 2) also suggest that the frequency at which blood can be discriminated from other tissues the best, is at 30 kHz.

## 7. Conclusion

### 7.1 Summary

The aim of this thesis is to develop a guidance and intra-arterial flow monitoring catheter. To accomplish this, three objectives are established, namely to detect a blood vessel from a short distance, detect when the needle penetrates a blood vessel and then to measure blood flow rate.

Literature shows several promising technologies that could be used to achieve these objectives. The literature in conjunction with some basic preliminary investigation indicates that near infrared (NIR) light, electrical impedance and thermal convection methods are the most appropriate methods to achieve the respective objectives.

#### 7.1.1 Near Infrared Blood Vessel Detection

NIR light is used to detect blood vessels from a short distance by transmitting the light via optic fibres. One fibre strand transmits light to the tissue and another receives and transmits reflected light back to a sensor. The difference in the optic properties of blood and other tissue causes the reflected light intensity to be different. The tests supported this hypothesis.

The *in vitro* tests clearly indicated that when pointing the NIR needle at different tissue types the response is different. Moreover, when pointing at an artificial blood vessel, filled with blood, the response differed from other tissue types. There was a statistically significant ( $p = 9.0996 \times 10^{-26}$ ) difference in readings between pointing at the blood vessel and away from the blood vessel. This was further supported by the *in vivo tests*. The tests were performed on New Zealand white rabbits. Pointing towards a blood vessel and away from a blood vessel also had a statistically significant ( $p \ll 0.0001$ ) different response, both when the blood vessel was visible and not visible. In the case where the blood was not visible, the physician relied on the real time response of the needle to locate the blood vessel. While it is certain that the needle pointed towards and away from the blood vessel, it is not entirely certain

## 7. CONCLUSION

---

which readings correspond to where the needle was pointing. For the same test at the skin surface there was also a statistically significant difference ( $p = 3.8791 \times 10^{-4}$ ) between pointing at the blood vessel and pointing away from it.

### 7.1.2 Electrical Impedance Blood Vessel Penetration Detection

Electric impedance is used to determine when the needle penetrates the blood vessel. The rationale behind this device is that if the electric impedance response in various biological tissues can be distinguished from blood flow, it is reasonable to assume that the needle can detect when it enters a blood vessel. The AD5934 impedance converter generates a voltage sine wave which is converted to a current sine wave. This is done by means of an enhanced Howland voltage controlled current source. For the purposes of testing, the sine waves starts at 5 kHz and sweeps through to 75 kHz. The AD5934 reads the return signal and calculates the real and imaginary part of the impedance.

The *in vitro* and *in vivo* tests both had very similar results. It was found that in both cases flowing blood could clearly be distinguished from muscle and fat at 29.85 kHz. This is the case for both the impedance magnitude and the impedance phase angle. The results showed a statistically significant difference ( $p \ll 0.0001$ ) between the impedance of blood and muscle and blood and fat at 29.85 kHz. This agrees with results obtained by both Schwartz (2013) and Martinsen *et al.* (2010) that also suggest that the frequency at which blood can be discriminated from other tissues the best, is at 30 kHz. It should be noted that from the test results, some minimum and maximum values of blood and other tissue types did interfere, but this did not fall in the 95 % confidence interval.

### 7.1.3 Thermal Convection Blood Flow Measurement

Thermal convection heat transfer is used to determine blood flow rate. Two thermistors are used to measure temperature. The one thermistor measures ambient temperature whereas the other is wrapped in a heating coil and measures that temperature. In the presence of fluid flow, heat is carried away from the sensor and causes a drop in temperature of the heater thermistor. This change in temperature can be related to the fluid flow rate.

This device is only conceptually tested on the *in vitro* flow model. The first set of tests were performed on distilled water. Flow rates from 0.1 ml/s to 0.45 ml/s were used. In this region the temperature difference fluctuated somewhat likely due to trapped heat in the heating coil. By removing the offset

## 7. CONCLUSION

---

of the different readings a clear trend was visible. In the flow measurement region, a linear fit is used with a coefficient of determination of  $R^2 = 0.9801$ . CFD results fall near the measured results, but when extended to 6 ml/s the results follow an exponential trend similar to that which is expected from convective heat transfer.

The blood tests had more erratic results. This is likely due to blood cells becoming trapped in the heating coil and not allowing internal heat to escape properly. Removing the offset of the results once again shows a trend. This time the most appropriate fit is a second order polynomial fit with a coefficient of determination of  $R^2 = 0.6056$ . This is only a moderate fit. The CFD results do however show that in theory the device could work, but physical elements such as the collecting of blood cells in the heater, need to be avoided. It should also be noted that this device will have to be calibrated over a number of diameters to accurately be used in practice. As the vessel diameter becomes closer to that of the probe, flow velocity is increased around the sensor and calibration is thus required.

### 7.2 Potential Future Work

The sensors in general provided mostly positive results. However, there are changes that could be made to future devices and additional testing that can improve the overall understanding of how these devices work.

The ability to detect blood vessels by means of near infrared light can further be tested in two ways. Firstly, the response can be tested when pointing the device at the center of the blood vessel and then at the side wall of the blood vessel. This can help determine whether the needle will penetrate the blood vessel at the correct place. Secondly, a test should be derived to determine the distance at which blood vessels can be detected. Changing the intensity of the light source for these tests can help find an optimal intensity depending on the required sensing distance.

The electrical impedance method detects when the needle penetrates the blood vessel. This can be further investigated by changing the number of electrodes on the needle. Additional electrodes may perhaps improve the accuracy of the device.

The thermal flow sensor has several changes that can potentially be made in the future. The most important change is to create a smooth heating element. A smooth element with a greatly reduced size can be obtained by etching the element on an appropriate material. This will avoid the trapping of heat in the heating element itself. Furthermore, the response of the device over a number of different tube diameters can provide information about whether calibration is truly required for the different tube sizes.

## 7. CONCLUSION

---

The eventual ideal is then to perform all the tests outlined in this thesis and in this section particularly, on humans. These clinical trials would inevitably provide the most accurate results of what can be expected if these devices are used in practise.

### 7.3 Conclusion

Physicians often have difficulty locating blood vessel and rely on their knowledge of the human anatomy to locate them. This is by no means a reliable method. Two devices were thus developed and tested to aid in guiding a needle into a blood vessel. The primary purpose of developing a guidance method, in the context of this thesis, is to create an access point for catheters to be inserted, in particular a flow monitoring catheter. Monitoring of blood flow, especially to the brain, is essential during surgical procedures to ensure that no brain damage occurs. A concept flow monitoring catheter is thus the third device that was developed and tested.

Guiding a needle into a blood vessel requires that the blood vessel be located first and then determine when the needle enters the blood vessel. Detecting the blood vessel from a short distance is done by means of near infrared light transmitted via optic fibres. The results obtained from both the *in vitro* and *in vivo* tests showed a statistically significant ( $p < 0.001$ ) difference in reflected light when pointing at a blood vessel and when pointing away from the blood vessel. This indicates that at short distances from the blood vessel, the device can in fact detect the vessel.

Determining when the needle enters the blood vessel is achieved by means of electrical impedance. It was found that at 29.85 kHz flowing blood can clearly be distinguished from fat and muscle. Both the impedance magnitude and phase angle between blood and fat and blood and muscle, significantly ( $p < 0.001$ ) differed from one another. This indicates that the device can detect when the tip of the needle enters a blood vessel.

Determining the blood flow rate is achieved by using the principle of convective heat transfer. In distilled water flow the sensor can determine the flow rate between the tested regions of 0.1 ml/s to 0.45 ml/s with a coefficient of determination of  $R^2 = 0.9801$ . This is however only once offsets have been removed. Blood could not be successfully measured in that region. Blood cells that got trapped in the heater caused the results to be erratic. A coefficient of determination of  $R^2 = 0.6056$  was achieved. However, CFD results show that in both water and blood the method can theoretically be used.

The devices have room for improvement, especially the thermal flow meter. However, the results are still relevant and contribute to the body of knowledge

## 7. CONCLUSION

---

about these topics. Developing a device that can efficiently guide a needle into a blood vessel has an important place in the medical field. In emergency situations, finding a blood vessel quickly is essential, whether it is to administer medication, fluids or adrenaline. Moreover it grants access to blood vessels that allow the insertion of catheters. A flow monitoring catheter also has an important place in the medical field. Measuring blood flow to organs can aid in diagnosing various diseases. Furthermore, measuring blood flow to the brain can ensure that the patient does not get brain ischemia which can result in the death of brain tissue.

The combination of near infrared light and the electrical impedance properties of biological tissue can guide a physician to insert a needle into a blood vessel. Thermal convection heat transfer can be used to determine blood flow rate, although some improvements to the current device needs to be made. These devices and the results obtained have the ability to contribute to the medical field.



# List of References

- Andreuccetti, D., Fossi, R. and Petrucci, C. (1996). An internet resource for the calculation of the dielectric properties of body tissues in the frequency range 10 hz - 100 ghz.  
Available at: <http://niremf.ifac.cnr.it/tissprop/>
- Bushberg, J.T. (2002). *The essential physics of medical imaging*. Lippincott Williams and Wilkins.
- Chang, Z.-y., Pop, G.A. and Meijer, G.C. (2008). A comparison of two-and four-electrode techniques to characterize blood impedance for the frequency range of 100 hz to 100 mhz. *IEEE Transactions on Biomedical Engineering*, vol. 55, no. 3, pp. 1247–1249.
- Chen, Z. and Luo, R. (1996 April 30). Solid-state micro proximity sensor. US Patent 5,512,836.
- Cheng, K.-S., Chen, C.-Y., Huang, M.-W. and Chen, C.-H. (2006). A multi-frequency current source for bioimpedance application. In: *5th International IEEE EMBS Special Topic Conference on Information Technology in Biomedicine*.
- Davies, T. (2005). An introduction to near infrared spectroscopy. *NIR news*, vol. 16, no. 1, p. 9.
- Dirnagl, U., Kaplan, B., Jacewicz, M. and Pulsinelli, W. (1989). Continuous measurement of cerebral cortical blood flow by laser-doppler flowmetry in a rat stroke model. *Journal of Cerebral Blood Flow & Metabolism*, vol. 9, no. 5, pp. 589–596.
- Du, W. (2014). *Resistive, Capacitive, Inductive, and Magnetic Sensor Technologies*. Series in Sensors. Taylor & Francis. ISBN 9781439812495.
- Franklin, D.L., Schlegel, W. and Rushmer, R.F. (1961). Blood flow measured by doppler frequency shift of back-scattered ultrasound. *Science*, vol. 134, no. 3478, pp. 564–565.
- Frobenius, W.D., Sanderson, A. and Nathanson, H. (1973). A microminiature solid-state capacitive blood pressure transducer with improved sensitivity. *Biomedical Engineering, IEEE Transactions on*, , no. 4, pp. 312–314.

## LIST OF REFERENCES

- Gabriel, C., Peyman, A. and Grant, E. (2009). Electrical conductivity of tissue at frequencies below 1 mhz. *Physics in medicine and biology*, vol. 54, no. 16, p. 4863.
- Gabriel, S., Lau, R. and Gabriel, C. (1996). The dielectric properties of biological tissues: Ii. measurements in the frequency range 10 hz to 20 ghz. *Physics in medicine and biology*, vol. 41, no. 11, p. 2251.
- Ganz, W. and Swan, H. (1972). Measurement of blood flow by thermodilution. *The American journal of cardiology*, vol. 29, no. 2, pp. 241–246.
- Gehlbach, S.M. (1992 July 21). Ultrasonic guided needle. US Patent 5,131,394.
- Giannoukos, G. and Min, M. (2014). Modelling of dynamic electrical bioimpedance and measurements safety. *AASRI Procedia*, vol. 6, pp. 12–18.
- Grimnes, S. and Martinsen, O.G. (2008). *Bioimpedance and bioelectricity basics*. Academic.
- Halperin, L.E., Miesel, K.A., Ufford, K.A., Svensk, J.R., Patrick, T., Hassler, B.A. and Varrichio, A.J. (1996 October 15). Implantable capacitive absolute pressure and temperature sensor. US Patent 5,564,434.
- Helfer, J.L., Switalski, S.C. and Liu, H.Y. (1993 March 30). Near infrared diagnostic method and instrument. US Patent 5,197,470.
- Islam, S.M.M., Reza, M.A.R. and Kiber, M.A. (2013). Performances of multi-frequency voltage to current converters for bioimpedance spectroscopy. *Bangladesh Journal of Medical Physics*, vol. 5, no. 1, pp. 71–76.
- Jaime, R.A., Basto, R.L., Lamien, B., Orlande, H.R., Eibner, S. and Fudym, O. (2013). Fabrication methods of phantoms simulating optical and thermal properties. *Procedia Engineering*, vol. 59, pp. 30–36.
- Jaspard, F., Nadi, M. and Rouane, A. (2003). Dielectric properties of blood: an investigation of haematocrit dependence. *Physiological measurement*, vol. 24, no. 1, p. 137.
- Jayanthy, A., Sujatha, N. and Reddy, M.R. (2011). Measuring blood flow: techniques and applications-a review. *Int. J. Res. Review Appl. Sci*, vol. 6, pp. 203–216.
- Johnson, B., Silverthorn, D., Ober, C., Ober, W., Silverthorn, A. and Pearson (2015). *Human Physiology: An Integrated Approach, Global Edition*. Always learning. Pearson Education, Limited. ISBN 9781292094939.
- Kalvøy, H., Frich, L., Grimnes, S., Martinsen, Ø.G., Hol, P.K. and Stubhaug, A. (2009). Impedance-based tissue discrimination for needle guidance. *Physiological measurement*, vol. 30, no. 2, p. 129.
- Li, C., Wu, P.-m., Wu, Z., Limnusun, K., Mehan, N., Mozayan, C., Golanov, E.V., Ahn, C.H., Hartings, J.A. and Narayan, R.K. (2015). Highly accurate thermal flow microsensors for continuous and quantitative measurement of cerebral blood flow. *Biomedical microdevices*, vol. 17, no. 5, pp. 1–7.

LIST OF REFERENCES

---

- Marieb, E.N. (2012). *Essentials of human anatomy and physiology*. Benjamin Cummings.
- Martinsen, Ø.G., Kalvøy, H., Grimnes, S., Nordbotten, B., Hol, P.K., Fosse, E., Myklebust, H. and Becker, L.B. (2010). Invasive electrical impedance tomography for blood vessel detection. *The open biomedical engineering journal*, vol. 4, p. 135.
- Menke, H. (2014). Basic operating principle of an inductive proximity sensor. Available at: <https://sensortech.wordpress.com/2014/03/05/basic-operating-principle-of-an-inductive-proximity-sensor/>
- Mohamadou, Y., Oh, T.I., Wi, H., Sohal, H., Farooq, A., Woo, E.J. and McEwan, A.L. (2012). Performance evaluation of wideband bio-impedance spectroscopy using constant voltage source and constant current source. *Measurement Science and Technology*, vol. 23, no. 10, p. 105703.
- Moore, J.E. and Zouridakis, G. (2004). *Biomedical technology and devices handbook*. CRC Press.
- Nelson, J. (1992 December 29). Thermocouple-based blood flow sensor. US Patent 5,174,299. Available at: <https://www.google.com/patents/US5174299>
- Ogle, J.S. (1999 August 10). Noninvasive blood flow sensor using magnetic field parallel to skin. US Patent 5,935,077.
- Pethig, R. (1987). Dielectric properties of body tissues. *Clinical Physics and Physiological Measurement*, vol. 8, no. 4A, p. 5.
- Schwartz, P. (2013). *Design of an impedance guided intra-arterial catheter*. Ph.D. thesis, Stellenbosch: Stellenbosch University.
- Shen-Xiu, Z. and Ti-Sheng, C. (1986). *Principles, techniques and applications in microsurgery*. World Scientific.
- Shepherd, A.P. and Öberg, P.A. (1990). *Laser-Doppler blood flowmetry*. Kluwer Academic Publishers.
- Siegman, A.E. (1986). *Lasers*. University Science Books.
- Smith, R., Arca, A., Chen, X., Marques, L., Clark, M., Aylott, J. and Somekh, M. (2011). Design and fabrication of ultrasonic transducers with nanoscale dimensions. In: *Journal of Physics: Conference Series*, vol. 278, p. 012035. IOP Publishing.
- Stolik, S., Delgado, J., Perez, A. and Anasagasti, L. (2000). Measurement of the penetration depths of red and near infrared light in human ex vivo tissues. *Journal of Photochemistry and Photobiology B: Biology*, vol. 57, no. 2, pp. 90–93.
- Strehle, E.-M. (2010). Making the invisible visible: near-infrared spectroscopy and phlebotomy in children. *Telemedicine and e-Health*, vol. 16, no. 8, pp. 889–893.

LIST OF REFERENCES

---

- Teferra, M.N. (2012). Electromagnetic blood flow meters. *Month*.
- Toffaletti, J. (2001). *Special Topics in Diagnostic Testing: Blood Gases and Electrolytes*. AACCC Press. ISBN 9781890883553.
- Tokarz-Deptuła, B., Niedźwiedzka-Rystwej, P., Adamiak, M., Hukowska-Szematowicz, B., Trzeciak-Ryczek, A. and Deptuła, W. (2014). Values of white and red blood cell parameters in polish mixed breed rabbits in the annual cycle. *Polish journal of veterinary sciences*, vol. 17, no. 4, pp. 643–655.
- Turner, L. (2013). *Electronics Engineer's Reference Book*. Elsevier Science. ISBN 9781483161273.
- Villarreal, M.R. (2009). Circulatory system.  
Available at: [https://upload.wikimedia.org/wikipedia/commons/2/29/Circulatory\\_System\\_en.svg](https://upload.wikimedia.org/wikipedia/commons/2/29/Circulatory_System_en.svg)
- Wang, P. and Liu, Q. (2011). *Biomedical Sensors and Measurement*. Advanced Topics in Science and Technology in China. Springer Berlin Heidelberg. ISBN 9783642195259.
- WHO (2005). Manual on the management, maintenance and use of blood cold chain equipment.
- Wyatt, D. (1961). Problems in the measurement of blood flow by magnetic induction. *Physics in medicine and biology*, vol. 5, no. 4, p. 369.

# Appendices

## A. Considered Technology

This appendix briefly covers technology that was considered for the design phase, but due to some drawbacks, were excluded.

### A.1 Ultrasonic Doppler

Ultrasonic Doppler was considered as a method to locate blood vessels. When ultrasound strikes moving objects, a frequency is reflected from the object, that is different from the original signal. This change in frequency is called a Doppler shift. By pointing the ultrasound at a blood vessel, the blood flow is expected to cause a Doppler shift, thereby allowing the user to locate a blood vessel.

A basic prototype was made to investigate how practical it would be to use Doppler as a method of locating blood vessels. A piezoelectric actuator, that generates ultrasound waves, was placed at the base of a needle. The electronics required to generate the ultrasound waves and to interpret the return signal are relatively complex. An existing 5 MHz fetal Doppler probe was thus used to test the concept as shown in Figure A.1.



**Figure A.1: Doppler probe with attached needle**

The probe that was used, generates a signal and interprets the return signal directly from the hardware. The signal processing works by means of a signal frequency mixer as shown in Figure A.2. The signal of the local oscillator (LO),

## A. CONSIDERED TECHNOLOGY

---

that actuates the piezoelectric crystal, enters the mixer along with the input of the receiver crystal (RF). The receiver crystal generates a signal equivalent to that of the transmitting crystal if there are no moving objects that can cause a Doppler shift. The mixer provides an output signal that has a component equal to  $LO - RF$  and  $LO + RF$ . By using a low-pass filter,  $LO + RF$  is removed and a signal with zero frequency is ideally returned.

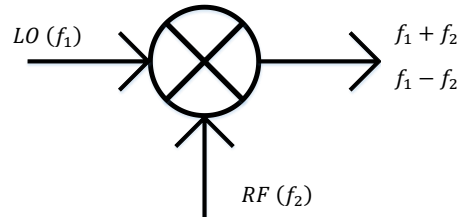


**Figure A.2: Frequency mixer**

Motion, such as blood flow, causes a Doppler shift and the frequency of the receiver will change relative to the local oscillator. This can then be seen in the  $LO - RF$  component of the output signal.

The needle has to be filled with a fluid, such as ultrasonic gel, as the high frequency sound waves will bounce off of human skin if it is transmitted through the air. The fluid thus allows the ultrasonic sound to propagate to the blood vessels.

A major drawback of this is that a signal will attenuate extremely fast over the length of the needle. Another drawback is the fact that the needle detects movement, so any movement of the needle on the skin or below the skin will cause noise. These are among some of the reasons why this technology is excluded from the final devices.

## A.2 Capacitance

The principle of using this technology to detect when a blood vessel is penetrated is very basic. A small diameter wire is coiled around a needle and attached to a resistor as shown in Figure A.3. One end of the wire is connected to a microcontroller output pin and the resistor is connected to an input pin. A short voltage pulse is then transmitted from the output pin. The time taken for the input pin to read this voltage is then measured. Refer to Figure A.4. When a dielectric material (such as blood) comes close to the needle, it acts as a capacitor. The result is that the input pin takes longer to receive the voltage signal by the output pin. This thus acts as a type of proximity detector.

## A. CONSIDERED TECHNOLOGY

---



Figure A.3: Capacitive sensing needle

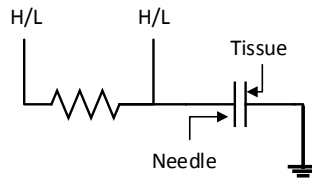


Figure A.4: Capacitive sensing circuit

The major drawback of this technology is that skin, fat, muscle and blood are all dielectric materials. This implies that this method will most likely not allow one to distinguish between different tissue types accurately. Also, if any grounded object comes near the device, the reading will also be affected. This makes it extremely difficult to use in a practical environment. These are among some of the reasons why this technology was excluded.



## B. Circuits

This appendix displays the full circuits of the devices discussed in Section 4

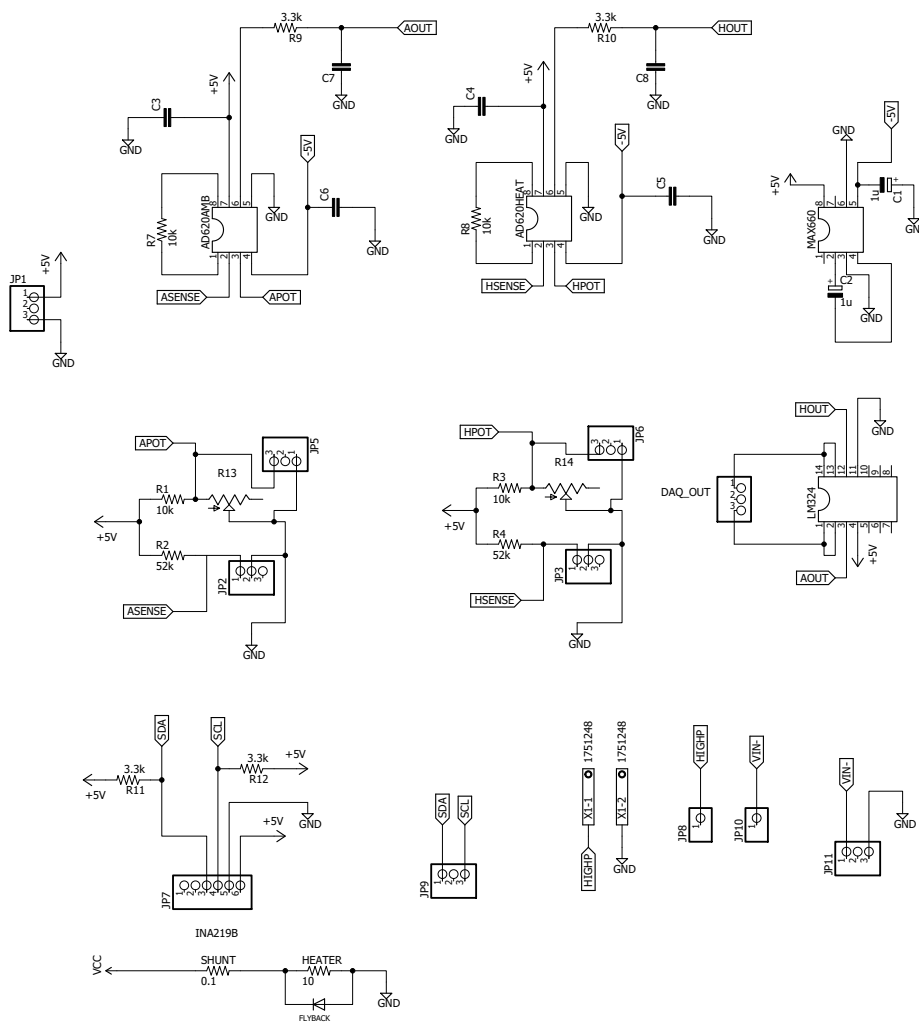


Figure B.1: Full thermal flow meter circuit

B. CIRCUITS

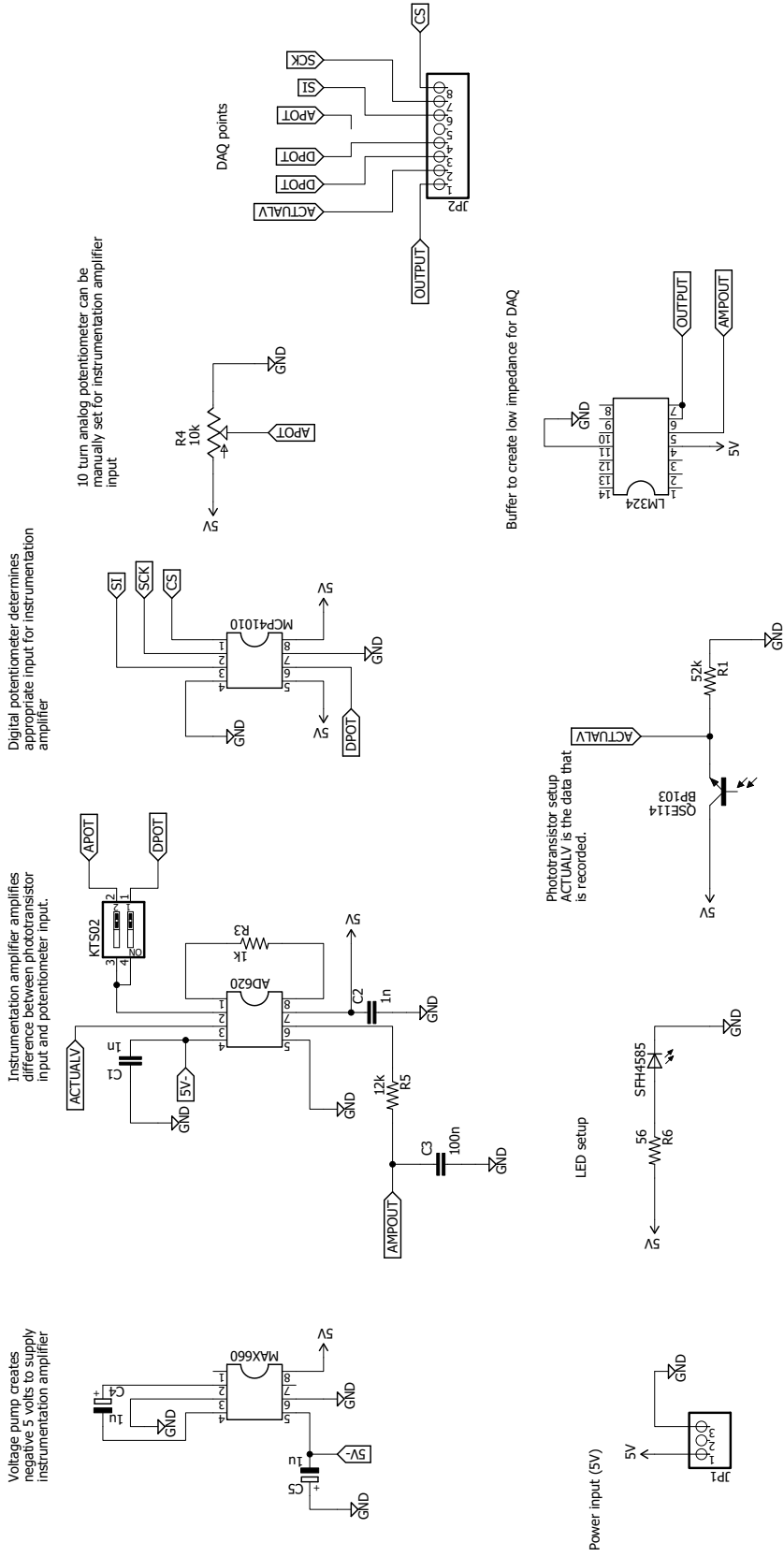


Figure B.2: Full near infrared device circuit

B. CIRCUITS

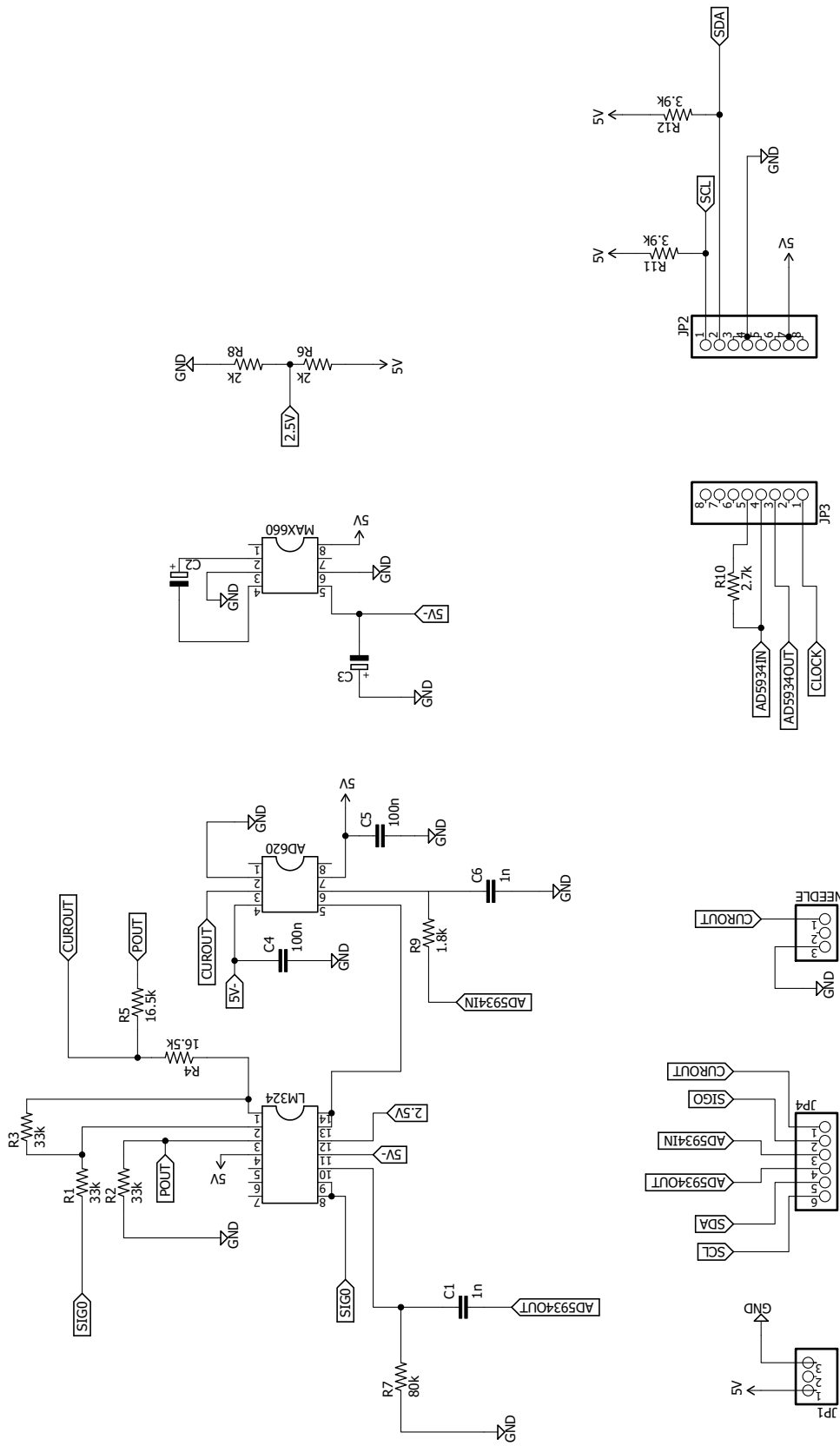


Figure B.3: Full impedance device circuit

## C. Near Infrared Device Housing

C. NEAR INFRARED DEVICE HOUSING

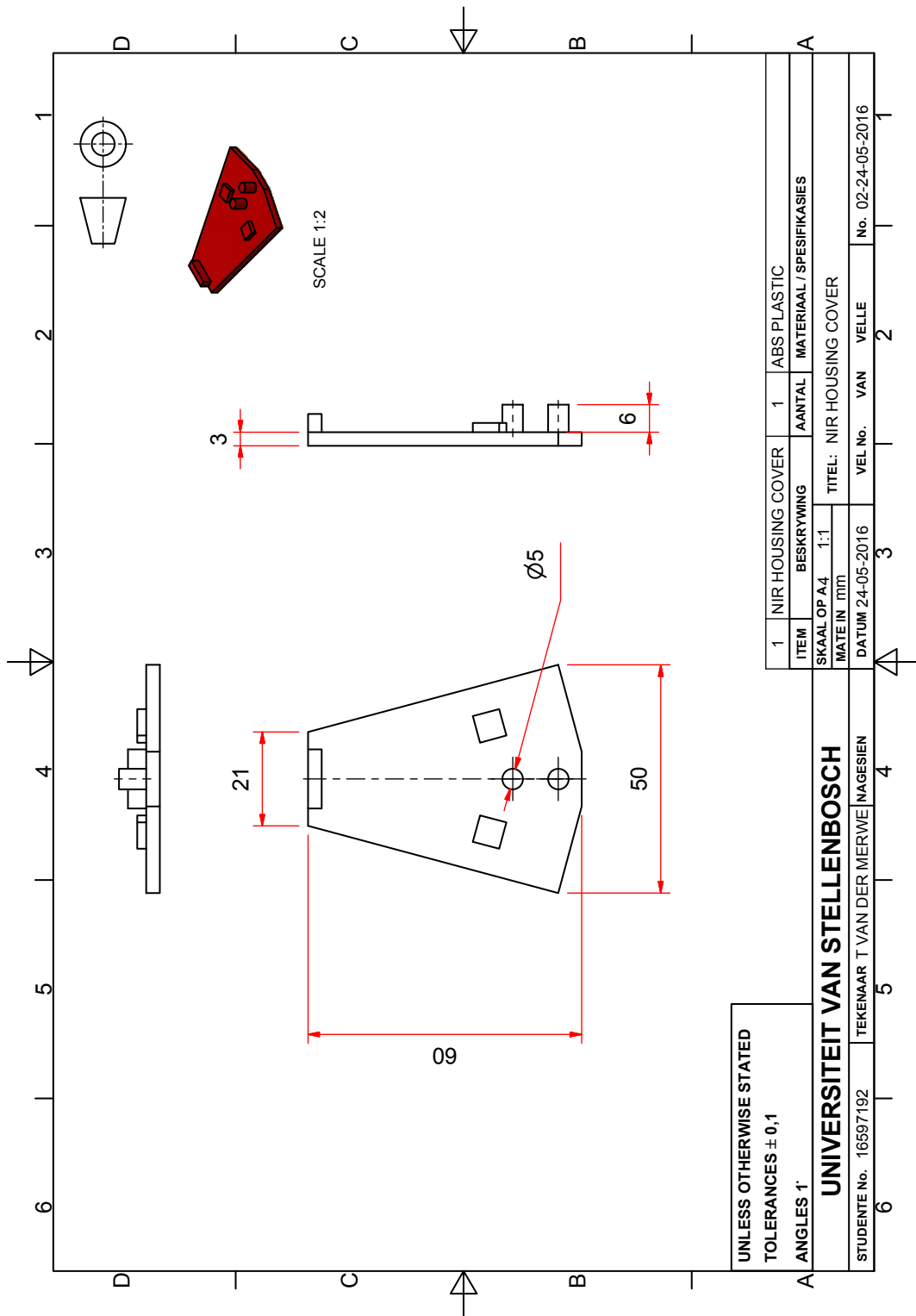


Figure C.1: Near infrared device housing top cover

C. NEAR INFRARED DEVICE HOUSING

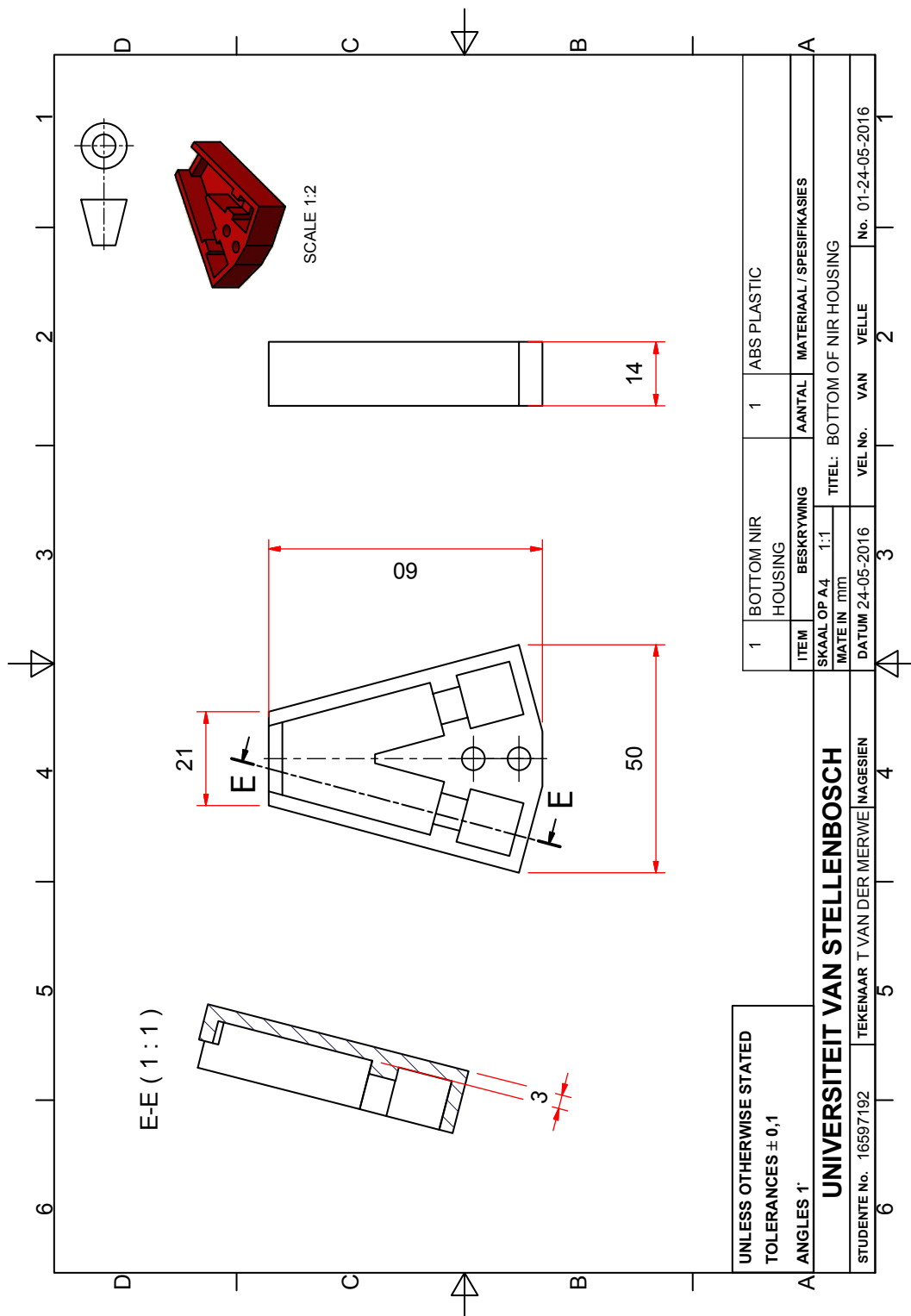


Figure C.2: Near infrared device bottom housing

## D. AD5934 Flow Chart

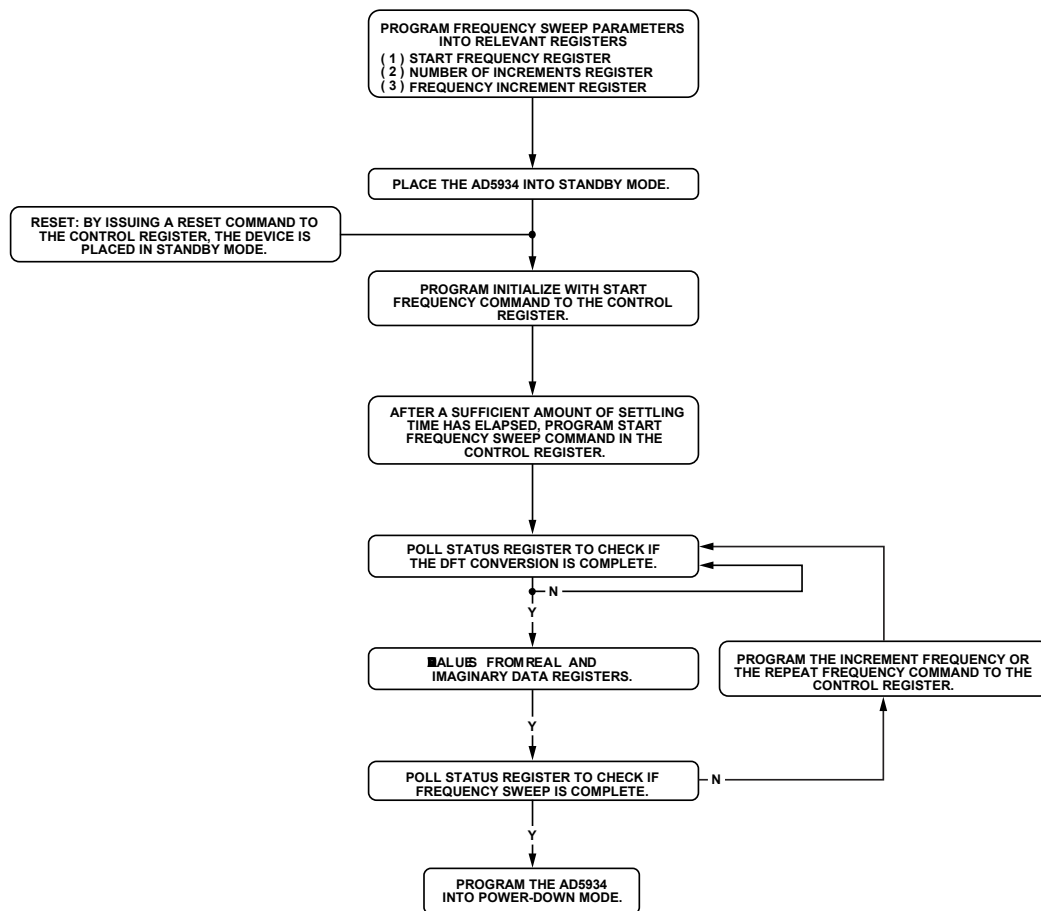
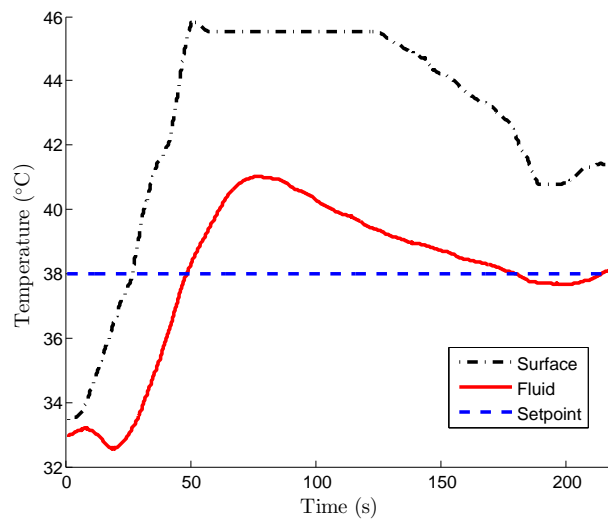


Figure D.1: AD5934 flow chart (AD5934 datasheet)

## E. Circulation System Heater Control

The *in vitro* tests (Section 5) are performed in a fluid circulation system. The system aims to regulate the temperature of the blood at approximately 38 °C. The temperature is regulated by means of PID control on an Arduino microcontroller. There are two thermocouples that provide input to the microcontroller. The one thermocouple measures the outlet temperature that serves as input to the PID control and the other measures the surface temperature of the heater. The surface temperature may not exceed 50 °C as red blood cells begin to damage at this temperature. Figure E.1 illustrates the subsequent response of water flow through the heater, with the PID constants set as 1,2 and 5 respectively.



**Figure E.1: PID control of infusion warmer**



## F. In Vitro Experimental Procedure

F. IN VITRO EXPERIMENTAL PROCEDURE

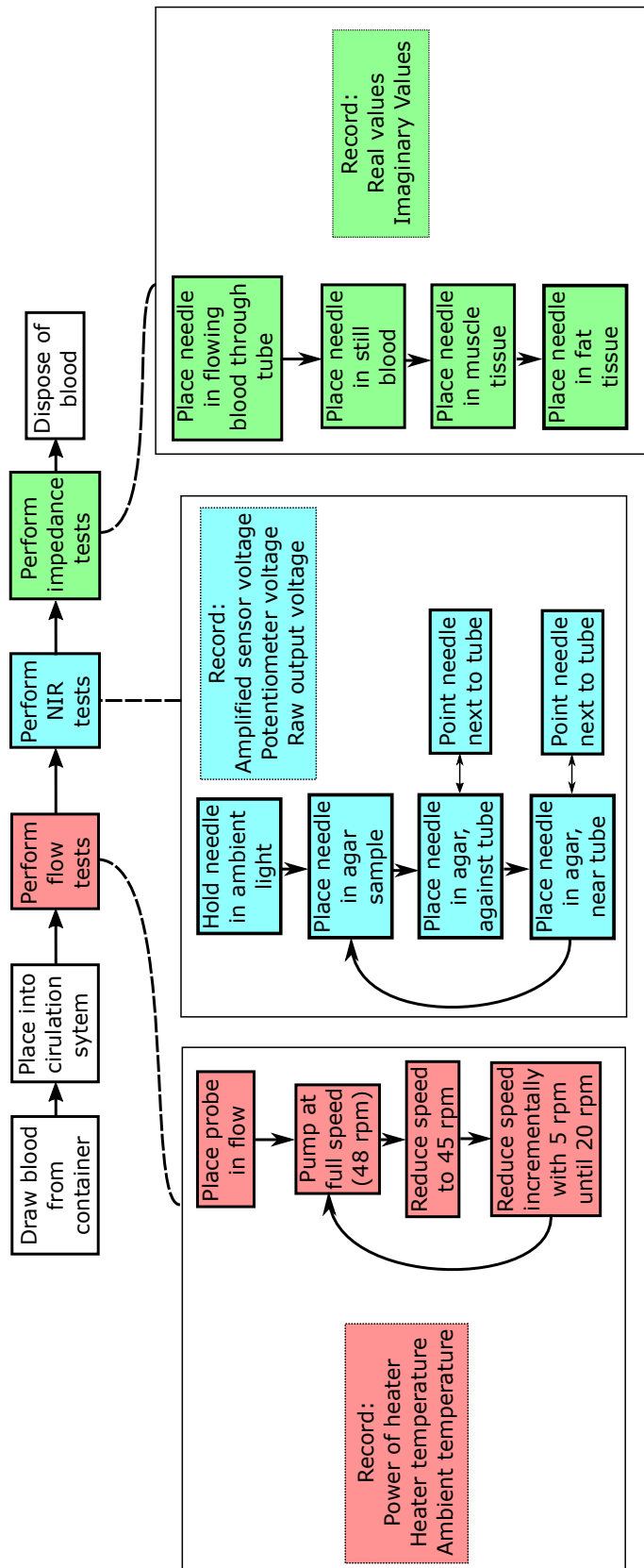


Figure F.1: *In vitro* testing procedure

## G. Pump Calibration

The Gilson Minipuls peristaltic pump is used to pump both blood and water through the circulation system discussed in Section 5. As shown in Figure G.1, the pump has ten rollers attached to a larger disc. The disc rotates and the rollers then pump the fluid in a peristaltic motion.



**Figure G.1: Gilson Minipuls peristaltic pump**

The pump has several RPM settings ranging from 0 to 48. The volume flow rate linearly increases with an increase in the RPM. A calibrated 50 ml burette was filled with water. The pump was then set to a specific RPM value, pumping water from the burette. This was done for 30 seconds, after which the volume pumped was determined. Figure G.2 illustrates the results obtained

## G. PUMP CALIBRATION

---

from the calibration. The volume flow rate (ml/s) as a function of the pump RPM is subsequently described by  $0.00842 \times \text{RPM}$  ( $R^2 = 0.9986$ ).

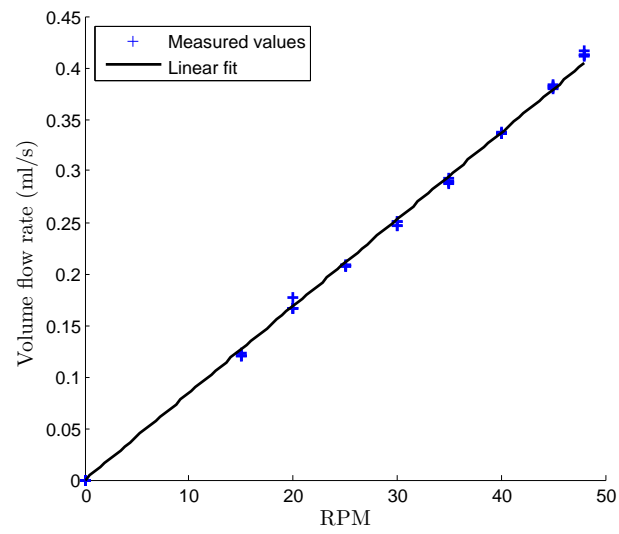


**Figure G.2: Pump calibration**

## H. Calibration

The ambient and heater thermistors are both calibrated by the Fluke 9142 metrology well. The thermistors are placed in an aluminium tube and then placed in the well. A pre-calibrated platinum resistance temperature detector (RTD), is used as a reference temperature. Both the resistances of the thermistors and the output voltage of the circuits were measured at a range of temperatures. Figure H.1 illustrates the calibration results along with the curve fits. Note that there is a considerable difference between the thermistors. The reason for this is that the wires that are attached to the thermistors add additional resistance and the difference in wire length contributes to the difference.

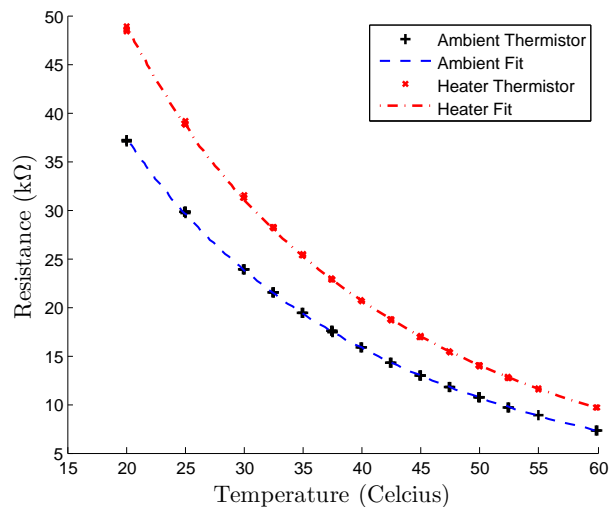


**Figure H.1: Thermistors Calibration**

The calibration data is fitted by means of the Steinhart-Hart equation for thermistors (as shown in Equation H.1).

$$\frac{1}{T} = C_1 + C_2 \ln(R) + C_3 [\ln(R)]^3 \quad (\text{H.1})$$

## H. CALIBRATION

---

Where  $T$  is the temperature in Kelvin,  $R$  is the thermistor resistance and  $C_1$ ,  $C_2$  and  $C_3$  are constants determined by calibration. The calibration constants for both the heater thermistor and ambient thermistor are displayed in Table H.1.

**Table H.1: Steinhart-Hart constants**

Thermistor usage	$C_1$	$C_2$	$C_3$	$R^2$
Heater	1.413e-02	-1.255e-03	2.675e-06	0.999
Ambient	1.365e-02	-1.222e-03	2.714e-06	0.999

A Wheatstone bridge is used to measure the resistance. As the resistance changes a voltage change in the Wheatstone bridge occurs. Thus, the measured voltage can be related to the resistance and subsequently the temperature. Figure H.2 illustrates how the voltage is related to the resistance of the ambient and heater thermistor circuits.

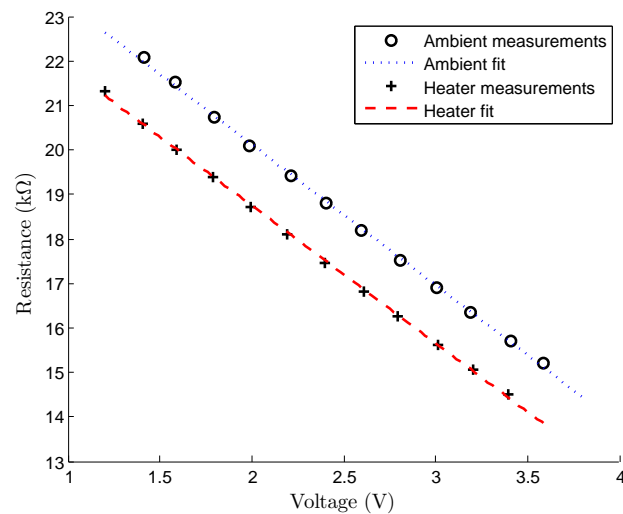


**Figure H.2: Ambient and heater thermistor Wheatstone bridge calibration**

# I. Ethical Clearance Letter of Approval



UNIVERSITEIT • STELLENBOSCH • UNIVERSITY  
jou kennisvennoot • your knowledge partner

## Protocol Approval

Date: 11-May-2016

PI Name: Van Der Merwe, Tys T

Protocol #: SU-ACUD15-00106

Title: Development of a Guidance and Intra-Arterial Flow  
Monitoring Catheter

Dear Tys Van Der Merwe, the Initial Application, was reviewed on 11-May-2016 by the Research Ethics Committee: Animal Care and Use via committee review procedures and was approved. Please note that this clearance is only valid for a period of twelve months. Ethics clearance of protocols spanning more than one year must be renewed annually through submission of a progress report, up to a maximum of three years.

Applicants are reminded that they are expected to comply with accepted standards for the use of animals in research and **teaching as reflected in the South African National Standards 10386: 2008. The SANS 10386: 2008 document is available on the** Division for Research Developments website [www.sun.ac.za/research](http://www.sun.ac.za/research).

As provided for in the Veterinary and Para-Veterinary Professions Act, 1982. It is the principal investigator's responsibility to ensure that all study participants are registered with or have been authorised by the South African Veterinary Council (SAVC) to perform the procedures on animals, or will be performing the procedures under the direct and continuous supervision of a SAVC-registered veterinary professional or SAVC-registered para-veterinary professional, who are acting within the scope of practice for their profession.

Please remember to use your protocol number, SU-ACUD15-00106 on any documents or correspondence with the REC: ACU concerning your research protocol.

Please note that the REC: ACU has the prerogative and authority to ask further questions, seek additional information, require further modifications or monitor the conduct of your research.

Any event not consistent with routine expected outcomes that results in any unexpected animal welfare issue (death, disease, or prolonged distress) or human health risks (zoonotic disease or exposure, injuries) must be reported to the committee, by creating an Adverse Event submission within the system.

We wish you the best as you conduct your research.

If you have any questions or need further help, please contact the REC: ACU secretariat at or .

Sincerely,

REC: ACU Secretariat